MycoKeys 51: 1–14 (2019)
doi: 10.3897/mycokeys.51.32272
http://mycokeys.pensoft.net

RESEARCH ARTICLE

A peer-reviewed open-access journal
MycoKeys
Launched to accelerate biodiversity research

The genus *Castanediella*

Chuan-Gen Lin[1,2], Darbhe J. Bhat[3,4], Jian-Kui Liu[5], Kevin D. Hyde[2], Yong Wang[1]

1 *Department of Plant Pathology, College of Agriculture, Guizhou University, Guiyang, Guizhou 550025, China* **2** *Center of Excellence in Fungal Research, Mae Fah Luang University, Chiang Rai 57100, Thailand* **3** *128/1-J, Azad Housing Society, Curca, Goa Velha 403108, India* **4** *Formerly, Department of Botany, Goa University, Goa, India* **5** *Center for Bioinformatics, School of Life Science and Technology, University of Electronic Science and Technology of China, Chengdu 611731, China*

Corresponding author: *Yong Wang* (yongwangbis@aliyun.com)

Academic editor: *C. Gueidan* | Received 9 December 2018 | Accepted 23 January 2019 | Published 15 April 2019

Citation: Lin C-G, Bhat DJ, Liu J-K, Hyde KD, Wang Y (2019) The genus *Castanediella*. MycoKeys 51: 1–14. https://doi.org/10.3897/mycokeys.51.32272

Abstract

Two new species, *Castanediella brevis* and *C. monoseptata*, are described, illustrated and compared with other *Castanediella* taxa. Evidence for the new species is provided by morphological comparison and sequence data analyses. *Castanediella brevis* can be distinguished from other *Castanediella* species by the short hyaline conidiophores and fusiform, aseptate hyaline conidia, while *C. monoseptata* differs from other *Castanediella* species by its unbranched conidiophores and fusiform, curved, 0–1-sepatate, hyaline conidia. Phylogenetic analysis of combined ITS and LSU sequence data was carried out to determine the phylogenetic placement of the species. A synopsis of hitherto described *Castanediella* species is provided. In addition, *Castanediella* is also compared with morphologically similar-looking genera such as *Idriella*, *Idriellopsis*, *Microdochium*, *Neoidriella*, *Paraidriella* and *Selenodriella.*

Keywords

new taxa, Castanediellaceae, hyphomycetes, phylogeny, Sordariomycetes

Introduction

Hernández-Restrepo et al. (2017) introduced the family *Castanediellaceae* for the genus *Castanediella* within Xylariales and it was consolidated in recent study by Wijayawardene et al. (2018). The asexual morphs in *Castanediellaceae* are hyphomycetous and characterized by macronematous, mononematous or sporodochial, branched, brown to pale brown conidiophores, with monoblastic or polyblastic, sympodial, discrete, cylindrical to lageni-

form, hyaline to subhyaline conidiogenous cells, that produce unicellular or transversely septate, cylindrical, fusiform or lunate, hyaline conidia (Hernández-Restrepo et al. 2017).

The genus *Castanediella* was established by Crous et al. (2015) to accommodate *C. acaciae*, *C. cagnizarii* and *C. ramosa* within *Xylariales* genera *incertae sedis*. The genus contains twelve species (Costa et al. 2018; Wanasinghe et al. 2018), each characterized by branched, hyaline to pale brown conidiophores, holoblastic, sympodial conidiogenous cells and falcate, cylindrical or fusiform, 0–3-sepate, hyaline conidia (Crous et al. 2015; Costa et al. 2018).

During a survey of hyphomycetes in Thailand, two hyaline-spored hyphomycetes were collected. They were shown to belong to the genus *Castanediella* based on morphology and phylogeny analyses of ITS and LSU sequence data. The new species *C. brevis* and *C. monoseptata* are introduced.

Materials and methods

Collection and isolation of fungi

Dead leaves from a variety of plants in two forests (Lampang province and Chiang Mai province) were collected in 2016 in Thailand. Samples were taken to the laboratory in Zip-lock plastic bags for examination. The specimens were incubated in sterile moist chambers and examined using a Motic SMZ 168 series microscope. Fungi were removed with a needle and placed in a drop of distilled water on a slide for morphological study. Photomicrographs of fungal structures were captured with a Canon 600D digital camera attached to a Nikon ECLIPSE Ni compound microscope. All measurements were made by the Tarosoft (R) Image FrameWork program. Photo-plates were made with Adobe Photoshop CS3 (Adobe Systems, USA). Isolation of the fungi on to potato dextrose agar (PDA) was performed by the single spore isolation method (Chomnunti et al. 2014). Dried material was deposited in the Herbarium of Mae Fah Luang University (**MFLU**), Chiang Rai, Thailand and herbarium of Kunming Institute of Botany, Chinese Academy of Sciences (**HKAS**), Kunming, China. Cultures were deposited at Mae Fah Luang University Culture Collection (**MFLUCC**), Chiang Rai, Thailand and Kunming Institute of Botany, Chinese Academy of Sciences (**KUMCC**), Kunming, China. FacesofFungi and Index Fungorum numbers were registered (Jayasiri et al. 2015; Index Fungorum 2018).

DNA extraction, PCR amplification and sequencing

Genomic DNA was extracted from fungal mycelium grown on PDA or malt extract agar (MEA) at room temperature using the Fungal gDNA Kit (BioMIGA, USA) according to the manufacturer's instructions. The internal transcribed spacer region of ribosomal DNA (ITS) and large subunit nuclear ribosomal DNA (LSU) genes were amplified via polymerase chain reaction (PCR) using the following primers: ITS5 and

ITS4 (White et al. 1990) for ITS, and LR0R and LR5 (Vilgalys and Hester 1990) for LSU. The PCR products were sequenced with the same primers. The PCR amplification was performed in a 25 μL reaction volume containing 12.5 μL of 2 × Power Taq PCR MasterMix (a premix and ready to use solution, including 0.1 Units/μl Taq DNA Polymerase, 500 μM dNTP Mixture each [dATP, dCTP, dGTP, dTTP], 20 mM Tris-HCl pH 8.3, 100 Mm KCl, 3 mM $MgCl_2$, stabilizer and enhancer), 1 μL of each primer (10 μM), 1 μL genomic DNA extract and 9.5 μL deionised water. The PCR thermal cycle program of ITS and LSU were followed as: initially 94 °C for 3 min., followed by 35 cycles of denaturation at 94 °C for 30 s, annealing at 55 °C for 50 s, elongation at 72 °C for 1 min., and final extension at 72 °C for 10 min.

Phylogenetic analyses

Original sequences were checked using BioEdit version 7.0.5.3 (Hall 1999), and most reference sequences were originated from previous publications. The remaining homogenous sequences were obtained by BLAST searches (Altschul et al. 1990) from GenBank. All sequences used in this study are listed in Table 1. Alignments for each locus were done in MAFFT v7.307 online version (Katoh and Standley 2016) and manually verified in MEGA 6.06 (Tamura et al. 2013). After alignment, the concatenation of different genes was done in SequenceMatrix 1.8 (Vaidya et al. 2011). The interleaved NEXUS files for Bayesian inference analyses were formatted with AliView v1.19-beta1k (Larsson 2014). Maximum parsimony (MP), maximum likelihood (ML) and Bayesian inference (BI) were used for phylogenetic analyses.

The best models of evolution for each gene region were determined using Akaike information criterion (AIC) as implemented in MrModeltest v2 (Nylander 2004). The analyses' results showed that the models GTR+I and GTR+I+G were the best ones for LSU and ITS sequence data, respectively.

MP analyses were performed in PAUP*4.0b10 (Swofford 2002) following Liu et al. (2016).

ML analyses were carried out in raxmlGUI v 1.5b1 (Silvestro and Michalak 2012) with RAxML v8.2.10 (Stamatakis 2014), using the ML + rapid bootstrap setting and the GTRGAMMAI (viz., GTR + GAMMA + I) substitution model with 1000 bootstrap replicates.

For BI analysis, Posterior probabilities (PP) (Rannala and Yang 1996; Zhaxybayeva and Gogarten 2002) were determined by Markov Chain Monte Carlo sampling (BMCMC) in MrBayes v 3.2.6 (Ronquist et al. 2012). For the combined dataset, the models were set to nst = 6 and rates = propinv for LSU and nst = 6 and rates = invgamma for ITS. Two independent analyses of two parallel runs and six simultaneous Markov chains were run for 1,000,000 generations, trees were sampled every 100th generation and the temperature value of the heated chains was set at 0.15. The first 25% sampled trees of each run were discarded as "burn-in", and the remaining trees were used for calculating posterior probabilities (PP) in the majority rule consensus tree with the sumt command in MrBayes.

Phylogenetic trees were drawn with TreeView 1.6.6 (Page 1996).

Table 1. GenBank accession numbers of isolates included in this study.

Taxa	Isolate[a]	ITS	LSU
Castanediella acaciae	CPC 24869, CBS 139896	NR_137985	KR476763
Castanediella brevis	KUMCC 18-0132	MH806361	MH806358
Castanediella cagnizarii	MUCL 41095	KC775732	KC775707
Castanediella cagnizarii	CBS 101043	KP859051	KP858988
Castanediella cagnizarii	CBS 542.96	KP859054	KP858991
Castanediella camelliae	CNUFC-DLHBS5-1	MF926620	MF926614
Castanediella camelliae	CNUFC-DLHBS5-2	MF926621	MF926615
Castanediella communis	CPC 27631	KY173393	–
Castanediella couratarii	CBS 579.71	NR_145250	KP858987
Castanediella eucalypti	CPC 24746, CBS 139897	NR_137981	KR476758
Castanediella eucalypticola	CPC 26539	NR_145254	KX228317
Castanediella eucalyptigena	CBS 143178, CPC 32055	MG386036	MG386089
Castanediella hyalopenicillata	CPC 25873	KX306751	KX306780
Castanediella malaysiana	CPC 24918	NR_154810	KX306781
Castanediella monoseptata	KUMCC 18-0133	MH806360	MH806357
Castanediella ramosa	MUCL 39857	KC775736	KC775711
Subsessila turbinata	MFLUCC 15-0831	KX762288	KX762289

[a] **CBS**, Centraalbureau voor Schimmelcultures, Utrecht, Netherlands; **CPC**, Culture collection of Pedro Crous, housed at CBS; **KUMCC**, Kunming Institute of Botany, Chinese Academy of Sciences, Kunming, China; **MFLUCC**, Mae Fah Luang University Culture Collection, Chiang Rai, Thailand; **MUCL**, Mycothèque de l'Université Catholique de Louvian, Belgium.

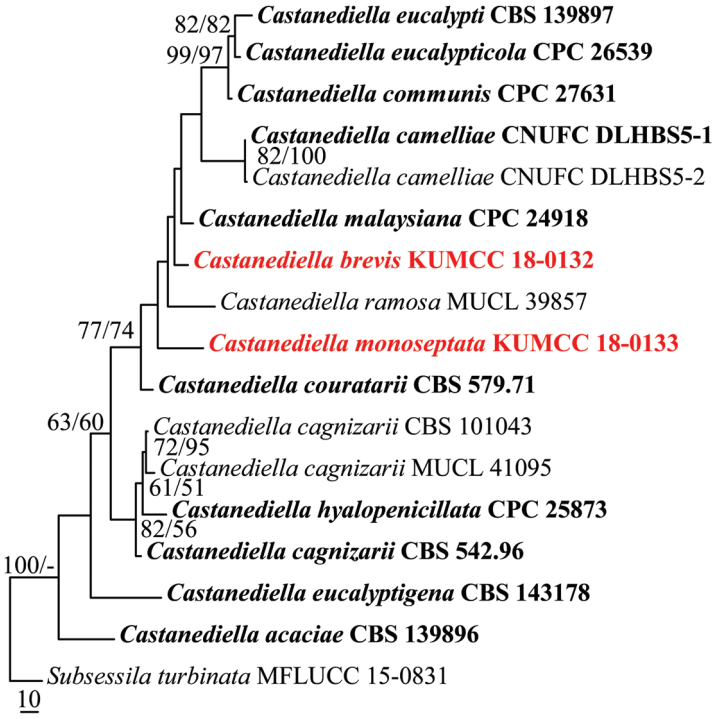

Figure 1. Phylogenetic tree generated from MP analysis based on combined LSU and ITS sequence data for the genus *Castanediella*. Bootstrap support values for maximum parsimony (MP, first set) and maximum likelihood (ML, second set) greater than 50% are indicated above or below the nodes. Ex-type strains are in bold, the new isolates are in red. The tree is rooted with *Subsessila turbinata* (MFLUCC 15-0831).

Results

Molecular phylogeny

The aligned sequence matrix comprises LSU and ITS sequence data for 16 taxa (ingroup) and one outgroup taxon with a total of 1438 characters after alignment including the gaps, of which 120 were parsimony informative, 77 parsimony-uninformative, and 1241 characters constant. The dataset consists of thirteen species within the genus. The tree was rooted with *Subsessila turbinata* (MFLUCC 15-0831). Maximum parsimony analysis resulted in two trees with TL = 391, CI = 0.657, RI = 0.642, RC = 0.422, HI = 0.343. For the Bayesian analysis, two parallel runs with six chains were run for 1,000,000 generations and trees were sampled every 100th generation, resulting in 20002 trees from two runs of which 15002 trees were used to calculate the posterior probabilities (each run resulted in 10001 trees of which 7501 trees were sampled).The MP and ML (lnL = -4041.301739) analyses based on combined LSU and ITS sequence data provided similar tree topologies, and the result of MP analysis is shown in Fig. 1.

The novelty of the species, *Castanediella brevis* and *C. monoseptata*, described in this study are supported by sequence data analyses as belonging to the genus *Castanediella*, but with low bootstrap support values. Isolates of *Castanediella brevis* and *C. monoseptata* formed separate clades in the phylogenetic inference, respectively. *Castanediella brevis* is sister to *C. malaysiana* and *C. ramosa*, while *C. monoseptata* shows close phylogenetic relationship to *C. couratarii* and *C. malaysiana*. Both the new taxa can be recognized as phylogenetically distinct species and are clearly novel based on the recommendations for molecular data (Jeewon and Hyde 2016).

MP, ML and BI were used for phylogenetic analyses in this study. The tree topologies of MP and ML resulted from the combined LSU and ITS sequence data are similar, but most of the nodes are in low bootstrap support (Fig. 1). Polytomy structure was formed in the BI tree generated from the combined LSU and ITS sequence data. More sequence data, especially the protein-coding genes, e.g. TEF1-α, RPB2, β-tubulin, are required in the future study of the genus *Castanediella*.

Taxonomy

Castanediella brevis **C.G. Lin & K.D. Hyde, sp. nov.**
MycoBank number: MB828879
Facesoffungi number: FoF04929
Figure 2

Holotype. THAILAND. Lampang: Amphoe Mueang Pan, Tambon Chae Son, on decaying leaves, 24 September 2016, Chuangen Lin, LCG 10-1 (MFLU 18-1695, holotype; HKAS 102198, isotype), ex-type living cultures KUMCC 18-0132.

GenBank number. ITS: MH806361, LSU:MH806358

Etymology. In reference to the short conidiophores.

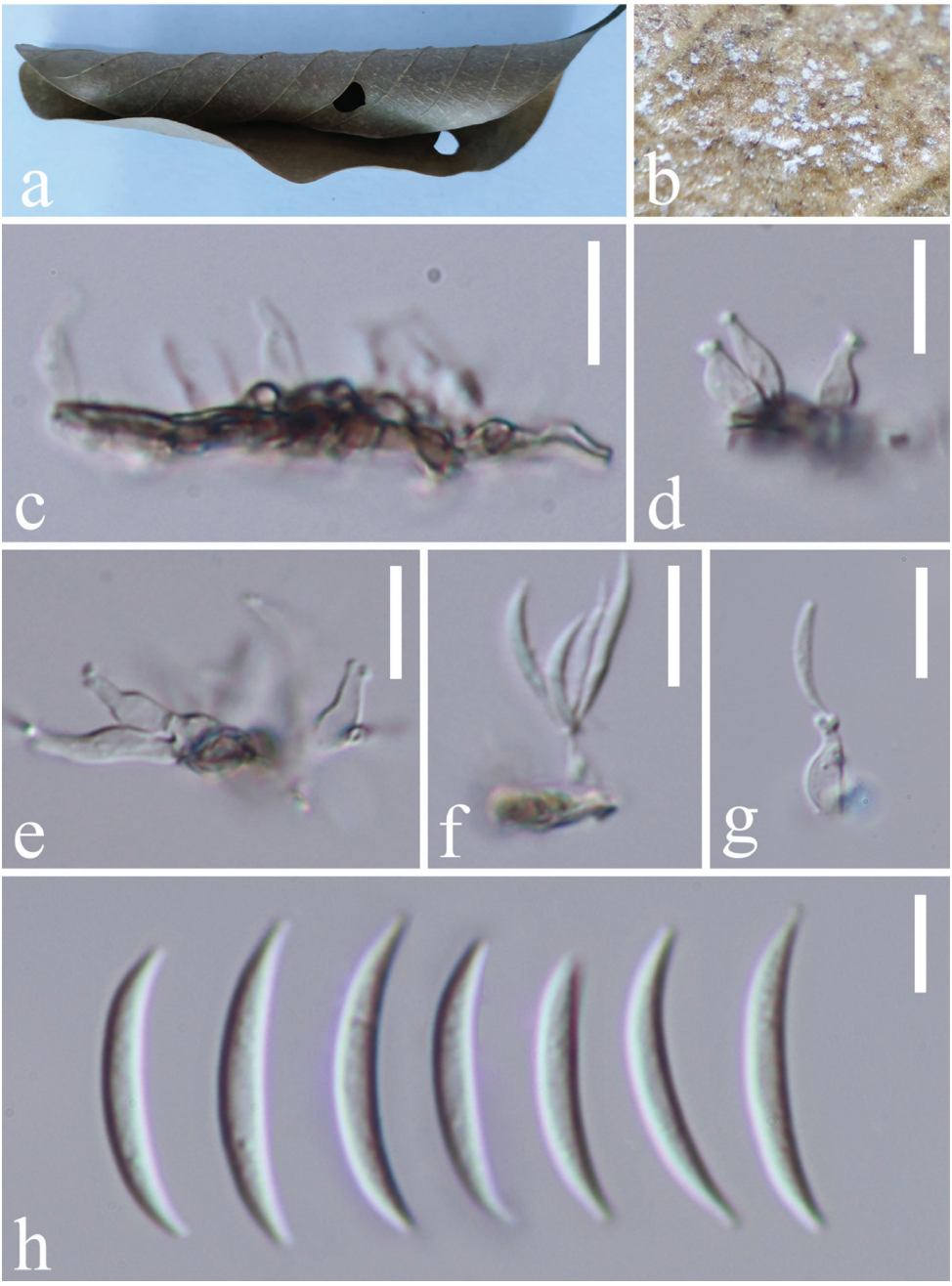

Figure 2. *Castanediella brevis* (MFLU 18-1695, holotype) **a** host material **b** conidiophores on the host surface **c–g** conidiophores, conidiogenous cells with conidia **h** conidia. Scale bars: 10 μm (**c–g**), 5 μm (**h**).

Saprobic on plant host. **Asexual morph:** *Colonies* on substrate effuse, white. *Mycelium* partly superficial, composed of septate, branched, smooth, hyaline to subhyaline hyphae. *Conidiophores* macronematous, mononematous, solitary, erect, unbranched,

straight or flexuous, short, 0–1-septate, hyaline, subcylindrical, ampulliform, smooth, often reduced to conidiogenous cells. *Conidiogenous cells* holoblastic, polyblastic, sympodial, integrated, terminal, subcylindrical, ampulliform, hyaline, denticulate, with 2–4 tiny protuberant denticles, 3–14 × 1.5–5.5 µm. *Conidia* solitary, dry, acropleurogenous, smooth, fusiform, curved, aseptate, hyaline, 12.5–21.7 × 1.2–3 µm (av. 16.95 × 2.2 µm, n = 60). **Sexual morph**: Undetermined.

Culture characteristics: Conidia germinating on PDA within 24 h. Colonies on PDA effuse, greyish white to dark from above and below, reaching a diam. of 5–7 cm in 30 days at 25 °C.

Notes. Based on a megablast search of the NCBI nucleotide database using the ITS sequence of the ex-type culture, the highest similarities found were with *Castanediella malaysiana* (GenBank NR_154810; identities = 526/537(98%), gaps = 1/537(0%)) and *C. couratarii* (GenBank KX960789; identities = 521/538(97%), gaps = 3/538(0%)). *Castanediella brevis* differs from these two species by its conidiophore morphology. *Castanediella couratarii* has pale brown conidiophores and longer conidiogenous cells (10.5–37 × 2–3.5 µm) whereas *C. malysiana* has pale brown and longer conidiophores (76–157 × 2.5–3 µm).

Among the species that produce more or less falcate and aseptate conidia, *Castanediella communis*, *C. eucalypti*, *C. eucalypticola* and *C. eucalyptigena* are most similar to *C. brevis*. However, *Castanediella brevis* differs from these species by its short, unbranched and 0–1-septate conidiophores.

Castanediella monoseptata **C.G. Lin & K.D. Hyde, sp. nov.**
MycoBank number: MB828881
Facesoffungi number: FoF04930
Figure 3

Holotype. THAILAND. Chiang Mai: on decaying leaves, 24 August 2016, Chuangen Lin, MRC 3-1 (MFLU 18-1696, holotype; HKAS 102199, isotype), ex-type living cultures KUMCC 18-0133.

GenBank number. ITS: MH806360, LSU: MH806357

Etymology. In reference to the 0–1-septate conidia

Saprobic on plant host. **Asexual morph:** *Colonies* on substrate effuse, white. *Mycelium* partly superficial, composed of septate, branched, hyaline to subhyaline, smooth hyphae. *Conidiophores* macronematous, mononematous, solitary, erect, unbranched, straight or flexuous, septate, hyaline, subcylindrical, smooth, 8–29 × 2–4 µm. *Conidiogenous cells* polyblastic, integrated, sympodial, subcylindrical, hyaline, with several scars. *Conidia* solitary, dry, acropleurogenous, smooth, fusiform, curved, 0–1-sepatate, hyaline, 15.4–25.8 × 1.5–2.3 µm (av. 23.03 × 1.98 µm, n = 45). **Sexual morph**: Undetermined.

Culture characteristics: Conidia germinating on PDA within 24 h. Colonies on PDA effuse, grayish white to dark from above and below, reaching a diam. of 5–7 cm in 30 days at 25 °C.

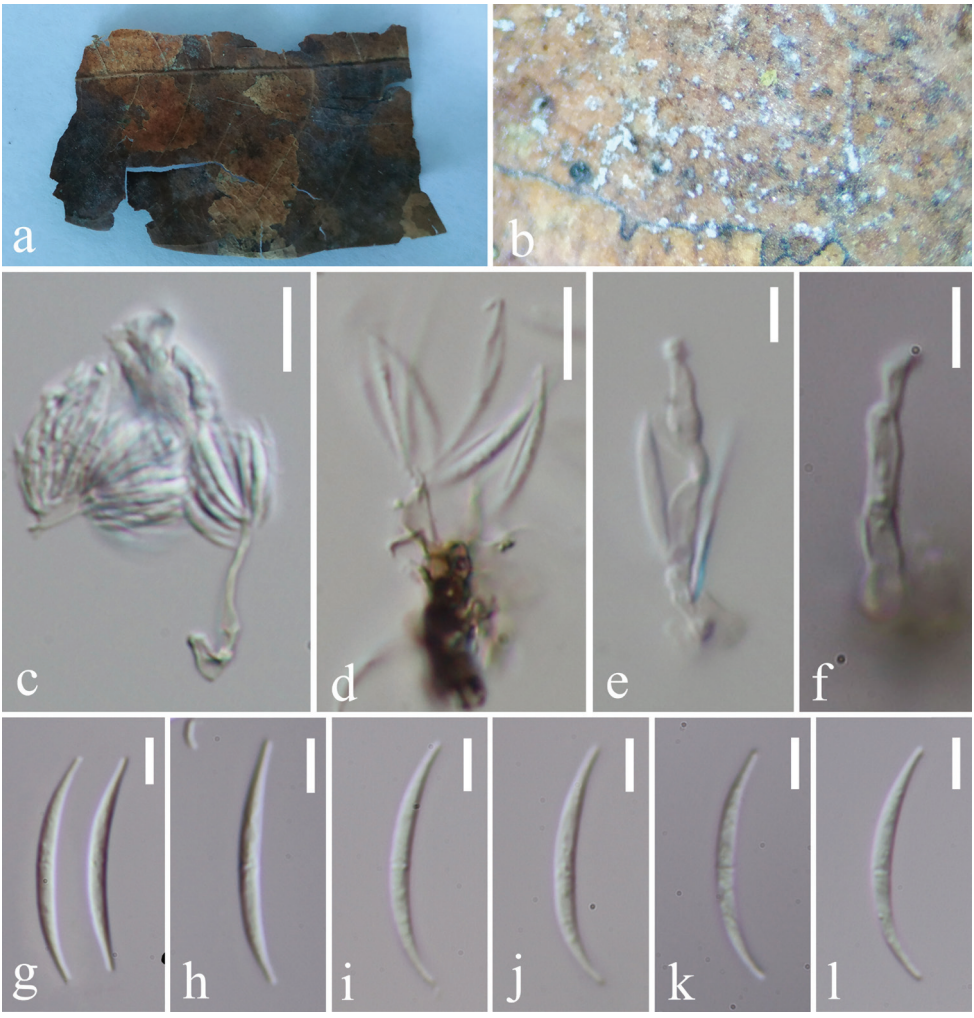

Figure 3. *Castanediella monoseptata* (MFLU 18-1696, holotype) **a** host material **b** conidiophores on the host surface **c–f** conidiophores, conidiogenous cells with conidia **g–l** conidia. Scale bars: 10 μm (**c, d**), 5 μm (**e–l**).

Notes. A megablast search of the NCBI nucleotide database using the ITS sequence of the ex-type culture showed the highest similarities with uncultured Sordariales fungi (GenBank GQ268569; identities = 518/539(96%), gaps = 3/539(0%)) and *Castanediella couratarii* (GenBank KX960789; identities = 516/540(96%), gaps = 4/540(0%)).

Five *Castanediella* species, *C. cagnizarii*, *C. diversispora*, *C. hyalopenicillata*, *C. malaysiana* and *C. ramosa*, were reported to produce 1-septate conidia. *Castanediella monoseptata* can be distinguished from these species by its unbranched conidiophores and falcate and 15.4–25.8 × 1.5–2.3 μm conidia. *Castanediella monoseptata* is phylogeneti-

cally closely related to *C. couratarii* and *C. ramosa*, but differs from both species by its conidial morphology. *Castanediella couratarii* has shorter conidia (9.5–19 × 2–3 µm) are aseptate and *C. ramosa* has larger conidia (26–44 × 2–3 µm) that are 0–3-septate.

Discussion

In this study, two new *Castanediella* species, *C. brevis* and *C. monoseptata*, were identified from decaying leaves in Thailand and a synopsis of hitherto described *Castanediella* species is provided (Table 2).

Table 2. Synopsis of *Castanediella* species.

Taxa	Conidiophores	Conidiogenous cells	Conidia			
			Shape	Size (µm)	Septa	Colour
C. acaciae	Subcylindrical, medium brown, 40–80 × 2–3 µm.	Polyblastic, ampulliform, pale brown, 10–15 × 2–3 µm.	Falcate with subobtuse ends	(8–)10–11(–12) × 1.5(–2)	0	Hyaline
C. brevis	Subcylindrical, ampulliform, hyaline, often reduced to conidiogenous cells	Polyblastic, cylindrical, hyaline, 3–14 × 1.5–5.5 µm	Fusiform, curved	12.5–21.7 × 1.2–3.0	0	Hyaline
C. cagnizarii	Cylindrical, brown at the base, subhyaline towards the apex, up to 45 µm long.	Polyblastic, sympodial, subhyaline, 5–22 × 3–4 µm.	Cylindrical to fusiform, curved at the ends	Two sizes, 10–15 × 2 or 20–26 × 2		Hyaline
C. camelliae	Conidiophores reduced to conidiogenous cell.	Cylindrical, ampulliform, globose to subglobose, or irregularly-shaped, 5.5–20.5 × 2–4.5 µm.	Straight to slightly curved, sometimes swollen in the middle part	18.5–51.5 × 1.6–2.5	Septum indistinct	Hyaline
C. communis	Subcylindrical, medium brown, 20–60 × 3–4 µm.	Polyblastic, subcylindrical to ampulliform, pale brown, 10–35 × 2–4 µm.	Falcate with subobtuse ends	(13–)17–20(–22) × (2–)2.5(–3)	0	Hyaline
C. couratarii	Pale brown	Lageniform to cylindrical, hyaline to pale brown, 10.5–37 × 2–3.5 µm	Lunate	9.5–19 × 2–3	0	Hyaline
C. diversispora	Pale brown to brown	Polyblastic, sympodial, pale brown to brown, 4–9 × 2–3.5 µm.	Type i) cylindrical, slightly uncinate at the ends, straight	Type i) 11.5–16 × 2	Type i) 1-septate	Hyaline
			Type ii) cylindrical to slightly subacerose, slightly uncinate at the apex, abruptly attenuated at the base, straight	Type ii) 19.5–25 × 1.5–2	Type ii) 1-septate	
			Type iii) long filiform, obtuse or rounded at the apex attenuated at the base, straight or curved	Type iii) 28.5–47 × 1	Type iii) 1–3-septate	

Taxa	Conidiophores	Conidiogenous cells	Conidia			
			Shape	Size (µm)	Septa	Colour
C. eucalypti	Subcylindrical, medium brown, 10–30 × 3–4 µm.	Polyblastic, subcylindrical to ampulliform, pale brown, 8–25 × 2.5–4 µm.	Falcate, slightly curved, widest in middle with subobtuse ends	(15–)18–21(–23) × 2–3	0	Hyaline
C. eucalypticola	Subcylindrical, medium brown, 5–30 × 3–5 µm.	Polyblastic, subcylindrical to ampulliform or lanceolate, pale brown, 5–20 × 3–3.5 µm.	Falcate, straight to curved, widest in the middle, apex subobtusely rounded, base truncate, 0.5 µm diam	(15–)20–26(–30) × (2.5–)3	0	Hyaline
C. eucalyptigena	Subcylindrical, hyaline, frequently reduced to conidiogenous loci on hyphae, up to 15 µm tall, 3–5 µm diam.	Polyblastic, hyaline, ampulliform or subcylindrical, 2–10 × 2–5 µm	Falcate, tapering to acute ends that are subobtusely rounded	(13–)18–24(–30) × 2(–2.5)	0	Hyaline
C. hyalopenicillata	Cylindrical, penicillate, mono-, bi-, and terverticillate, hyaline, 24–69 × 1.5–3 µm.	Mono- and polyblastic, short cylindrical, ampulliform, hyaline, 6.5–14 × 2–4 µm	Fusiform, base pointed, apex obtuse	14–24 × 2–3	0–1	Hyaline
C. malaysiana	Cylindrical, biverticillate, pale brown, 76–157 × 2.5–3 µm.	Polyblastic, cylindrical, subcylindrical, hyaline, 19–28 × 2.5–3.5 µm.	Fusiform, curved, apex acuminate, and base acuminate or slightly flattened	18–30 × 2–3	0–1	Hyaline
C. monoseptata	Subcylindrical, unbranched, hyaline, 8–29 × 2–4 µm	Polyblastic, cylindrical, hyaline	Fusiform, curved	15.4–25.8 × 1.5–2.3	0–1	Hyaline
C. ramosa	Cylindrical, penicillate, brown at the base, subhyaline at the apex, up to 70 µm long	Polyblastic, subhyaline, 10–20 x 2.5–3.5 µm	Falcate	26–44 × 2.2–3	(0–) 1 (–3)	Hyaline

Presently, the genus *Castanediella* contains 14 species, and is shown to be diverse in its habitats. Most of *Castanediella* species have been collected from plant leaves. *Castanediella acaciae*, *C. camelliae*, *C. communis*, *C. eucalypti*, and *C. eucalypticola* were isolated from disease symptoms on different host plant leaves (Crous et al. 2015, 2016a, b; Wanasinghe et al. 2018) whereas *C. cagnizarii* is the only species found on decaying leaves submerged in a stream (Castañeda Ruiz et al. 2005). Some *Castanediella* species were reported from decaying leaves, such as *C. brevis*, *C. cagnizarii*, *C. diversispora*, *C. hyalopenicillata* and *C. monoseptata* (Castañeda Ruiz et al. 2005; Hernández-Restrepo et al. 2016b; Costa et al. 2018). *Castanediella couratarii* was reported from dead wood (Hernández-Restrepo et al. 2016a).

The genus *Castanediella* is morphologically similar to *Idriella*, *Idriellopsis*, *Microdochium*, *Neoidriella*, *Paraidriella*, *Selenodriella* (Seifert et al. 2011; Crous et al.

2015; Hernández-Restrepo et al. 2016a). However, these genera can be distinguished by the branching pattern of their conidiophores and conidial shape and septation (Hernández-Restrepo et al. 2016a). *Castanediella* differs from these genera by its branched conidiophores, ampulliform conidiogenous cells with scars instead of denticles, and filiform, 0–1-septate, straight to curved conidia (Crous et al. 2015). These similar-looking genera are phylogenetically distinct (Crous et al. 2015; Hernández-Restrepo et al. 2016a). A comparative synopsis of these genera is provided (Table 3).

Table 3. Synopsis of *Castanediella*-like genera.

Genera	Conidiophores	Conidiogenous cells	Conidia	Chlamydospores
Castanediella	Branched, pale brown to brown at the base and subhyaline at the apex.	Sympodial, small denticles or scars, subhyaline.	0–1-sepate, falcate, lunate, cylindrical or fusiform, hyaline	Not observed.
Idriella	Brown, mostly reduced to conidiogenous cells	Denticulate, sympodial	Aseptate, lunate, curved, hyaline	Brown, uni- or pluricellular.
Idriellopsis	Unbranched, brown at the base, almost hyaline at the apex, mostly reduced to conidiogenous cells	Terminal, denticulate	0–1-septate, falcate, curved, hyaline	Not observed
Microdochium	More or less verticillate, reduced to conidiogenous cells, hyaline	Hyaline, sympodial or percurrent, sometimes denticulate	Aseptate or multiseptate, lunate, falcate, fusiform, filiform, obovoid or subpyriform, straight or curved, hyaline	Terminal or intercalary, solitary, in chains or grouped in clusters, brown.
Neoidriella	Mostly unbranched, pale brown, mostly reduced to conidiogenous cells	Sympodial, denticulate, terminal.	Aseptate, cylindrical to obovoid, hyaline	Intercalary or terminal, pale brown.
Paraidriella	Unbranched, pale brown, mostly reduced to conidiogenous cells.	Sympodial, denticulate, terminal.	Aseptate, cylindrical to oblong, hyaline	Not observed.
Selenodriella	Unbranched or verticillate, brown.	Sympodial, denticulate, terminal and intercalary.	Aseptate, falcate, hyaline	Not observed

Acknowledgements

We would like to thank Dr. Shaun Pennycook (Landcare Research Manaaki Whenua, New Zealand) for advising on the fungal names. The research is supported by the Thailand Research grants entitled The future of specialist fungi in a changing climate: baseline data for generalist and specialist fungi associated with ants, *Rhododendron* species and *Dracaena* species (grant no: DBG6080013), Impact of climate change on fungal diversity and biogeography in the Greater Mekong Subregion (grant no: RDG6130001). Y. Wang would like to thank the projects of the National Natural Science Foundation of China (No. 31560489, 31500451), Talent project of Guizhou science and technology cooperation platform ([2017]5788-5), Bijie Science and Technology Project ([2016]19) and Guizhou science and technology department international cooperation base project ([2018]5806). J.K. Liu would like to thank the National Natural Science Foundation of China (NSFC 31600032) and the Science and Technology Foundation of Guizhou Province (LH [2015]7061).

References

Altschul SF, Gish W, Miller W, Myers EW, Lipman DJ (1990) Basic local alignment search tool. Journal of Molecular Biology 215: 403–410.

Castañeda Ruiz RF, Heredia GP, Arias RM, Stadler M, Minter DW (2005) Two Hyphomycetes from submerged plant material of México. Mycotaxon 91: 333–338.

Chomnunti P, Hongsanan S, Aguirre-Hudson B, Tian Q, Persoh D, Dhami MK, Alias AS, Xu J, Liu X, Stadler M, Hyde KD (2014) The sooty moulds. Fungal Diversity 66: 1–36. https://doi.org/10.1007/s13225-014-0278-5

Costa PM, Barbosa MA, Da Silva GV, Sosa D, Pérez-Martinez S, Castañeda-Ruiz RF, Malosso E (2018) *Castanediella diversispora* sp. nov. from the Brazilian Atlantic Forest. Mycotaxon 133: 63–69.

Crous PW, Wingfield MJ, Burgess TI, Hardy GESJ, Crane C, Barrett S, Cano-Lira JF, Leroux JJ, Thangavel R, Guarro J, Stchigel AM, Martín MP, Alfredo DS, Barber PA, Barreto RW, Baseia IG, Cano-Canals J, Cheewangkoon R, Ferreira RJ, Gené J, Lechat C, Moreno G, Roets F, Shivas RG, Sousa JO, Tan YP, Wiederhold NP, Abell SE, Accioly T, Albizu JL, Alves JL, Antoniolli ZI, Aplin N, Araújo J, Arzanlou M, Bezerra JDP, Bouchara JP, Carlavilla JR, Castillo A, Castroagudín VL, Ceresini PC, Claridge GF, Coelho G, Coimbra VRM, Costa LA, da Cunha KC, da silva SS, Daniel R, de beer ZW, Dueñas M, Edwards J, Enwistle P, Fiuza PO, Fournier J, García D, Gibertoni TB, Giraud S, Guevara-Suarez M, Gusmão LFP, Haituk S, Heykoop M, Hirooka Y, Hofmann TA, Houbraken J, Hughes DP, Kautmanová I, Koppel O, Koukol O, Larsson E, Latha KPD, Lee DH, Lisboa DO, Lisboa WS, López-Villalba Á, Maciel JLN, Manimohan P, Manjón JL, Marincowitz S, Marney TS, Meijer M, Miller AN, Olariaga I, Paiva LM, Piepenbring M, Poveda-Molero JC, Raj KNA, Raja HA, Rougeron A, Salcedo I, Samadi R, Santos TAB, Scarlett K, Seifert KA, Shuttleworth LA, Silva GA, Silva M, Siqueira JPZ, Souza-Motta CM, Stephenson SL (2016a) Fungal Planet description sheets: 469–557. Persoonia - Molecular Phylogeny and Evolution of Fungi 37: 218–403.

Crous PW, Wingfield MJ, Guarro J, Hernández-Restrepo M, Sutton DA, Acharya K, Barber PA, Boekhout T, Dimitrov RA, Duenas M, Dutta AK, Gene J, Gouliamova DE, Groenewald M, Lombard L, Morozova OV, Sarkar J, Smith MT, Stchigel AM, Wiederhold NP, Alexandrova AV, Antelmi I, Armengol J, Barnes I, Cano-Lira JF, Castaneda Ruiz RF, Contu M, Courtecuisse PR, da Silveira AL, Decock CA, de Goes A, Edathodu J, Ercole E, Firmino AC, Fouriem A, Fournier J, Furtado EL, Geering ADW, Gershenzon J, Giraldo A, Gramaje D, Hammerbacher A, He XL, Haryadi D, Khemmuk W, Kovalenko AE, Krawczynski R, Laich F, Lechat C, Lopes UP, Madrid H, Malysheva EF, Marin-Felix Y, Martin MP, Mostert L, Nigro F, Pereira OL, Picillo B, Pinho DB, Popov ES, Pelaez CAR, Rooney-Latham S, Sandoval-Denis M, Shivas RG, Silva V, Stoilova-Disheval MM, Telleria MT, Ullah C, Unsickern SB, van der Merwe NA, Vizzini A, Wagner HG, Wong PTW, Wood AR, Groenewald JZ (2015) Fungal Planet description sheets: 320–370. Persoonia 34: 167–266. https://doi.org/10.3767/003158515x688433

Crous PW, Wingfield MJ, Richardson DM, Leroux JJ, Strasberg D, Edwards J, Roets F, Hubka V, Taylor PWJ, Heykoop M, Martín MP, Moreno G, Sutton DA, Wiederhold NP, Barnes CW, Carlavilla JR, Gené J, Giraldo A, Guarnaccia V, Guarro J, Hernández-Restrepo M, Kola, Ik

M, Manjón JL, Pascoe IG, Popov ES, Sandoval-Denis M, Woudenberg JHC, Acharya K, Alexandrova AV, Alvarado P, Barbosa RN, Baseia IG, Blanchette RA, Boekhout T, Burgess TI, Cano-Lira JF, moková A, Dimitrov RA, Dyakov MY, Dueñas M, Dutta AK, Esteve-Raventós F, Fedosova AG, Fournier J, Gamboa P, Gouliamova DE, Grebenc T, Groenewald M, Hanse B, Hardy GESJ, Held BW, Jurjevi, Kaewgrajang T, Latha KPD, Lombard L, Luangsa-ard JJ, Lysková P, Mallátová N, Manimohan P, Miller AN, Mirabolfathy M, Morozova OV, Obodai M, Oliveira NT, Ordóñez ME, Otto EC, Paloi S, Peterson SW, Phosri C, Roux J, Salazar WA, Sánchez A, Sarria GA, Shin HD, Silva BDB, Silva GA, Smith MT, Souza-Motta CM, Stchigel AM, Stoilova-Disheva MM, Sulzbacher MA, Telleria MT, Toapanta C, Traba JM, Valenzuela-Lopez N, Watling R, Groenewald JZ (2016b) Fungal Planet description sheets: 400–468. Persoonia - Molecular Phylogeny and Evolution of Fungi 36: 316–458.

Hall TA (1999) BioEdit: a user-friendly biological sequence alignment editor and analysis program for Windows 95/98/NT. Nucleic Acids Symposium Series 41: 95–98.

Hernández-Restrepo M, Gené J, Castañeda-Ruiz RF, Mena-Portales J, Crous PW, Guarro J (2017) Phylogeny of saprobic microfungi from Southern Europe. Studies in Mycology 86: 53–97. https://doi.org/10.1016/j.simyco.2017.05.002

Hernández-Restrepo M, Groenewald JZ, Crous PW (2016a) Taxonomic and phylogenetic re-evaluation of *Microdochium*, *Monographella* and *Idriella*. Persoonia – Molecular Phylogeny and Evolution of Fungi 36: 57–82.

Hernández-Restrepo M, Schumacher RK, Wingfield MJ, Ahmad I, Cai L, Duong TA, Edwards J, Gené J, Groenewald JZ, Jabeen S (2016b) Fungal Systematics and Evolution: FUSE 2. Sydowia 68: 193–230.

Jayasiri SC, Hyde KD, Ariyawansa HA, Bhat J, Buyck B, Cai L, Dai Y-C, Abd-Elsalam KA, Ertz D, Hidayat I, Jeewon R, Jones EBG, Bahkali AH, Karunarathna SC, Liu J-K, Luangsa-ard JJ, Lumbsch HT, Maharachchikumbura SSN, McKenzie EHC, Moncalvo J-M, Ghobad-Nejhad M, Nilsson H, Pang K-L, Pereira OL, Phillips AJL, Raspé O, Rollins AW, Romero AI, Etayo J, Selçuk F, Stephenson SL, Suetrong S, Taylor JE, Tsui CKM, Vizzini A, Abdel-Wahab MA, Wen T-C, Boonmee S, Dai DQ, Daranagama DA, Dissanayake AJ, Ekanayaka AH, Fryar SC, Hongsanan S, Jayawardena RS, Li W-J, Perera RH, Phookamsak R, Silva NI, Thambugala KM, Tian Q, Wijayawardene NN, Zhao R-L, Zhao Q, Kang J-C, Promputtha I (2015) The Faces of Fungi database: fungal names linked with morphology, phylogeny and human impacts. Fungal Diversity 74: 3–18. https://doi.org/10.1007/s13225-015-0351-8

Jeewon R, Hyde KD (2016) Establishing species boundaries and new taxa among fungi: recommendations to resolve taxonomic ambiguities. Mycosphere 7: 1669–1677. https://doi.org/10.5943/mycosphere/7/11/4

Katoh K, Standley DM (2016) A simple method to control over-alignment in the MAFFT multiple sequence alignment program. Bioinformatics 32: 1933–1942. https://doi.org/10.1093/bioinformatics/btw108

Larsson A (2014) AliView: a fast and lightweight alignment viewer and editor for large data sets. Bioinformatics 30: 3276–3278. https://doi.org/10.1093/bioinformatics/btu531

Liu JK, Yang J, Maharachchikumbura SSN, McKenzie EHC, Jones EBG, Hyde KD, Liu ZY (2016) Novel chaetosphaeriaceous hyphomycetes from aquatic habitats. Mycological Progress 15: 1157–1167.

Nylander J (2004) MrModeltest v2. Program distributed by the author. Evolutionary Biology Centre, Uppsala University.

Page RDM (1996) TreeView: an application to display phylogenetic trees on personal computers. Computer Applications in the Biosciences 12: 357–358. https://doi.org/10.1093/bioinformatics/12.4.357

Rannala B, Yang Z (1996) Probability distribution of molecular evolutionary trees: A new method of phylogenetic inference. Journal of Molecular Evolution 43: 304–311. https://doi.org/10.1007/BF02338839

Ronquist F, Teslenko M, van der Mark P, Ayres DL, Darling A, Höhna S, Larget B, Liu L, Suchard MA, Huelsenbeck JP (2012) MrBayes 3.2: efficient Bayesian phylogenetic inference and model choice across a large model space. Systematic Biology 61: 539–542.

Seifert KA, Morgan-Jones G, Gams W, Kendrick B (2011) The genera of hyphomycetes. CBS-KNAW Fungal Biodiversity Centre, Utrecht, The Netherlands.

Silvestro D, Michalak I (2012) raxmlGUI: a graphical front-end for RAxML. Organisms Diversity & Evolution 12: 335–337.

Stamatakis A (2014) RAxML version 8: a tool for phylogenetic analysis and post-analysis of large phylogenies. Bioinformatics 30: 1312–1313. https://doi.org/10.1093/bioinformatics/btu033

Swofford DL (2002) PAUP*: Phylogenetic Analysis Using Parsimony and other methods, version 4.0 b10. Sinauer Associates.

Tamura K, Stecher G, Peterson D, Filipski A, Kumar S (2013) MEGA6: Molecular Evolutionary Genetics Analysis version 6.0. Molecular Biology and Evolution 30: 2725–2729. https://doi.org/10.1093/molbev/mst197

Vaidya G, Lohman DJ, Meier R (2011) SequenceMatrix: concatenation software for the fast assembly of multi-gene datasets with character set and codon information. Cladistics 27: 171–180. https://doi.org/10.1111/j.1096-0031.2010.00329.x

Vilgalys R, Hester M (1990) Rapid genetic identification and mapping of enzymatically amplified ribosomal DNA from several *Cryptococcus* species. Journal of Bacteriology 172: 4238–4246.

Wanasinghe DN, Phukhamsakda C, Hyde KD, Jeewon R, Lee HB, Gareth Jones EB, Tibpromma S, Tennakoon DS, Dissanayake AJ, Jayasiri SC, Gafforov Y, Camporesi E, Bulgakov TS, Ekanayake AH, Perera RH, Samarakoon MC, Goonasekara ID, Mapook A, Li W-J, Senanayake IC, Li J, Norphanphoun C, Doilom M, Bahkali AH, Xu J, Mortimer PE, Tibell L, Tibell S, Karunarathna SC (2018) Fungal diversity notes 709–839: taxonomic and phylogenetic contributions to fungal taxa with an emphasis on fungi on Rosaceae. Fungal Diversity 89: 1–236. https://doi.org/10.1007/s13225-018-0395-7

White TJ, Bruns T, Lee S, Taylor J (1990) Amplification and direct sequencing of fungal ribosomal RNA genes for phylogenetics. In: Innis MA, Gelfand DH, Sninsky JJ, White TJ (Eds) PCR protocols: a guide to methods and applications. Academic Press, California, 315–322.

Wijayawardene NN, Hyde KD, Lumbsch HT, Liu JK, Maharachchikumbura SSN, Ekanayaka AH, Tian Q, Phookamsak R (2018) Outline of Ascomycota: 2017. Fungal Diversity 88: 167–263. https://doi.org/10.1007/s13225-018-0394-8

Zhaxybayeva O, Gogarten JP (2002) Bootstrap, Bayesian probability and maximum likelihood mapping: exploring new tools for comparative genome analyses. BMC Genomics 3: 4–4. https://doi.org/10.1186/1471-2164-3-4

MycoKeys 51: 15–28 (2019)
doi: 10.3897/mycokeys.51.32775
http://mycokeys.pensoft.net

RESEARCH ARTICLE

A peer-reviewed open-access journal
MycoKeys
Launched to accelerate biodiversity research

Type studies of *Rossbeevera bispora*, and a new species of *Rossbeevera* from south China

Md. Iqbal Hosen[1,*], Xiang-Jing Zhong[2,*], Genevieve Gates[3], Takamichi Orihara[4], Tai-Hui Li[1]

1 *State Key Laboratory of Applied Microbiology Southern China, Guangdong Provincial Key Laboratory of Microbial Culture Collection and Application, Guangdong Institute of Microbiology, Guangzhou 510070, Guangdong, China* **2** *Administration of Guangdong Xiangtoushan National Nature Reserve, Huizhou 516001, Guangdong, China* **3** *Tasmanian Institute of Agriculture, Private Bag 98, Hobart, Tasmania 7001, Australia* **4** *Kanagawa Prefectural Museum of Natural History, 499 Iryuda, Odawarashi, Kanagawa 250-0031, Japan*

Corresponding author: *Md. Iqbal Hosen* (iqbalmyco@gmail.com); *Tai-Hui Li* (mycolab@263.net)

Academic editor: *M.P. Martín* | Received 1 January 2019 | Accepted 5 March 2019 | Published 15 April 2019

Citation: Hosen MI, Zhong X-J, Gates G, Orihara T, Li T-H (2019) Type studies of *Rossbeevera bispora*, and a new species of *Rossbeevera* from south China. MycoKeys 51: 15–28. https://doi.org/10.3897/mycokeys.51.32775

Abstract

The type of *Rossbeevera bispora* and additional collections from the type location and adjacent areas were studied. Molecular data for *R. bispora* derived from the new collections are provided. In addition, *R. griseobrunnea*, a new species of *Rossbeevera*, is described from Xiangtoushan National Nature Reserve, Guangdong Province of China. The new species is characterized by its globose to subglobose sequestrate basidiomata with grayish white to grayish brown pileus, pale bluish discoloration in some parts of the hymenophore when injured becoming rusty brown to dark brown after being exposed to the air, fusoid (star-shaped in cross section) basidiospores 17–20 × 9–12 µm, and subcutis elements in the pileus. Based on multi-locus (ITS+nrLSU+*tef1-a*+*rpb2*) molecular phylogenetic analyses, both species appear as sister to *R. paracyanea*. We present color photos, macro- and micro-description, SEM basidiospores, molecular affinities of the species and compare them with morphologically similar taxa within the genus. A key to the species known from northern and southern hemispheres is provided.

Keywords

Boletaceae, East Asia, multi-locus phylogeny, new taxon, taxonomy

* Contributed equally to this work.

Introduction

Rossbeevera T. Lebel & Orihara, a sequestrate ectomycorrhizal genus of Boletaceae, was erected in 2012 to accommodate *Chamonixia pachydermis* Zeller & C.W. Dodge as the type of the genus (Lebel et al. 2012). The genus represents a distinct monophyletic group in the subfamily Leccinoideae, and is strongly supported as a sister to another sequestrate genus *Turmalinea* Orihara & N. Maek. (Orihara et al. 2016). Species of *Rossbeevera* are easy to recognize in the field as they have rubbery sequestrate basidiomata, with or without bluish discoloration of either the pileus or the hymenophore and usually a thin pileipellis. Microscopically, they have a hymenium that is developed when the basidiomata is immature and collapses at maturity, and ornamented basidiospores with 3–5 longitudinal ridges (Lebel et al. 2012, Orihara et al. 2016).

Presently *Rossbeevera* includes 10 species (Lebel et al. 2012, Orihara et al. 2012, 2016), only known from Asia (China, Japan and Singapore/Malaysia) and Australasia (Australia and New Zealand). Prior to this study, two of them (*R. bispora* (B.C. Zhang & Y.N. Yu) T. Lebel & Orihara and *R. yunnanensis* Orihara & M.E. Sm.) were known from China (Zhang and Yu 1989, Orihara et al. 2012). In 2018, Orihara reported *R. yunnanensis* from Japan. Of the remaining eight species: four (*R. cryptocyanea* Orihara, *R. eucyanea* Orihara, *R. griseovelutina* Orihara and *R. paracyanea* Orihara) are known from Japan (Lebel et al. 2012; Orihara et al. 2016), two (*R. vittatispora* (G.W. Beaton, Pegler & T.W.K. Young) T. Lebel and *R. westraliensis* T. Lebel, Orihara & N. Maek) from Australia (Lebel et al. 2012), one (*R. pachydermis* (Zeller & C.W. Dodge) T. Lebel) (orthographic variant *R. pachyderma*) from New Zealand (Lebel et al. 2012) and one (*R. mucosa* (Petri) T. Lebel, Orihara & N. Maek.) from Singapore/Malaysia (Lebel et al. 2012, Orihara et al. 2016).

In this study, several collections of *Rossbeevera* resembling *R. bispora* have repeatedly been found in south China (Guangdong Province: Dinghushan Nature Reserve, a type locality of *R. bispora*; Baiyunshan Mountain, Tianluhu Park and Xiangtoushan National Nature Reserve). Among the collections examined in this study two of them appeared to be clearly different from *R. bispora* (although all collections were originally treated as *R. bispora*). Therefore, we studied the type material of *R. bispora* for comparison with the recent collections. A combination of morphological data and multi-locus phylogenetic analyses including sequences of the nuclear ribosomal internal transcribed spacer (ITS) region, nuclear ribosomal large subunit (nrLSU), translation elongation factor 1-α (*tef1-a*), and the second largest subunit of RNA polymerase II (*rpb2*) were used for the delimitation of a new species within the genus *Rossbeevera*.

Materials and methods

Sampling and morphological studies

The specimens were collected from south China (Guangdong Province: Dinghushan Nature Reserve, Tianluhu Park, Baiyunshan Mountain and Xiangtoushan National Nature Reserve). After being examined and described the dried specimens were depos-

ited in the Fungal Herbarium of the Guangdong Institute of Microbiology, Guangzhou, China (GDGM).

Macromorphological descriptions were based on field notes and photographs. Micromorphological observations were made from small pieces of dried specimens mounted in H_2O, 5% aqueous KOH (w/v), Congo Red and Melzer's solution. In the description of the basidiospore measurements, the notation [n/m/p] is used, which means *n* basidiospores from *m* basidiomata of *p* collections. Dimensions for basidiospores are given as (a–)b–c(–d), in which 'b–c' contains a minimum of 90% of the measured values and extreme values 'a' and 'd' are given in parentheses, whenever necessary. Q denotes the length/width ratio of a measured basidiospore, Q_m denotes the average of *n* basidiospores, and SD is their standard deviation. Results are presented as $Q_m \pm SD$. For describing the species, we used the taxonomic terminology pileus for 'peridium', hymenophore for 'gleba' and stipe for 'columella'.

Molecular studies

Protocols for genomic DNA extraction, PCR amplification, and sequencing followed Hosen et al. (2013) and references therein. The ITS1-F/ITS4 (White et al. 1990), LROR/LR5 (Vilgalys and Hester 1990), ef1-983F/ef1-1567R (Rehner and Buckley 2005) and rpb2-B-F/rpb2-B-R (Wu et al. 2014) primer pairs were used for the amplification of ITS, nrLSU, *tef1-a* and *rpb2* regions.

Currently molecular data are available for eight of the 10 reported species. The final dataset consisted of 10 species of *Rossbeevera* including *R. bispora* and a new species (see taxonomy). Representative sequences (ITS, nrLSU, *tef1-a* and *rpb2*) of *Rossbeevera* and its allied genera from the subfamily Leccinoideae were retrieved from GenBank. Individual gene fragments were aligned in MAFFT v.6.8 (Katoh et al. 2005), and manually edited in BioEdit v.7.0.9 (Hall 1999) using default settings. Prior to concatenating the multi-locus (ITS+nrLSU+*tef1-a*+*rpb2*) dataset, an individual aligned dataset was analyzed separately to detect the topologies (BS ≥70%). There was no significant incongruence detected while reconstructing ITS, nrLSU or ITS+nrLSU/ITS+nrLSU+*tef1-a* except for the individual dataset of *tef1-a* and *rpb2* (because of the lack of representative *tef1-a* and *rpb2* sequences for *Rossbeevera* species) phylogenetic trees. A multi-locus dataset was built using Phyutility (Smith and Dunn 2008) for further phylogenetic analyses, and the resulting dataset was deposited in TreeBASE (S23404). Maximum Likelihood (ML) was used to analyze the multi-locus dataset. ML was performed in RAxML v.7.2.6 (Stamatakis 2006) with default settings. Statistical support values were obtained using nonparametric bootstrapping (BS) with 1000 replicates.

Results

Molecular phylogenetic results

In this study, 15 new sequences were generated from the Chinese collections of *Rossbeevera* and deposited in GenBank (Table 1). The combined aligned dataset included

Table 1. List of fungal taxa of Boletaceae with voucher number, country of origin and GenBank accession numbers used in the molecular phylogeny.

Name of the species	Voucher/collection no.	Country	GenBank accession number			
			ITS	nrLSU	*tef1-α*	*rpb2*
Borofutus dhakanus	HKAS 73785*	Bangladesh	JQ928605	JQ928615	JQ928577	JQ928596
Leccinellum sp.	KPM-NC-0018041	Japan	–	KC552053	KC552094	–
Leccinum scabrum	KPM-NC-0017840	Japan	KC552012	JN378515	JN378455	–
Leccinum versipelle	KPM-NC-0017833	Japan	–	JN378514	JN378454	–
Octaviania decimae	KPM-NC-0017763	Japan	JN257991	JN378465	JN378409	–
Octaviania tasmanica	MEL2341996	Australia	KC552004	JN378495	JN378436	–
Retiboletus sinensis	HKAS 59832	China	–	KT990633	KT990827	KT990464
Rhodactina himalayensis	CMU25117	Thailand	–	–	MG212603	–
Rhodactina rostratispora	OR1055	Thailand	–	–	MG212604	MG212644
Rossbeevera westraliensis	Trappe14692	Australia	HQ647131	HQ647153	–	–
Rossbeevera bispora	GDGM 45612	China	**MK035705**	**MK036346**	–	**MK350308**
Rossbeevera bispora	GDGM 45639	China	–	**MK036347**	–	**MK350309**
Rossbeevera bispora	GDGM 46631	China	**MK035705**	**MK036348**	–	–
Rossbeevera bispora	GDGM 46638	China	–	**MK036349**	–	–
Rossbeevera cryptocyanea	KPM-NC0023387	Japan	KP222893	KP222899	KP222913	–
Rossbeevera eucyanea	KPM-NC-0018043	Japan	KC551983	KC552029	KC552071	–
Rossbeevera eucyanea	TNS-F-36986*	Japan	HQ693875	HQ693880	KC552068	–
Rossbeevera griseobrunnea	GDGM 45266	China	**MH532533**	**MH537792**	–	**MK350310**
Rossbeevera griseobrunnea	GDGM 45913*	China	**MH532534**	**MH537793**	**MK350307**	**MK350311**
Rossbeevera griseovelutina	TNS-F-36989*	Japan	HQ693876	KC552031	KC552076	–
Rossbeevera griseovelutina	TNS-F-36991	Japan	KC551985	KC552032	KC552077	–
Rossbeevera pachydermis	MEL2079350	New Zealand	HQ647138	HQ647157	–	–
Rossbeevera pachydermis	PDD:89084	New Zealand	GU222301	–	–	–
Rossbeevera paracyanea	KPM-NC-0018023	Japan	KC551988	KC552035	–	–
Rossbeevera paracyanea	KPM-NC0023940	Japan	KP222894	–	–	–
Rossbeevera vittatispora	MEL2329434	Australia	KJ001084	KJ001097	KJ001075	–
Rossbeevera vittatispora	TO-AUS-72	Australia	KC551977	KC552025	KC552065	–
Rossbeevera westraliensis	MEL2231712	Australia	HQ647140	HQ647162	–	–
Rossbeevera yunnanensis	HKAS 70689*	China	–	JN979437	–	–
Rossbeevera yunnanensis	KPM-NC 23352	Japan	MF357925	MF354015	–	–
Spongiforma squarepantsii	LHFB14	Malaysia	HQ724511	HQ724509	–	–
Spongiforma thailandica	DED7873*	Thailand	EU685113	EU685108	KF030436	KF030387
Turmalinea chrysocarpa	HKAS 70601*	China	–	KF112448	–	KF112729
Turmalinea mesomorpha subsp. *sordida*	KPM-NC-0018015*	Japan	KC552001	KC552049	KC552092	–
Turmalinea persicina	KPM-NC-0018001*	Japan	KC551991	KC552038	KC552082	–

Highlighted in bold are newly generated sequences in this study. *holotype. En dash (–) indicates information is not available.

35 specimens from 24 species in the Boletaceae (10 of *Rossbeevera*, three of *Turmalinea*, two each of *Leccinum* Gray, *Octaviania* Vittad., *Rhodactina* Pegler & T.W.K. Young and *Spongiforma* Desjardin, Manfr. Binder, Roekring & Flegel, and one each of *Borofutus* Hosen & Zhu L. Yang, *Leccinellum* Bresinsky & Manfr. Binder and *Retiboletus* Manfr. Binder & Bresinsky). The combined alignment contained 3928 nucleotide sites (gaps included) for each sample, of which 1118 were ITS, 916 were nrLSU, 1128 were *tef1-a* and 766 were *rpb2*. *Rossbeevera bispora* is nested in a clade containing *R. paracyanea* and *R. griseobrunnea* with strong support (95% ML BS, Fig. 1). Two collections of *R. griseobrunnea* (GDGM 45266 and GDGM 45913) formed a monophyletic clade and sister to the Japanese *R. paracyanea* with moderate support (68% ML BS, Fig. 1). Interestingly, these three East Asian species formed a sister clade with the Australasian

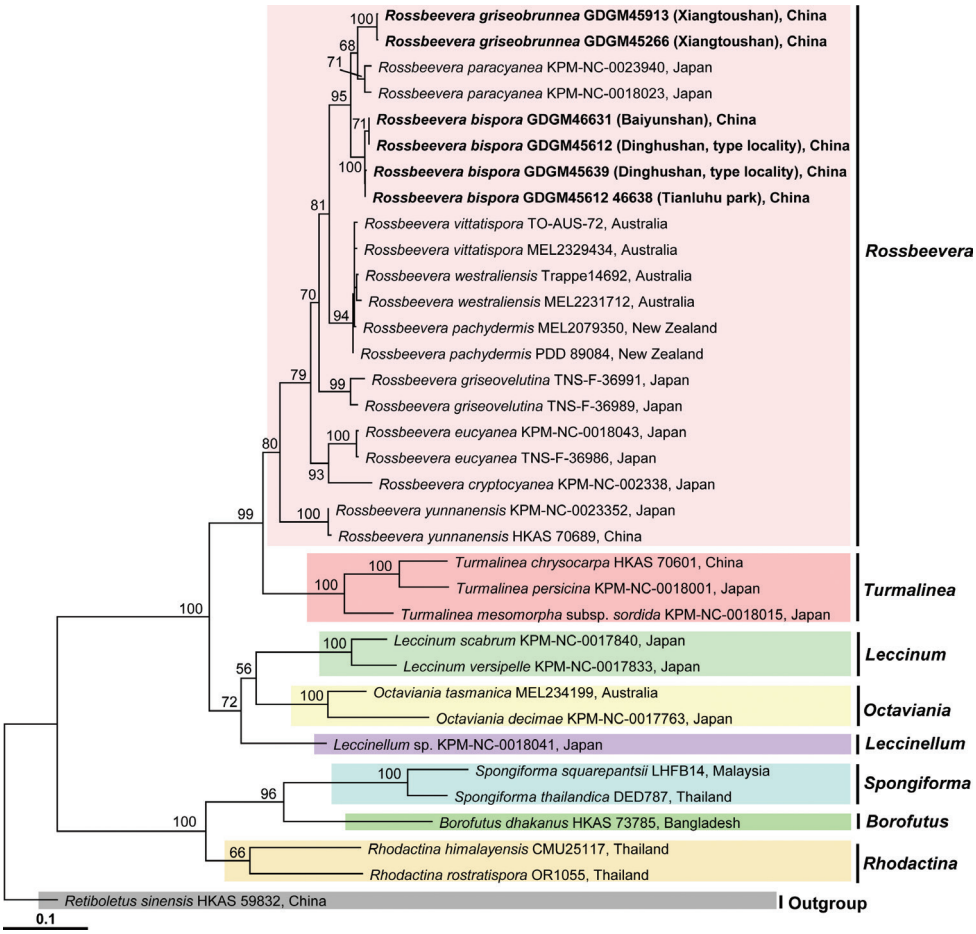

Figure 1. Phylogenetic relationships of *Rossbeevera* and its allied genera inferred from multi-locus (ITS+nrLSU+*tef1-a*+*rpb2*) analyses. *Rossbeevera bispora* and *R. griseobrunnea* are highlighted in bold on the tree. RAxML bootstrap (BS) support values (ML BS>50%) are indicated on the branches at nodes. Voucher number/collection number are provided after each species followed by country name.

Rossbeevera species including *R. westraliensis*, *R. vittatispora* and *R. pachydermis* with moderate strong support (81% ML BS, Fig. 1). The summarized result of the phylogenetic analysis is presented in Fig. 1.

Taxonomy

Rossbeevera bispora **(B.C. Zhang & Y.N. Yu) T. Lebel & Orihara, Fungal Diversity 52(1): 58 (2012)**

Figs 2, 3, 6a, b

≡ *Chamonixia bispora* B.C. Zhang & Y.N. Yu, Mycotaxon 35(2): 278 (1989).

Figure 2. Type specimen of *Rossbeevera bispora* (as *Chamonixia bispora,* GDGM 5688, holotype) **a** dried basidiomata of *Rossbeevera bispora* **b** basidiospores.

Description. *Basidiomata* hypogeous, 25–45 mm broad, 20–30 mm high, small, globose to subglobose, napiform, sometimes deformed or reniform, fleshy when fresh, firm when dry. *Pileus* thin, surface glabrous to slightly velvety in some cases, shiny, sometimes alveolate or cracking with age, dull white, grayish white to grayish brown, whitish at the lower portion, turning blue to deep blue when touched or injured or when mature, occasionally basal part covered with yellowish white mycelia. *Hymenophore* off-white, white to dull white when young, blue to dark blue immediately when cut or injured, fleshy, soft and smooth, composed of minute, irregular locules, becoming partially collapsed with many small empty chambers when dried. *Stipe* absent. *Sterile base* present but reduced, white, dull white to grayish white, somewhat dendroid or as a small basal pad or rhizomorph. *Odor and taste* not recorded.

Basidiospores [80/4/4] 16–21 × 9–11.5 µm [mean 18.55 × 10.58 µm, Q = 1.63–1.83(–1.90), Q_m = 1.75 ± 0.11], fusoid, ornamented with 4-longitudinal ridges (star-shaped in cross section), inamyloid, brown to dark brown in KOH and H_2O, thick-walled up to 2 µm thick, hilar appendages 1–3 µm long. *Basidia* 12–25 × 5–8 µm, narrowly clavate to cylindro- clavate, hyaline to pale yellow, usually 2-spored, occasionally 1-spored. Hymenial cystidia absent. *Hymenium* developed when immature but collapsed at maturity, hyaline to pale yellowish; subhymenium not developed. *Hymenophoral trama* 60–160 µm wide, subgelatinous, composed of hyaline, cylindrical, loosely interwoven to parallel, frequently branched, thin-walled, cylindrical hyphae 2–5 µm wide. *Pileipellis* a repent cutis, terminal cells short, clavate to cylindro-clavate, yellowish brown to brownish pigmented, smooth, thin-walled. *Clamp connections* absent in all tissues.

Habit and habitat. Solitary or in small groups beneath or on the ground, hypogeous or partially epigeous in a subtropical evergreen broad-leaved forest, putatively

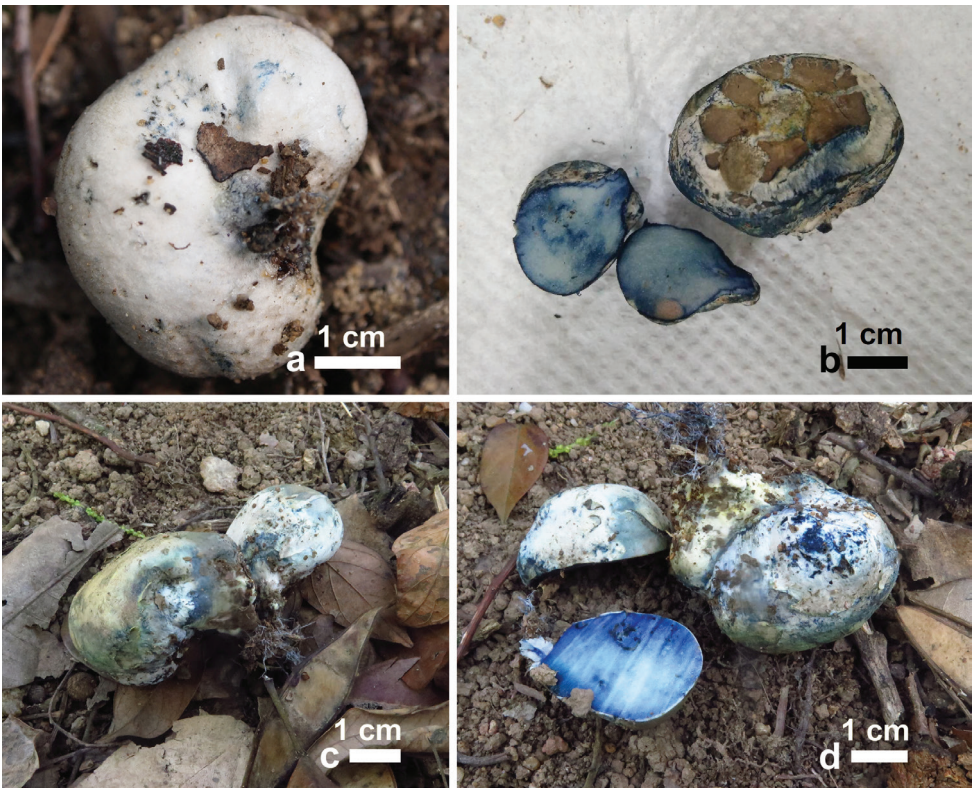

Figure 3. Basidiomata of *Rossbeevera bispora* (new collections). **a** Dull white to grayish brown pileus with blue tinges in some portion (GDGM 45612) **b** Bluing hymenophore (after injured) and pileus surface (GDGM 46631) **c** Bluing pileus with reduced stipe (GDGM 46638) **d** Bluing hymenophore (after injured) and pileus surface (GDGM 46638).

associated with *Castanopsis fissa* Rehder & E.H.Wilson, *C. chinensis* (Spreng.) Hance, *C. fabri* Hance and *Schima superba* Gardner & Champ.

Known distribution. Currently known from south China (Guangdong Province: (Baiyunshan Mountain, Dinghushan Nature Reserve and Tianluhu Park).

Specimens examined. CHINA. Guangdong Province, Zhaoqing City, Dinghushan Nature Reserve, 13 October 1982, You-Zao Wang, Wan-Ling Zhen, Jinag-Qing Li (GDGM 5688, holotype); 7 March 2013, Karl (GDGM 45612 and GDGM 45639); Baiyun Mountain, 7 April 2017, Yong He (GDGM 46631); Tianluhu Park, 21 March 2018, Tai-Hui Li, Chenghua Zhang, Xishen Liang (GDGM 46638).

Comments. Zhang and Yu (1989) described *R. bispora* as *Chamonixia bispora* B.C. Zhang & Y.N. Yu from south China (Dinghushan Nature Reserve, Guangdong Province) based on a single collection (Fig. 2). Lebel et al. (2012) transferred this species to *Rossbeevera* as it fits within the generic concept of *Rossbeevera*. This species is characterized by its whitish to grayish brown pileus turning bluish when injured, 2-spored basidia, and is associated with broad-leaved trees in south China.

Rossbeevera griseobrunnea **Iqbal Hosen & T.H.Li, sp. nov.**
MycoBank: MB826880
Figs 4, 5, 6c, d

Diagnosis. Basidiomata hypogeous, small; pileus grayish white to grayish brown, surface bluing slightly when injured; hymenophore dull white to very pale blue in some portion when injured, finally rusty brown to dark brown at maturity; stipe absent; basidiospores 17–20 × (8–)9–12 µm, fusoid, ornamented with 4-longitudinal ridges (star-shaped in cross section), brown to dark brown; pileipellis a subcutis, with terminal elements short cylindro-clavate.

Typification. CHINA. Guangdong Province, Boluo County, Xiangtoushan National Nature Reserve, 19 November 2015, Tai-Hui Li, Ting Li, Hao Huang & Jun-Ping Zhou (GDGM 45913, holotype).

Etymology. The epithet name '*griseobrunnea*' (Lat.) refers to the grayish brown pileus.

Description. *Basidiomata* hypogeous, 15–35 mm broad, 12–25 mm high, small, globose to subglobose, napiform, sometimes deformed or reniform, fleshy when fresh, firm when dry. *Pileus* very thin, surface glabrous to slightly velvety, shiny, grayish white to grayish brown, whitish at the lower portion, turning to pale blue when touched or injured. *Hymenophore* off-white, white to dull white when young, becoming pale blue to bluish in some parts/patches then rusty brown to dark brown when exposed to air for 3–5 minutes, often greenish brown around insect damage, firm, composed of minute, irregular locules, becoming partially collapsed with many small empty chambers when dried. *Stipe* absent. *Stipe* base present but reduced, white, dull white to grayish white, somewhat dendroid or as a small basal pad or rhizomorph. *Odor and taste* not recorded.

Basidiospores [50/2/2] 17–20(–21) × (8–)9–12(–13) µm [mean = 18.5 × 10.5 µm, Q = (1.52–)1.63–1.91(–2.1), Q_m = 1.81 ± 0.18] fusoid, ornamented with 4-longitudinal ridges (star-shaped in cross section) (up to 2.5 µm high), inamyloid, non-dextrinoid, brown to dark brown in KOH and H_2O, thick-walled up to 2 µm thick, hilar appendages 1.5–3 µm long. *Basidia* 15–27 × 5–9 µm, narrowly clavate to cylindro-clavate, hyaline to pale yellow, usually 2-spored, occasionally 1-spored; basidioles 18–25 × 8–10 µm, clavate to short clavate. *Hymenial* cystidia absent. *Hymenium* developed when immature but collapsed at maturity, hyaline to pale yellowish; subhymenium not developed. *Hymenophoral trama* 60–130 µm wide, subgelatinous, composed of hyaline, cylindrical, loosely interwoven to parallel, frequently branched, thin-walled, cylindrical hyphae 2–5 µm wide. *Pileipellis* a subcutis with terminal elements 15–20 × 7–9 µm, short clavate to cylindro-clavate, yellowish brown to brownish pigmented, smooth, thin-walled. *Clamp connections* absent in all tissues.

Additional specimen examined. CHINA, Guangdong Province, Boluo County, Xiangtoushan National Nature Reserve, 19 November 2015, Tai-Hui Li, Ting Li, Hao Huang & Jun-Ping Zhou (GDGM 45266).

Habit and habitat. Solitary or in small groups beneath or on the ground, hypogeous or partially epigeous in a subtropical evergreen broad-leaved forest, putatively associated with *Castanopsis fissa*, *C. chinensis*, *C. fabri* and *Schima superba*.

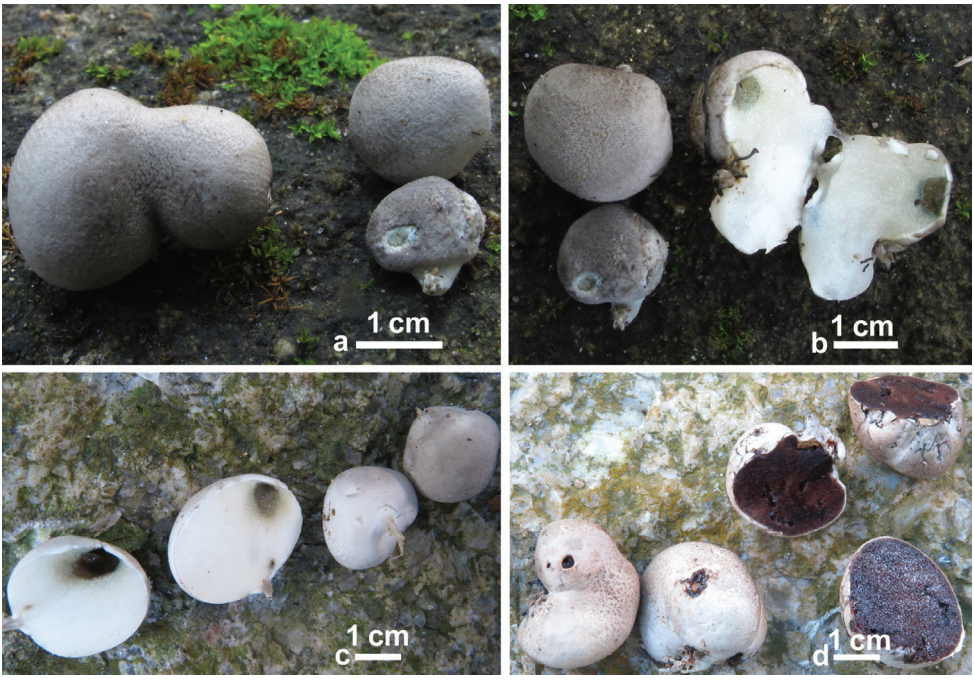

Figure 4. Basidiomata of *Rossbeevera griseobrunnea*. **a** Unchanged pileus surface with reduced stipe (GDGM 45266) **b** Unchanged pileus surface and pale blue (in some patches) hymenophore when injured (GDGM 45266) **c** Pale bluing hymenophore (after injured) with reduced stipe (GDGM 45913, holotype) **d** Dark brownish hymenophore after exposed to air (GDGM 45913, holotype).

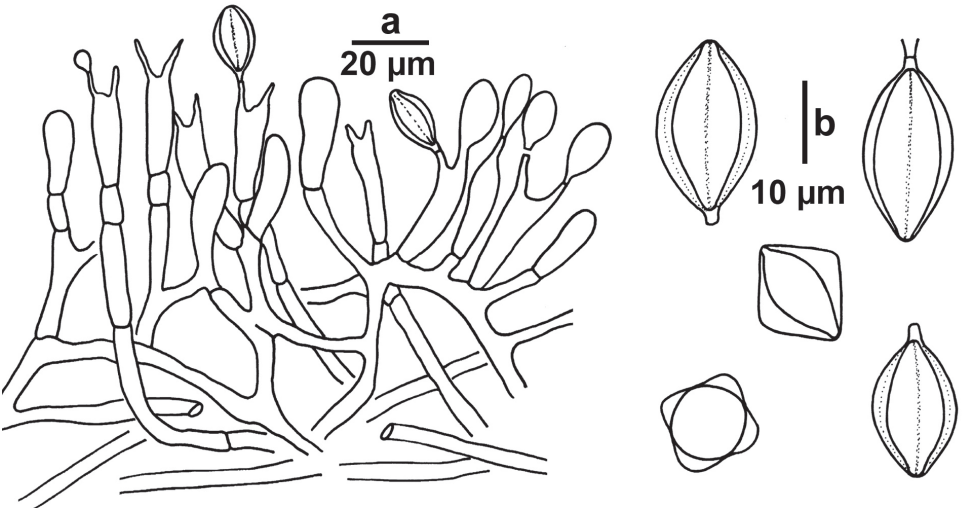

Figure 5. Microscopic features of *Rossbeevera griseobrunnea*. **a** Basidia and basidioles development at different stages (GDGM 45266) **b** Basidiospores in different views (star-shaped in side view and quadrangular in polar view) (GDGM 45913, holotype).

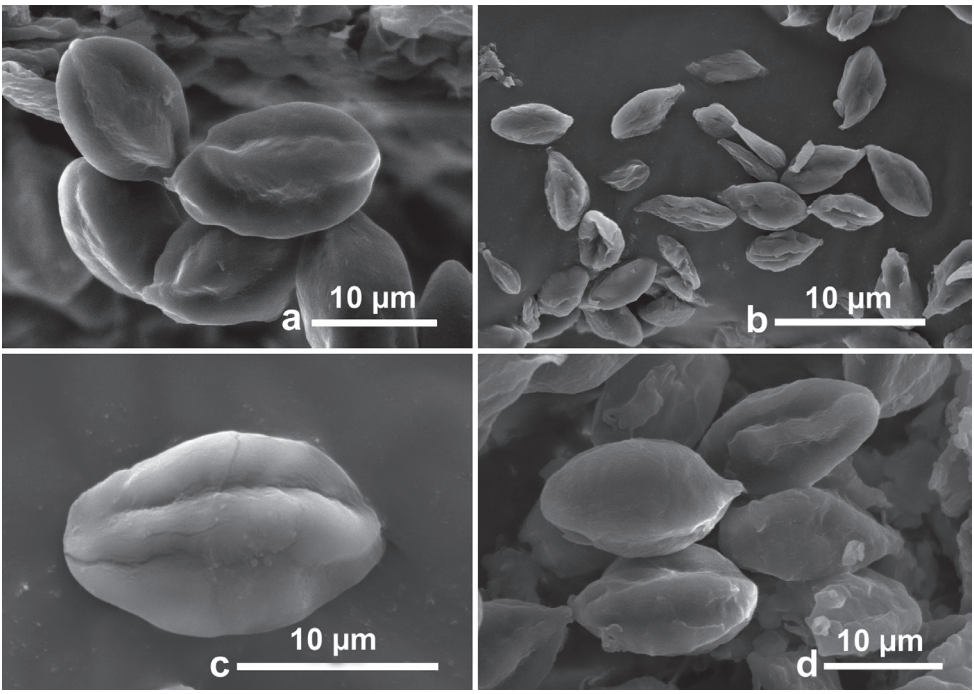

Figure 6. SEM of basidiospores of *Rossbeevera* species. **a, b** *Rossbeevera bispora* (**a** GDGM 45612 **b** GDGM 45639) **c, d** *Rossbeevera griseobrunnea* (**c** GDGM 45266 **d** GDGM 45913, holotype).

Known distribution. Currently known only from south China (Guangdong Province, Xiangtoushan National Nature Reserve).

Comments. The voucher specimen (GDGM 45266) was cited as *Rossbeevera* sp. by Hosen et al. (2018), while studying boletes from the Xiangtoushan National Nature Reserve, Guangdong Province, China. After morphological and molecular comparisons with other known species of *Rossbeevera* the voucher specimen (GDGM 45266) is described here as *R. griseobrunnea*. It is characterized by its dull white, grayish white to grayish brown basidiomata, with hymenophore that discolors very slowly in some portions (pale blue in some patches becoming rusty brown to dark brown) after being cut or injured, fusoid ornamented basidiospores with mostly 4-longitudinal ridges and subcutis elements (short clavate terminal cells) in the pileus.

Discussion

Most of the species within *Rossbeevera* share common features like globose to subglobose sequestrate basidiomata with bluish discoloration (due to oxidation of pulvinic acid) when injured (either pileus or hymenophore), usually 1–2-spored but sometimes 4-spored basidia, ornamented basidiospores with 4–5 longitudinal ridges (star-shaped in cross section), absence of hymenial cystidia (except *R. griseovelutina*), and loose ar-

rangement of hymenophoral trama with 2–5 µm wide hyphae. However, continental distance, habitat with different hosts, molecular data or genetic distance and some macro- and micro-morphological differences make them distinct species within *Rossbeevera*.

In the protologue, the basidiospore size of *R. bispora* is 15–21 × 10–12 µm (Zhang and Yu 1989). Our re-examination of the type material of *R. bispora* (GDGM 5688) showed that the basidiospore size is 16–21 × 10–12 µm [mean 18.35 × 11.02 µm, Q = [1.56–1.72(–1.81), Q_m = 1.66 ± 0.11], which is similar to that of the original description. The Q values [(1.63–1.83(–1.90), Q_m = 1.75 ± 0.11] of basidiospores derived from the new collections are slightly higher than the type material of *R. bispora*. However, the color changes of the pileus and hymenophore, 2-spored basidia and their association with broad-leaved trees suggest that the modern collections (including those from the type locality, Dinghushan Nature Reserve) are conspecific with *R. bispora*. Extraction of DNA sequences from the type material of *R. bispora* (GDGM 5688) was not successful due to the poor quality of the DNA from the aged specimen (collection date: October 13, 1982; Zhang and Yu 1989). For examination of evolutionary relationships within *Rossbeevera* and phylogenetic stability of this species we provide DNA sequences derived from the new collections. Prior to this study, *R. bispora* was known only from the type locality (Guangdong Province: Dinghushan Biosphere Reserve Forest), but we demonstrate it has a wide geographic distribution in south China (Guangdong Province: Baiyun Mountain and Tianluhu Park).

The rusty brown to dark brown or chocolate brown hymenophore (after exposure to air for 3–5 minutes or at maturity) in *R. griseobrunnea* occurs also in *R. vittatispora*, *R. pachydermis* and *R. griseovelutina* Orihara. However, *R. vittatispora*, originally described from Australia has a white to pale grayish to buff pileus staining greenish blue or indigo blue in some patches on the surface and shorter and narrower basidiospores measuring 9–12(–13) × 4–5.5(–6) µm (Lebel et al. 2012). *Rossbeevera pachydermis*, originally described from New Zealand, has a restricted distribution to that country and differs from the new species in having large basidiomata (up to 50 mm broad), relatively smaller basidiospores measuring 11–14 × 8–10 µm, and is mainly associated with *Nothofagus* (Lebel et al. 2012). The East Asian *R. griseovelutina* is distinctive on account of its velvety basidiomata, abundant hymenial cystidia, trichodermal elements in the pileus, and relatively longer basidiospores 14.4–31.9 × 6.7–10.4 µm (Lebel et al. 2012, Orihara et al. 2012). Phylogenetically, *R. paracyanea*, originally described from Japan, is a close sister species to *R. griseobrunnea* with moderate support value (68% ML BS, Fig. 1), but significantly differs from the latter species in having white to grayish basidiomata when young, becoming blue-gray to dark gray with age, an off-white hymenophore when young that turns indigo blue very quickly and strongly when touched or exposed to air, relatively narrower basidiospores (14–19.3 × 6.0–9.2 µm), and it occurs with *Quercus gilva* Blume and *Castanopsis cuspidata* Schottky (Orihara et al. 2016).

Besides the comparisons with the closely related species of *Rossbeevera*, two known Chinese species, *R. bispora* and *R. yunnanensis* can be compared with *R. griseobrunnea*. Both *R. griseobrunnea* and *R. bispora* share 2-spored basidia, brown to dark brown hymenophore at maturity, and are putatively associated with broad-leaved trees. However, *R. bispora* can be differentiated from *R. griseobrunnea* by the deep bluing reaction of the pileus and hymenophore when bruised or exposed to air (Zhang and Yu 1989) and it

is also a phylogenetically distinct species (Fig. 1). *Rossbeevera yunnanensis*, known as the earliest divergence lineage within *Rossbeevera*, is distinguished from *R. griseobrunnea* in having a very thin, whitish pileus which becomes blue-green when injured and a reddish brown to blackish brown hymenophore at maturity (Orihara et al. 2012, Orihara 2018). Apart from China, *R. yunnanensis* is known also from Japan which is about 3150 km from the type locality (Chuxiong, Yunnan Province, China vs Hiroshima Prefecture, Japan) (Orihara 2018), suggesting that the species has a wide geographic distribution.

Key to the taxa *Rossbeevera* known from Northern Hemisphere (China, Japan and Singapore/Malaysia) and Southern Hemisphere (Australia and New Zealand)

1 Geographical distribution- Southern Hemisphere (Australasia) **2**
– Geographical distribution- Northern Hemisphere (Asia) **4**
2 Distributed in Australia, basidiospores within 9–15 × 3–6 µm **3**
– Distributed in New Zealand, basidiospores 11–14 × 8–10 µm, associated with mainly *Nothofagus* spp., no grayish tints on the surface ..... ***R. pachydermis***
3 Basidiospores 12–14 × 3–4.5 µm, basidiomata turn deep blue on bruising, restricted to western Australia ..... ***R. westraliensis***
– Basidiospores 9–12 × 4–5.5 µm, basidiomata turn blue to deep blue in some patches, widespread in eastern Australia ..... ***R. vittatispora***
4 Distributed in East Asia **5**
– Distributed in Southeast Asia (Singapore/Malaysia), (13–)15–17 × (7–)8–9 µm, with Q values = 1.76–2.05 ..... ***R. mucosa***
5 Distributed in both Japan and China ..... ***R. yunnanensis***
– Distributed either in Japan or China **6**
6 Basidia constantly 1 or 2-spored, either dark/strong or partial bluing pileus and hymenophore **7**
– Basidia 2-, 3-and 4-spored, bluing pileus and hymenophore **8**
7 Pileus and hymenophore not bluing or partially pale bluing when injured or exposed to air, turn rusty brown to dark brown after exposure to air for a long time, found in China ..... ***R. griseobrunnea***
– Pileus and hymenophore bluing, basidiospores 15–21 × 10–12 µm, found in China ..... ***R. bispora***
8 Strong bluing reaction, basidiospores mean 5–18 × 6.5–9.4 µm **9**
– Strong bluing reaction, velvety pileus, cystidia present, basidiospores mean >22.2 × 8.7 µm, found in Japan ..... ***R. griseovelutina***
9 Hilar appendages (HA) 1.6–3.2 µm, basidiospores Q_m = 1.9, found in Japan ..... ***R. eucyanea***
– Hilar appendages 2.1–5.9 µm, basidiospores Q_m = 2.1–2.4 ..... **10**
10 Hilar appendages 2.1–4.5 µm, basidiospores 14–19.3 × 6.9–9.2 µm (mean 16.7 × 8 µm), found in Japan ..... ***R. paracyanea***
– Hilar appendages 2.4–5.9 µm, basidiospores 13.4–18.3 × 5.8–7.3 µm (mean 15.8 × 6.5), found in Japan ..... ***R. cryptocyanea***

Acknowledgements

This work was supported by the 11th Special Fund of the China Postdoctoral Science Foundation (No. 2018T110854), the GDAS' Special Project of Science and Technology Development (2019GDASYL-0104011), the China Postdoctoral Science Foundation (No. 2017M610514, 61st phase) and the NSFC Research Fund for International Young Scientists (No. 31750110476) to the first author (MIH). Thanks to Mr. Xishen Liang (Guangdong Institute of Microbiology, Guangzhou, China) for conducting partial molecular experiment. Mr. Ting Li, Mr. Huang Hao, Mr. Jun-ping Zhou and Yong He (Guangdong Institute of Microbiology, Guangzhou, China) are acknowledged for providing the voucher specimens. The authors also thank the reviewers for the suggestions and corrections to improve this work.

References

Hall TA (1999) BioEdit: a user-friendly biological sequence alignment editor and analysis program for Windows 95/98/NT. Nucleic Acids Symposium Series 41: 95–98.

Hosen MI, Feng B, Wu G, Zhu XT, Li YC, Yang ZL (2013) *Borofutus*, a new genus of Boletaceae from tropical Asia: phylogeny, morphology and taxonomy. Fungal Diversity 58: 215–226. https://doi.org/10.1007/s13225-012-0211-8

Hosen MI, Zhong XJ, Li T, Zhang M, Li TH (2018) Exploration of boletes from Xiangtoushan National Nature Reserve, Guangdong Province, China. Open Access Journal of Mycology & Mycological Sciences 1: 000101.

Katoh K, Kuma K, Toh H, Miyata T (2005) MAFFT version 5: improvement in accuracy of multiple sequence alignment. Nucleic Acids Research 33: 511–518. https://doi.org/10.1093/nar/gki198

Lebel T, Orihara T, Maekawa N (2012) The sequestrate genus *Rossbeevera* T. Lebel & Orihara gen. nov. (Boletaceae) from Australasia and Japan: new species and new combinations. Fungal Diversity 52: 49–71. https://doi.org/10.1007/s13225-011-0109-x

Orihara T (2018) First report of a rare sequestrate fungus, *Rossbeevera yunnanensis* (Boletaceae, Boletales) from Japan. Truffology 1: 5–8.

Orihara T, Lebel T, Ge ZW, Smith ME, Maekawa N (2016) Evolutionary history of the sequestrate genus *Rossbeevera* (Boletaceae) reveals a new genus *Turmalinea* and highlights the utility of ITS minisatellite-like insertions for molecular identification. Persoonia 37: 173–198. https://doi.org/10.3767/003158516X691212

Orihara T, Smith ME, Ge ZW, Maekawa N (2012) *Rossbeevera yunnanensis* (Boletaceae, Boletales), a new sequestrate species from southern China. Mycotaxon 120: 139–147. https://doi.org/10.5248/120.139

Rehner SA, Buckley EP (2005) A *Beauveria* phylogeny inferred from nuclear ITS and *EF1-a* sequences: evidence for cryptic diversification and links to *Cordyceps* teleomorphs. Mycologia 97:84–98.

Smith SA, Dunn CW (2008) Phyutility: a phyloinformatics tool for trees, alignments and molecular data. Bioinformatics 24: 715–716. https://doi.org/10.1093/bioinformatics/btm619

Stamatakis A (2006) RAxML-VI-HPC: maximum likelihood-based phylogenetic analyses with thousands of taxa and mixed models. Bioinformatics 22: 2688–2690. https://doi.org/10.1093/bioinformatics/btl446

Vilgalys R, Hester M (1990) Rapid genetic identification and mapping of enzymatically amplified ribosomal DNA from several *Cryptococcus* species. Journal of Bacteriology 172: 4238–4246. https://doi.org/10.1128/jb.172.8.4238-4246.1990

White TJ, Bruns T, Lee S, Taylor J (1990) Amplification and direct sequencing of fungal ribosomal RNA genes for phylogenetics. In: Innis MA, Gelfand DH, Sninsky JJ, White TJ (Eds) PCR Protocols: a guide to methods and applications. Academic Press, San Diego, 315–322. https://doi.org/10.1016/B978-0-12-372180-8.50042-1

Wu G, Feng B, Xu J, Zhu XT, Li YC, Zeng NK, Hosen MI, Yang ZL (2014) Molecular phylogenetic analyses redefine seven major clades and reveal 25 new generic lineages in the fungal family Boletaceae. Fungal Diversity 69: 93–115. https://doi.org/10.1007/s13225-014-0283-8

Zhang BC, Yu YN (1989) *Chamonixia bispora* sp. nov. (Boletales) from China. Mycotaxon 35: 277–281.

MycoKeys 51: 29–53 (2019)
doi: 10.3897/mycokeys.51.31957
http://mycokeys.pensoft.net

RESEARCH ARTICLE

A peer-reviewed open-access journal
MycoKeys
Launched to accelerate biodiversity research

Myrothecium-like new species from turfgrasses and associated rhizosphere

Junmin Liang[1,*], Guangshuo Li[1,2,*], Shiyue Zhou[3], Meiqi Zhao[4,5], Lei Cai[1,3]

1 *State Key Laboratory of Mycology, Institute of Microbiology, Chinese Academy of Sciences, Beichen West Road, Chaoyang District, Beijing 100101, China* **2** *College of Life Sciences, Hebei University, Baoding, Hebei Province, 071002, China* **3** *College of Life Sciences, University of Chinese Academy of Sciences, Beijing 100049, China* **4** *College of Plant Protection, China Agricultural University, Beijing 100193, China* **5** *Forwardgroup Turf Service & Research Center, Wanning, Hainan Province, 571500, China*

Corresponding author: *Lei Cai* (cail@im.ac.cn)

Academic editor: *I. Schmitt* | Received 27 November 2018 | Accepted 26 February 2019 | Published 18 April 2019

Citation: Liang J, Li G, Zhou S, Zhao M, Cai L (2019) Myrothecium-like new species from turfgrasses and associated rhizosphere. MycoKeys 51: 29–53. https://doi.org/10.3897/mycokeys.51.31957

Abstract

Myrothecium sensu lato includes a group of fungal saprophytes and weak pathogens with a worldwide distribution. *Myrothecium* s.l. includes 18 genera, such as *Myrothecium*, *Septomyrothecium*, *Myxospora*, all currently included in the family Stachybotryaceae. In this study, we identified 84 myrothecium-like strains isolated from turfgrasses and their rhizosphere. Five new species, i.e., *Alfaria poae*, *Alf. humicola*, *Dimorphiseta acuta*, *D. obtusa*, and *Paramyrothecium sinense*, are described based on their morphological and phylogenetic distinctions. Phylogenies were inferred based on the analyses of sequences from four DNA loci (ITS, *cmdA*, *rpb2* and *tub2*). The generic concept of *Dimorphiseta* is broadened to include a third type of seta, i.e. thin-walled, straight with obtuse apices.

Keywords

Stachybotryaceae, soil fungi, turfgrass disease, multi-locus phylogeny, cup-shaped sporodochia

Introduction

Myrothecium was first introduced by Tode (1790) based on *M. inundatum*. The typical characters of these fungi are cup-shaped sporodochia covered by a mass of slimy, green to black conidia. The generic concept of *Myrothecium* has been emended several times

* These authors contributed equally to this study.

(Link 1809; von Höhnel 1905; Pidoplichko and Kirilenko 1971). Decock et al. (2008) reported that the genus *Myrothecium* is not monophyletic based on internal transcribed spacer regions and the intervening 5.8S rDNA (ITS). Chen et al. (2015) re-evaluated the phylogeny of *Myrothecium* based on ITS and elongation factor 1-alpha (EF1-α) gene sequences, suggesting the polyphyly of *Myrothecium* within Stachybotryaceae. These studies did not make taxonomic conclusions accordingly. Lombard et al. (2016) constructed a backbone tree of *Myrothecium* s.l. based on a multi-locus phylogeny and resolved *Myrothecium* s.l. to 18 genera including 13 new genera introduced. Under the current concept of *Myrothecium* sensu stricto, only two species were included, *M. inundatum* and *M. simplex* (Lombard et al. 2016).

Most myrothecium-like species are saprobes in soils (Ellis and Ellis 1985). Many species were named referring to their substrates such as *Alfaria terrestris*, *Albifimbria terrestris*, *Simorphiseta terrestris* and *Parvothecium terrestre.* Some species were also reported as weak plant pathogens. For instance, *Paramyrothecium roridum* (syn. *Myrothecium roridum*) can infect coffee plants, causing bark canker (Tulloch 1972). *Albifimbria verrucaria* (syn. *Myrothecium verrucaria*) is pathogenic to mulberry causing leaf spot (Murakami et al. 2005). In addition, myrothecium-like species are also well-studied for their natural compounds, which are able to inhibit the activity of liver cancer and tumors (Pope 1944; Okunowo et al. 2010). Some myrothecium-like species can also produce a cocktail of secondary metabolites, which have strong antifungal and antibiotic activity (Kobayashi et al. 2004; Liu et al. 2006; Ruma et al. 2015). Hereto, more than 50 of these bioactive compounds have been reported from *P. roridum* and *Alb. verrucaria* (Wagenaar and Clardy 2001).

In a survey of turfgrass diseases from 2017, a number of myrothecium-like strains were collected from leaves and roots of turfgrasses and their rhizosphere. The aim of this study was to characterize these strains based on morphology and molecular phylogenetic analyses.

Materials and methods

Fungal isolates

From May 2017 to March 2018, turfgrass diseases were investigated on cold-season species in Beijing and on warm-season species in Hainan Province. Atotal of 130 samples were collected. Each sample was treated as an underground part of soil sample and a ground part of diseased grasses. Soil samples were isolated following the modified dilution plate method (Zhang et al. 2017). Five grams of each soil sample were suspended in 30 mL sterile water in a 50 mL bioclean centrifuge tube. The suspension was mixed thoroughly using Vortex-Genie 2 (Scientific Industries, New York) with maximum speed and then diluted to a series of concentration, i.e., 10^{-1}, 10^{-2}, 10^{-3} and 10^{-4}. The 100 μL suspensions of each concentration were spread on to antibiotic potato dextrose agar (PDA, 4 g potato starch, 5 g dextrose and 15 g agar, 50 mg ampicillin

and streptomycin sulfate in 1 L sterile water). The first few samples suggested that 10^{-2} was the best-diluted concentration for colony pickup. Diseased samples were isolated following a tissue isolation protocol (Chen et al. 2015). All plates were incubated at room temperature (23–25 °C) for 3–4 weeks, and from which all single colonies were picked up and transferred to clean PDA plates. Purified strains were stored at 4 °C for further studies. For phylogenetic analysis, associated sequences of 73 myrothecium-like strains and one outgroup strain were retrieved from GenBank (NCBI, https://www.ncbi.nlm.nih.gov/; Table 1).

Morphology and culture characteristics

Descriptions of macromorphological features are based on 7-d old materials incubated in the dark at room temperature (20–25 °C) and grown on potato dextrose agar (2% w/w; PDA), oatmeal agar (OA), cornmeal agar (CMA) and synthetic low-nutrient agar (SNA; Nirenberg 1981). Color description followed the color guide by Kornerup and Wanscher (1978). Digital images of colonies were made with a Nikon Eclipse 80i light microscope (Tokyo, Japan) with differential interference contrast (DIC) illumination and a LV2000 digital camera (Beijing, China). Slides mounted in clear lactic acid were also prepared to observe conidiogenesis, conidiophores and conidia.

DNA extraction and PCR amplification

Genomic DNA was extracted from 1–2 weeks' old cultures grown on potato dextrose agar (2% w/w; PDA) incubated at room temperature using a modified Cetyltrimethyl Ammonium Bromide (CTAB) method (Rogers and Bendich 1994). Partial sequences of four genes, ITS, RNA polymerase II second largest subunit (*rpb2*), *β-tubulin* (*tub2*) and calmodulin (*cmdA*) gene sequences were amplified using the following pairs of primers, ITS1 and ITS4 (White et al. 1990) for ITS, RPB2-5F2 and RPB2-7cR (O'Donnell et al. 2007) for *rpb2*, Bt2a and Bt2b (Glass and Donaldson 1995) for *tub2* and CAL-228F (Carbone and Kohn 1999) and CAL2Rd (Groenewald et al. 2013) for *cmdA.* Amplification for each locus followed the PCR protocols as described in Lombard et al. (2016). The PCR was performed in a 25 μL reaction volume including 2.5 μL 10 × PCR Buffer (Dingguo, Beijing, China), 2 mM $MgCl_2$, 50 μM dNTPs, 0.1 μM of each primer, 0.5 U Taq DNA polymerase and 10 ng genomic DNA. PCR reactions were conducted in ProFlex™ PCR system (Applied Biosystems, California, USA) under the following reaction conditions: predenaturation at 94 °C for 5 min, followed by 35 cycles of denaturation at 94 °C for 30 s, annealing at 52 °C (for ITS) or 54 °C (for *rpb2* and *cmdA*) or 56 °C (for *tub2*) for 40 s and elongation at 72 °C for 1 min, a final elongation at 72 °C for 5 min.

The purified PCR products were sequenced in both forward and reverse directions on an ABI-3730 XL DNA Analyzer (Applied Biosystems, California, USA). The se-

Table 1. Strains and NCBI GenBank accessions used in the phylogenetic analyses.

Species	Isolate no. [a]	Host/Substrate	Country	NCBI accession numbers			
				cmdA	**ITS**	***tub2***	***rpb2***
Myrothecium simplex	CBS 582.93^{T}	Decaying agaric	Japan	KU846439	NR145079	KU846537	–
	CBS 100287	*Russula nigricans*	Japan	KU846440	KU846457	KU846538	–
M. inundatum	CBS 275.48^{T} = IMI 158855	*Russula adusta*	England	KU846435	KU846452	KU846533	–
	CBS 116539	Agaric	Canada	KU846437	KU846454	KU846535	–
Albifimbria lateralis	CBS117712^{T}	Unknown	USA	KU845865	KU845881	KU845957	KU845919
Alb. terrestris	CBS 1261^{8}6T	Soil in mopane woodlands	Namibia	KU845867	KU845883	KU845959	KU845921
	CBS 109378 = NRRL 31066	Dead hardwood	USA	KU845866	KU845882	KU845958	KU845920
	CBS 127838	Soil	Namibia	KU845868	KU845884	KU845960	KU845922
	LC12196	rhizosphere soils of *Poa* sp.	China	MK500260	MK478879	MK500277	–
Alb. verrucaria	CBS 328.52^{T} = NRRL 2003 = ATCC 9095	deteriorated baled cotton	USA	KU845875	KU845893	KU845969	KU845931
	CBS 189.46 = IMI 140060	*Solanum tubersum*	Cyprus	KU845872	KU845889	KU845965	KU845927
	LC12191	Rhizosphere soils of *Poa* sp.	China	MK500255	MK478874	MK500272	MK500264
	LC12192	Rhizosphere soils of *Poa* sp.	China	MK500256	MK478875	MK500273	MK500265
	LC12193	Rhizosphere soils of *Poa* sp.	China	MK500257	MK478876	MK500274	MK500266
	LC12194	Rhizosphere soils of *Poa* sp.	China	MK500258	MK478877	MK500276	MK500267
	LC12195	Rhizosphere soils of *Poa* sp.	China	MK500259	MK478878	MK500275	MK500268
Alb. viridis	CBS 449.71^{T} = BCC 37540	Unknown	India	KU845879	KU845898	KU845974	KU845936
	CBS 127346	Soil	USA	KU845880	KU845899	KU845975	KU845937
Alfaria. ossiformis	CBS 324.^{5}4T	Prairie soil	USA	KU845977	KU845984	KU846015	KU846002
***Alf. humicola* sp. nov.**	CGMCC3.19213^{T} = LC12143	Rhizosphere soils of *Poa* sp.	Beijing, China	MH885432	MH793291	MH793317	MH818829
	LC12144	Rhizosphere soils of *Poa* sp.	Beijing, China	MH885434	MH793293	MH793318	MH818830
***Alf. poae* sp. nov.**	CGMCC3.19198^{T} = LC12140	Leaves of *Poa* sp.	Hainan, China	MH885419	MH793278	MH793314	MH818826
	LC12141	Rhizosphere soils of *Poa* sp.	Hainan, China	MH885420	MH793279	MH793315	MH818828
	LC12142	Rhizosphere soils of *Poa* sp.	Hainan, China	MH885421	MH793280	MH793316	MH818827
Alf. putrefolia	CBS 112037^{T}	Rotten leaf	Brazil	–	KU845985	KU846016	KU846003
	CBS 112038	Rotten leaf	Brazil	–	KU845986	KU846017	KU846004
Alf. terrestris	CBS 477.91^{T}	Soil	Turkey	KU845979	KU845988	KU846019	KU846006
Alf. thymi	CBS 447.83^{T}	*Thymus serpyllum*	The Netherlands	KU845981	KU845990	KU846021	–
Capitofimbria compacta	CBS 111739^{T}	Decaying leaf	Brazil	KU846261	KU846287	KU846404	KU846349
	MUCL 50238	Bark	Zimbabwe	–	KU878556	KU878559	KU878558
Dimorphiseta terrestris	CBS 127345^{T}	Soil collected in *tallgrass prairie*	USA	KU846284	KU846314	KU846431	KU846375
***D. acuta* sp. nov.**	CGMCC3.19208^{T} = LC12122	Rhizosphere soils of *Poa pratensis*	Beijing, China	MH885429	MH793288	–	MH818815
	LC12123	Leaves of *Digitaria sanguinalis*	Beijing, China	MH885417	MH793276	MH793300	MH818811
	LC12124	Leaves of *Poa pratensis*	Beijing, China	MH885418	MH793277	MH793297	MH818812

Species	Isolate no. [a]	Host/Substrate	Country	NCBI accession numbers			
				cmdA	ITS	*tub2*	*rpb2*
***D. acuta* sp. nov.**	LC12125	Rhizosphere soils of *Poa pratensis*	Beijing, China	MH885427	MH793286	MH793298	MH818813
	LC12126	Rhizosphere soils of *Poa pratensis*	Beijing, China	MH885428	MH793287	MH793299	MH818814
	LC12127	Rhizosphere soils of *Poa pratensis*	Beijing, China	MH885430	MH793289	MH793301	MH818820
***D. obtusa* sp. nov.**	CGMCC3.19206^{T} = LC12128	*Poa pratensis*	Beijing, China	MH885426	MH793285	MH793307	MH818816
	LC12129	Rhizosphere soils of *Agrostis stolonifera*	Beijing, China	MH885415	MH793274	MH793303	MH818821
	LC12130	Rhizosphere soils of *Poa pratensis*	Beijing, China	MH885431	MH793290	MH793308	MH818817
	LC12131	rhizosphere soils of *Poa* sp.	Beijing, China	MH885416	MH793275	MH793304	–
	LC12132	Rhizosphere soils of *Festuca arundinacea*	Beijing, China	MH885422	MH793281	MH793305	MH818818
	LC12133	Rhizosphere soils of *Poa pratensis*	Beijing, China	MH885423	MH793282	MH793306	MH818819
	LC12134	Roots of *Poa pratensis*	Beijing, China	MH885424	MH793283	MH793309	–
	LC12135	Roots of *Poa pratensis*	Beijing, China	MH885425	MH793284	MH793302	–
Gregatothecium humicola	CBS 205.96^{T}	Soil	Papua New Guinea	KU846285	KU846315	KU846432	KU846376
Peethambara sundara	CBS 646.77^{T}	Dead twig	India	–	KU846471	KU846551	KU846509
	CBS 521.96 = MUCL 39093	Dead twig	Nepal	–	KU846470	KU846550	KU846508
Inaequalispora prestonii	CBS 175.73^{T}	Forest soil	Malaysia	KU846286	KU846316	KU846433	KU846377
	MUCL 52636	rhizoplane and roots of plants	Ecuador	–	KY389317	KY366447	KY389355
Myxospora masonii	CBS 174.73^{T}	Leaves of *Glyceria* sp.	England	KU846445	KU846462	KU846543	KU846500
My. graminicola	CBS 116538^{T}	Decaying grass leaf	USA	KU846444	KU846461	KU846542	KU846499
My. aptrootii	CBS 101263^{T}	Leaf litter	China	KU846441	KU846458	KU846539	KU846496
My. musae	CBS 265.71^{T}	*Musa* sp.	Madagascar	–	KU846463	KU846544	KU846501
	CPC 25150	Tarspot lesion	South Africa	KU846446	KU846464	KU846545	KU846502
My. crassiseta	CBS 731.^{8}3T	Dead twig	Japan	KU846442	KU846459	KU846540	KU846497
	CBS 121141 = NRRL 45891	Pyrenomycete	Hawaii	KU846443	KU846460	KU846541	KU846498
Paramyrothecium humicola	CBS 127295^{T}	Soil collected in tallgrass prairie	USA	–	KU846295	KU846412	KU846356
P. parvum	CBS 257.35^{T}	*Viola* sp.	United Kingdom	–	KU846298	KU846415	KU846359
	CBS 142.422= IMI 155923= MUCL 7582	Dune sand	France	KU846268	KU846297	KU846414	KU846358
P. foeniculicola	CBS 331.51^{T}	*Foeniculum vulgare* leaf sheath	The Netherlands	–	KU846292	KU846409	KU846354
P. nigrum	CBS 116537^{T}	Soil	Spain	KU846267	KU846296	KU846413	KU846357
	LC12188	Rhizosphere soils of *Poa* sp.	China	MK500252	MK478871	MK500269	MK500261
P. cupuliforme	CBS 1277^{8}9T	Surface soil in desert	Namibia	KU846264	KU846291	KU846408	KU846353
P. viridisporum	CBS 873.85^{T}	Soil	Turkey	KU846278	KU846308	KU846425	KU846369
	CBS 125835	Soil	USA	KU846280	KU846310	KU846427	KU846371
P. acadiense	CBS 123.96^{T}	*Tussilago farfara*	Canada	–	KU846288	KU846405	KU846350
P. terrestris	CBS 564.86^{T}	Soil	Turkey	KU846273	KU846303	KU846420	KU846364
	CBS 566.86	Soil	Turkey	KU846275	KU846305	KU846422	KU846366
P. tellicola	CBS 478.91^{T}	Soil	Turkey	KU846272	KU846302	KU846419	KU846363
P. foliicola	CBS 113121^{T}	Decaying leaf	Brazil	KU846266	KU846294	KU846411	–
	CBS 419.93	Air	Cuba	KU846265	KU846293	KU846410	KU846355

Species	Isolate no. [a]	Host/Substrate	Country	NCBI accession numbers			
				cmdA	ITS	*tub2*	*rpb2*
P. breviseta	CBS 544.75[T]	Unknown	India	KU846262	KU846289	KU846406	KU846351
P. roridum	CBS 357.89[T]	*Gardenia* sp.	Italy	KU846270	KU846300	KU846417	KU846361
	CBS 212.95	Water	The Netherlands	KU846269	KU846299	KU846416	KU846360
	CBS 372.50 = IMI 140050	*Coffea* sp.	Colombia	KU846271	KU846301	KU846418	KU846362
P. guiyangense	GUCC 201608S01[T]	*Soil*	Guiyang, China	KY196193	KY126418	KY196201	–
	HGUP 2016-8001	*Soil*	Guiyang, China	KY196192	KY126417	KY196200	–
P. verruridum	HGUP 2016-8006[T]	*Soil*	Guizhou, China	KY196197	KY126422	KY196205	–
***P. sinense* sp. nov.**	CGMCC3.19212[T] = LC12136	Rhizosphere soils of *Poa* sp.	Beijing, China	MH885437	MH793296	MH793313	MH818824
	LC12137	Rhizosphere soils of *Poa* sp.	Beijing, China	MH885436	MH793295	MH793312	MH818822
	LC12138	Rhizosphere soils of *Poa* sp.	Beijing, China	MH885433	MH793292	MH793310	MH818823
	LC12139	Rhizosphere soils of *Poa* sp.	Beijing, China	MH885435	MH793294	MH793311	MH818825
Parvothecium terrestre	CBS 198.89[T]	Soil in virgin forest	Brazil	KU846449	KU846468	KU846548	KU846506
Neomyrothecium humicola	CBS 310.96[T]	Soil	Papua New Guinea	KU846448	KU846467	–	KU846505
Gregatothecium humicola	CBS 205.96[T]	Soi	Papua New Guinea	KU846285	KU846315	KU846432	KU846376
Xepicula crassiseta	CBS 392.71[T]	Soil	Spain	KU847222	KU847247	KU847337	KU847296
X. jollymannii	CBS 276.48[T]= MUCL 11830	*Nicotiana tabacum*	Malawi	KU847223	KU847248	KU847338	KU847297
	CBS 126168	Soil	Namibia	KU847224	KU847250	KU847340	KU847298
X. leucotricha	CBS 131.64= IMI 103664= ATCC 16686	Soil	India	KU847225	KU847251	KU847341	KU847299
	CBS 483.78	Soil	Colombia	KU847228	KU847254	KU847344	KU847302
Smaragdiniseta bisetosa	CBS 459.82[T]	Rotten bark	India	KU847206	KU847229	KU847319	KU847281
Striaticonidium brachysporum	CBS 513.71[T] = IMI 115293	Dune sand	Iran	KU847209	KU847232	KU847322	KU847284
S. brachysporum	CBS 131.71= IMI 158441= ATCC 22270	Soil	Ukrain	KU847207	KU847230	KU847320	KU847282
	LC12189	Rhizosphere soils of *Poa* sp.	Beijing, China	MK500253	MK478872	MK500270	MK500262
	LC12190	Rhizosphere soils of *Poa* sp.	Beijing, China	MK500254	MK478873	MK500271	MK500263
S.synnematum	CBS 479.85[T]	Palm leaf	Japan	KU847218	KU847242	KU847332	KU847292
S. cinctum	CBS 932.69[T]	Soil	The Netherlands	KU847216	KU847239	KU847329	KU847290
	CBS 277.48 = IMI 001526	Soil	New Zealand	KU847213	KU847236	KU847326	KU847288
S. humicola	CBS 388.97	Soil	Papua New Guinea	KU847217	KU847241	KU847331	KU847291
Tangerinosporium thalictricola	CBS 317.61[T] = IMI 034815	*Thalictrum flavum*	UK	KU847219	KU847243	KU847333	–
Xenomyrothecium tongaense	CBS 598.80[T]	*Halimeda* sp.	Tonga	KU847221	KU847246	KU847336	KU847295
Virgatospora echinofibrosa	CBS 110115	*Theobroma cacao*	Ecuador	KU847220	KU847244	KU847334	KU847293
	MUCL 39092 = ATCC 200437	*Trewia nudiflora*	Nepal	–	KU847245	KU847335	KU847294
Fusarium sambucinum	CBS 146.95	*Solanum tuberosum*	UK	KM231391	KM231813	KM232078	KM232381

† ATCC: American Type Culture Collection, Manassas, USA; BCC: BIOTEC Culture Collection, National Center for Genetic Engineering and Biotechnology (BIOTEC), Bangkok, Thailand; CBS: CBS-KNAW Fungal Diversity Centre, Utrecht, The Netherlands; CGMCC: China General Microbiological Culture Collection Center, Beijing, China; GUCC: Guizhou University Culture Collection, Guiyang, China; HGUP: Herbarium of the Department of Plant Pathology, Guizhou University, China; IMI: International Mycological Institute, England, UK; LC: Collection of Lei Cai, Institute of Microbiology, Chinese Academy of Sciences, Beijing, China; MUCL: Mycothèque de l'Université Catholique de Louvian, Belgium; NRRL: Northern Regional Research Laboratory, USA.

[T] Ex-type and ex-epitype cultures.

quences were checked and manually corrected where necessary. A consensus contig was assembled with BioEdit v. 7.0.9 (Hall 1999) and the reference sequences were downloaded from GenBank (Table 1). Sequences were aligned with MAFFT v. 7 (Kazutaka and Standley 2013) and manually trimmed to equal length by cutting the unaligned sequences at both ends.

Phylogenetic analyses

Phylogenetic analyses were based on Bayesian inference (BI) and Maximum Likelihood (ML). For BI analysis, the optimal evolutionary model was estimated in MrModeltest v. 2.3 (Nylander 2004) using the Akaike Information Criterion (AIC) for each locus. For the selected substitution models for each locus see Table 2. MrBayes v. 3.2.1 (Ronquist and Huelsenbeck 2003) was used to generate tree topology and a Markov Chain Monte Carlo (MCMC) algorithm of four chains was started with a random seed and a burn in of first 25% trees. The MCMC analysis lasted until the average standard deviation of split frequencies came below 0.01. The ML analysis was performed using RAxML servers (http://phylobench.vital-it.ch/raxml-bb/index.php), with a maximum likelihood bootstrap (LB) of 1,000 replicates, under the GTR-GAMMA model (Stamatakis 2006).

Results

In this study, 603 fungal strains were isolated. Based on colony morphologies and preliminary sequence comparison of ITS via BLASTn in GenBank, 84 myrothecium-like strains were selected. Phylogenetic analyses of above 84 strains were performed on single locus and concatenated datasets (ITS, *cmdA, tub2* and *rpb2*), with 70 strains in *Myrothecium* s.l. as reference and *Fusarium sambucinum* (CBS 146.95) as outgroup. After alignment, the concatenated datasets of four loci contained 569 characters (with gaps) for ITS, 318 for *tub2*, 732 for *cmdA* and 724 for *rpb2*. The characters of different alignments and statistics of phylogenetic analyses were shown in Table 2. The four single locus trees of all strains showed essentially similar topology (Supp. materials 1–4), with only minor differences affecting unsupported nodes on the trees. The resulting multi-locus ML tree was presented in Fig. 1 together with BI posterior probability values. Among 84 myrothecium-like strains, 14 strains were identified as four known species, *Albifimbria verrucaria* (10 strains), *Alb. terrestris* (1 strain), *Striaticonidium brachysporum* (2 strains) and *Paramyrothecium nigrum* (1 strain). The rest of them were grouped into five distinct clades with high supported values. Based on the morphological and phylogenetic distinctions, five novel species (i.e. *Alfaria humicola, Alf. poae*, *Dimorphiseta acuta*, *D. obtusa* and *Paramyrothecium sinense*) were described in this paper.

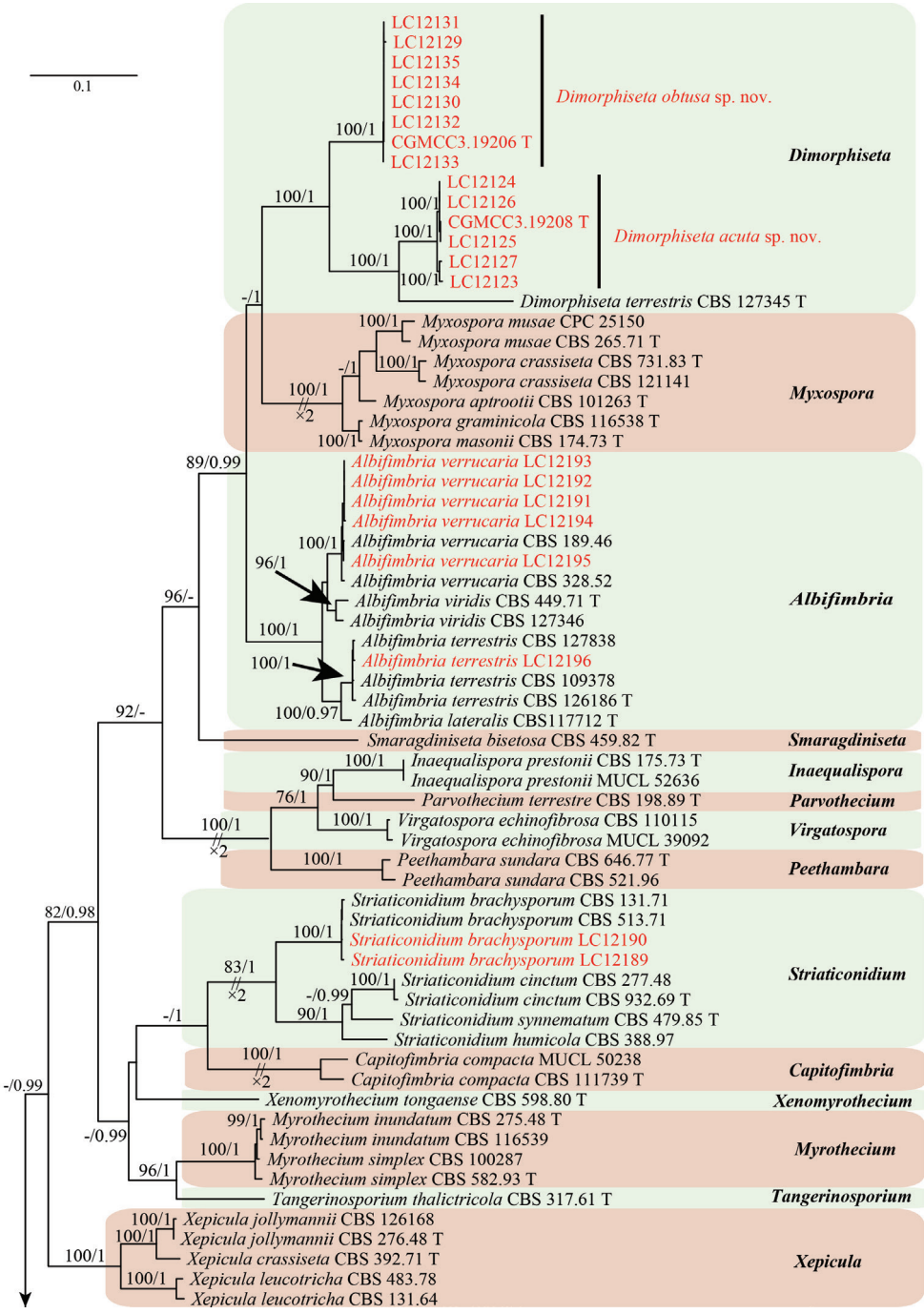

Figure 1. The ML consensus tree inferred from a four-locus concatenated alignment (ITS, *cmdA*, *rpb2* and *tub2*). Bootstrap values (1,000 replicates) over 70% for ML and posterior probability (PP) over 0.95 are added to the left of a node (ML/PP). The type strains are labeled with "T". Strains obtained from this study are in red. The tree is rooted using *Fusarium sambucinum* (CBS 146.95).

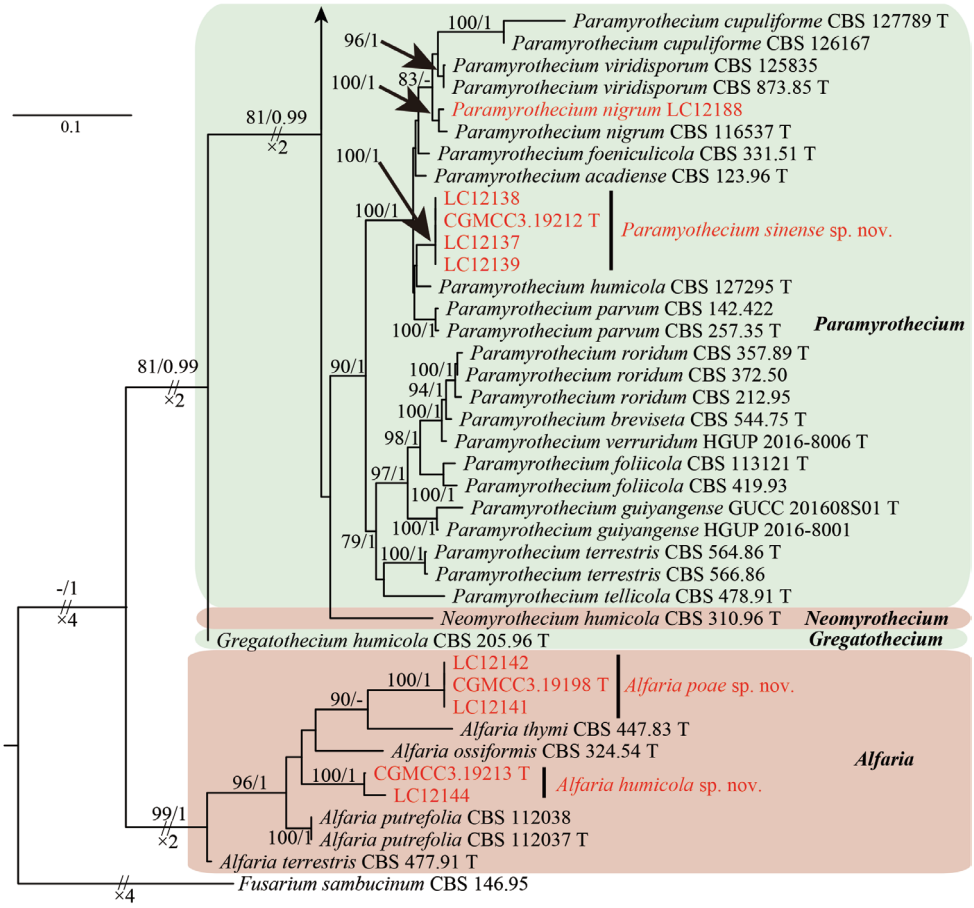

Figure 1. Continued.

Table 2. Characteristics of the different datasets and statistics of phylogenetic analyses used in this study.

Locus†	Number of sites*				Evolutionary model‡	Number of tree sampled in B	Maximum-likelihood statistics	
	Total	Conserved	Phylogenetically informative	B unique patterns			Best tree optimised likelihood	Tree length
ITS	569	334	193	247	GTR+I+G	7501	-32666.73	5.36
tub2	318	168	140	159	HKY+I+G			
cmdA	732	258	381	490	HKY+I+G			
rpb2	724	360	367	367	GTR+I+G			

† ITS, the internal transcribed spacer regions and 5.8s rRNA gene; *tub2, β-tubulin*; *cmdA*, calmodulin; *rpb2*: RNA polymerase II second largest subunit.

* B = Bayesian inference.

‡ G: Gamma distributed rate variation among sites. GTR: Generalised time-reverisble. I: Proportion of invariable sites. HKY: Hasegawa-Kishino-Yano.

Taxonomy

Dimorphiseta L. Lombard & Crous., Persoonia. 36: 188. 2016. emend. J.M.Liang & L.Cai.

Dimorphiseta terrestris L. Lombard & Crous. Persoonia. 36: 188. 2016. (Type species)

Note. *Dimorphiseta* was a monotypic genus, introduced based on *D. terrestris*, which showed both type I (thin-walled, flexuous to circinate, narrowing to a sharp apex) and type II (thick-walled, straight to slightly curved, narrowing to a sharp apex) setae. Our study demonstrated that there is a third type of setae (type III: thin-walled, straight, terminating in an obtuse apex) in the genus.

Dimorphiseta acuta J.M. Liang, G.S. Li & L. Cai, sp. nov.

MycoBank MB 829693
Fig. 2

Type. China, Beijing, isolated from rhizosphere soils of *Poa pratensis*, 26 Aug 2017, J.M. Liang, holotype HMAS 247957, dried culture on PDA, ex-holotype culture CGMCC3.19208 = LC12122.

Description. *Colonies* on PDA, CMA and OA approx. 7–8 cm diam. after 7 d at room temperature (approx. 25 °C), mycelium white and abundant, with conidiophores forming on the aerial mycelium, carrying slimy olivaceous green to black conidial masses, reverse on PDA buff. *Conidiomata* sporodochial, stromatic, superficial, cupulate to discoid, scattered, rarely gregarious, irregular in outline, 50–300 μm diam., 60–150 μm deep, consisting of bundles of parallel, longitudinal, closely compacted hyphae, terminating in whorls of 3–5 conidiogenous cells, covered by an olivaceous green to black slimy mass of conidia without marginal hyphae. *Stroma* poorly developed, hyaline, of a textura angularis. *Setae* arising from the conidial mass, thick-walled, subhyaline, smooth, 5–15-septate, tapering to sharp apices, 120–370 μm long, 10–13 μm wide at the broadest part, 2–4 μm wide at the apex. *Conidiophores* macronematous, irregularly, unbranched, smooth to lightly verrucose, arising from the basal stroma. *Conidiogenous cells* phialidic, subcylindrical, hyaline, smooth, 10–20 μm long, 2–3 μm wide. *Conidia* aseptate, smooth, hyaline, ellipsoidal, rounded at the base, pointed at the apex with a funnel-shaped appendage, 7–12 × 2–3 μm (av. 10 ± 0.7 × 3 ± 1.3 μm, n = 50).

Distribution. China.

Etymology. Name refers to the setae with tapered and sharp apices.

Additional isolates examined. China, Beijing, from leaves of *Digitaria sanguinalis*, 21 Aug 2017, J.M. Liang, LC12123; China, Beijing, from leaves of *Poa pratensis*, 21 Aug 2017, J.M. Liang, LC12124; China, Beijing, from rhizosphere soils of *P. pratensis*, 21 Aug 2017, J.M. Liang & G.S. Li, LC12125, 21 Jul 2017, J.M. Liang, LC12126, 25 Jul 2017, J.M. Liang, LC12127.

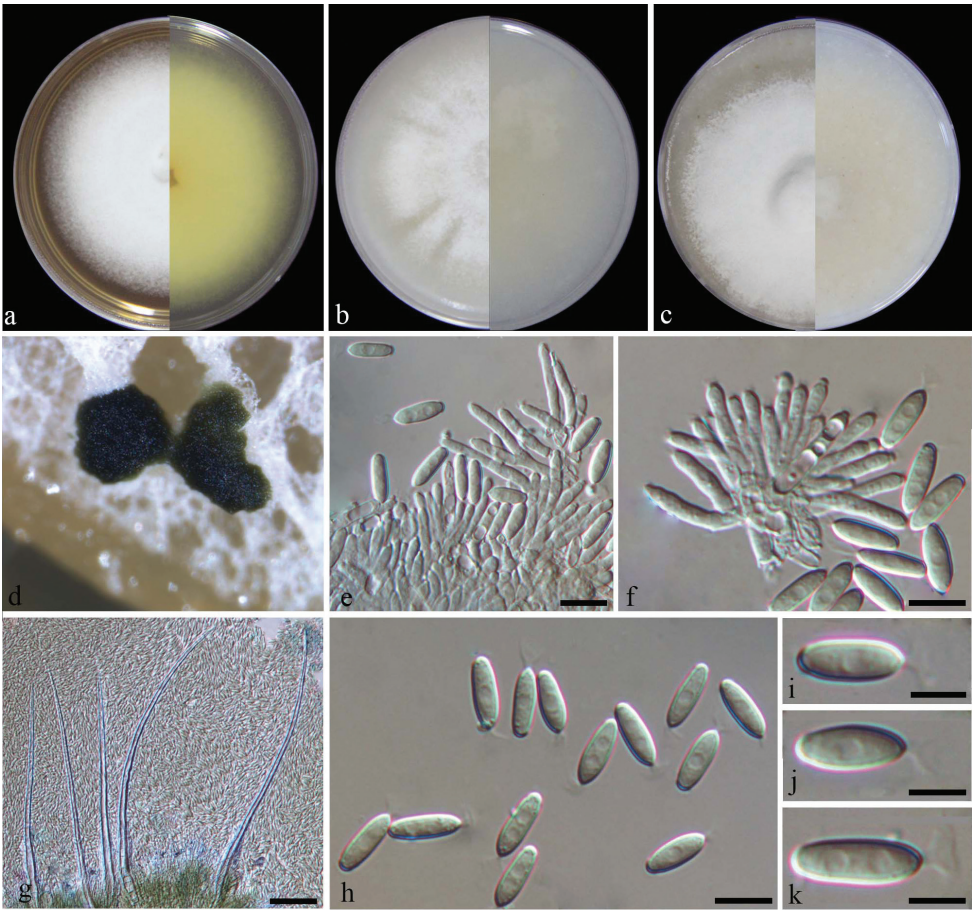

Figure 2. *Dimorphiseta acuta* (from ex-type strain CGMCC3.19208) **a–c** colony on PDA, CMA, OA **d** conidiomata on SNA **e** conidiophores **f** conidiogenous cells **g** setae **h–k** conidia. Scale bars: 5 µm (**e, f, h**): 50 µm (**g**); 2 µm (**i, j, k**).

Notes. The multi-locus phylogenetic analyses indicated that *D. acuta* formed a sister clade to *D. terrestris*, but differs from the latter in the type and size of setae. *Dimorphiseta terrestris* produces both types of setae, the thin-walled and circinate type (Type I) and the thick-walled sharp-edged type (Type II), whereas *D. acuta* only produces the type I setae. In addition, the setae of *D. acuta* are much longer and wider than that in *D. terrestris* (120–370 µm × 10–13 µm vs. 70–95 × 3–4 µm) (Lombard et al. 2016). Morphologically, *D. acuta* should also be compared with *M. miconiae* and *M. xigazense*, which also produce sharp-edged setae. *Myrothecium miconiae,* however, differs from *D. acuta* in producing 1-septate conidia (Alves et al. 2010), while *M. xigazense* differs in producing conidia that are truncate at both ends (Wu et al. 2014).

Dimorphiseta obtusa **J.M. Liang, G.S. Li & L. Cai, sp. nov.**
MycoBank MB 829694
Fig. 3

Type. China, Beijing, isolated from rhizosphere soils of *P. pratensis*, 23 Jun 2017, J.M. Liang, holotype HMAS 247954, ex-holotype culture CGMCC3.19206 = LC12128.

Description. *Colonies* on PDA, OA and CMA approx. 5–6 cm diam. after 7 d at room temperature (approx. 25 °C), mycelium white and abundant, with conidiophores forming on the aerial mycelium, carrying slimy olivaceous green to black conidial masses, reverse on PDA pale luteous to buff. *Conidiomata* sporodochial, stro-

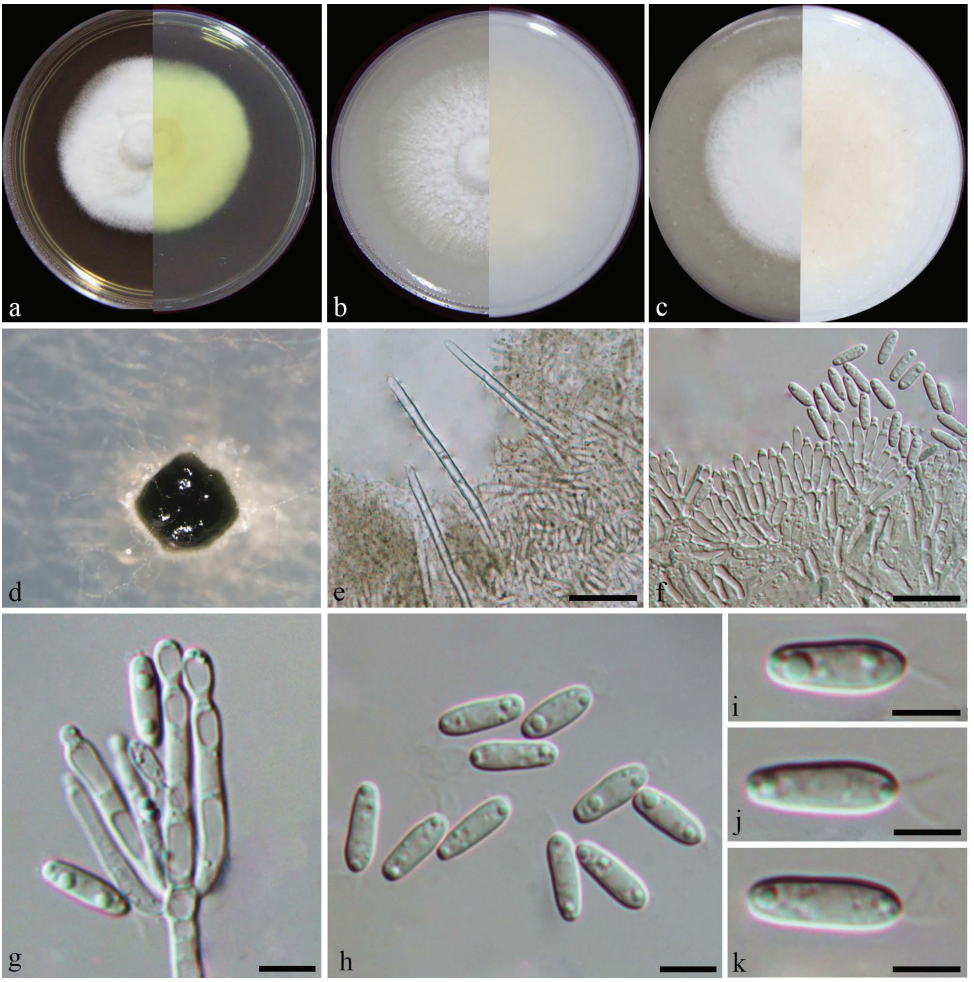

Figure 3. *Dimorphiseta obtusa* (from ex-type strain CGMCC3.19206) **a–c** colony on PDA, CMA, OA **d** conidioma on SNA **e** setae **f** conidiophores **g** conidiogenous cells **h–k** conidia. Scale bars: 50 μm (**e**); 10 μm (**f, g**); 5 μm (**h**); 2 μm (**i, j, k**).

matic, superficial, scattered, rarely gregarious, oval to elongate or irregular in outline, 60–280 µm diam., 40–120 µm deep, with a setose fringe surrounding green to black slimy mass of conidia. *Stroma* poorly developed, hyaline, smooth to verrucose, of textura angularis. *Setae* arising from the basal stroma, thin-walled, 3–6-septate, unbranched, hyaline, smooth, 80–250 µm long, 2–4 µm wide at the broadest, terminating in a blunt apex. *Conidiophores* macronematous, irregularly, unbranched, smooth to lightly verrucose, arising from the basal stroma, up to 18 µm long. *Conidiogenous cells* phialidic, hyaline, smooth to verrucose, cylindrical, 7–19 × 2–3 µm, becoming narrowed at the tip with collarette. *Conidia* aseptate, ellipsoidal or cylindrical, hyaline, smooth, rounded both ends, with a funnel-shaped apical appendage, 9–11 × 2–4 µm (av. 10 ± 0.5 × 3 ± 0.3 µm, n = 50).

Distribution. China.

Etymology. Named refers the setae with obtuse apices.

Additional isolates examined. China, Beijing, from rhizosphere soils of *Agrostis stolonifera*, 24 Jul 2017, J.M. Liang, LC12129; China, Beijing, from rhizosphere soils of *P. pratensis*, 25 Aug 2017, J.M. Liang & G.S. Li, LC12130, 19 Jul 2017, J.M. Liang, LC12133; China, Beijing, from rhizosphere soils of *Poa* sp., 19 Jul 2017, J.M. Liang, LC12131; China, Beijing, from rhizosphere soils of *Festuca arundinacea*, 19 Jul 2017, J.M. Liang, LC12132; China, Beijing, from leaves of *P. pratensis*, 23 Jun 2017, J.M. Liang, LC12134, LC12135.

Notes. *Dimorphiseta obtusa* formed a highly supported cluster with *D. terrestris* and *D. acuta,* but can be distinguished from the latter two by having setae with erect and obtuse apices. In addition, *D. obtusa* is also morphologically similar to two old un-sequenced *Myrothecium* taxa, i.e. *M. biforme* and *M. dimorphum*, but both of these two taxa have two types of conidia. *Myrothecium biforme* produces short cylindrical and ellipsoidal to navicular conidia (Jiang et al. 2014) and *M. dimorphum* has ovate and ellipsoidal conidia (Watanabe et al. 2003).

***Alfaria humicola* J.M. Liang, G.S. Li & L. Cai, sp. nov.**
MycoBank MB 829696
Fig. 4

Type. China, Beijing, Olympic Park, from rhizosphere soil of *Poa* sp., 13 Dec 2017, S.Y. Zhou, holotype HMAS 247955, ex-holotype culture CGMCC3.19213 = LC12143.

Description. *Colonies* on PDA, CMA and OA approx. 7–8 cm diam. after 7 d at 25 °C. *Hyphae* hyaline, smooth, branched, 1–2 µm wide. *Conidiomata* sporodochial, stromatic, superficial, cupulate to discoid, scattered to gregarious, oval to elongate or irregular in outline, 50–200 µm diam., 70–150 µm deep, without setose hyphae, covered by a green to black agglutinated slimy mass of conidia. *Stroma* well-developed, hyaline, of textura globulose or textura angularis. *Setae* absent. *Conidiophores* arising from the basal stroma, unbranched or branched, initially hyaline and smooth, becoming pigmented and verrucose with age, 11–25 µm long.

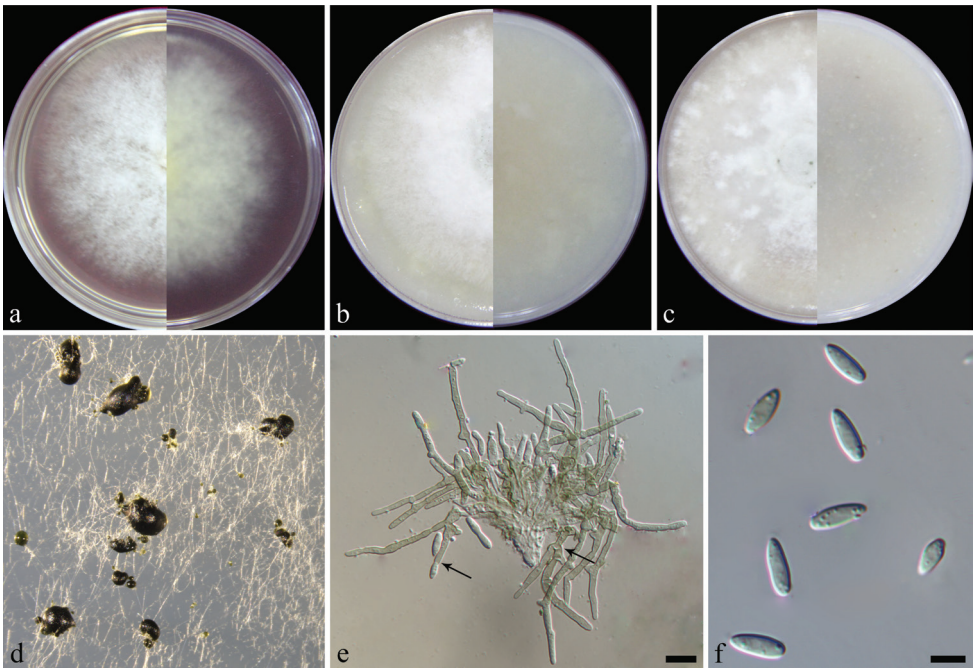

Figure 4. *Alfaria humicola* (from ex-type CGMCC3.19213) **a–c** colony on PDA, CMA, OA **d** conidiomata on SNA **e** sporodochial conidioma, arrows showing branched conidiosphores and conidiogenous cells **f** conidia. Scale bars: 10 μm (**e**); 5 μm (**f**).

Conidiogenous cells phialidic, cylindrical to allantoid, initially hyaline and smooth becoming pigmented and verrucose with age, 14–33 × 2–3 μm. *Conidia* aseptate, smooth, hyaline, elongated ellipsoidal to limoniform, straight, 7–9(–10) × 2–3 μm (av. 8 ± 0.6 × 3 ± 0.2 μm, n = 50).

Distribution. China.

Etymology. Name refers the substrate, soil, from which this fungus was isolated.

Additional isolate examined. China, Beijing, Olympic Park, from rhizosphere soil of *Poa* sp., 13 Dec 2017, S.Y. Zhou, LC12144.

Notes. *Alfaria humicola* represents another distinct lineage in *Alfaria* (Fig. 1). *Alfaria humicola* lacks setae, distinguishing it from *Alf. caricicola* and *Alf. thymi*. Furthermore, the conidiogenous cells of *Alf. humicola* (14–33 × 2–3 μm) are much longer than that of *Alf. arenosa* (5–10 × 1–2 μm), *Alf. ossiformis* (5–10 × 2–3 μm) and *Alf. terrestris* (5–11 × 1–3 μm). Compared with those old *Myrothecium* taxa lacking sequences, *Alf. humicola* is morphologically similar to *M. atrocarreum* (Berkeley & Broome, 1877), *M. conicum* (Fuckel, 1870), *M. ellipsosporum* (Fuckel, 1866), *M. fragosianum* (Saccardo, 1917), *M. leucomelas* (Höhnel, 1925) and *M. oryza* (Saccardo, 1917), but *Alf. humicola* produces limoniform conidia which makes it distinguishable. In addition, the conidiogenous cells of *Alf. humicola* show conspicuous collarettes which were not described in previous old taxa.

Alfaria poae **J.M. Liang, G.S. Li & L. Cai, sp. nov.**
MycoBank MB 829697
Fig. 5

Type. China, Hainan Province, Haikou, isolated from leaves of *Imperata cylindrica*, 10 Mar 2018, J.M. Liang and L. Cai, holotype HMAS 247953, ex-holotype culture CGMCC3.19198 = LC12140.

Description. *Colonies* on PDA, CMA and OA with white aerial mycelium, approx. 6–7 cm diam. after 7 d at 25 °C, giving rise to dark green or blank sporodochia scattered or gregarious on the surface, covered by olivaceous green pillars of conidia,

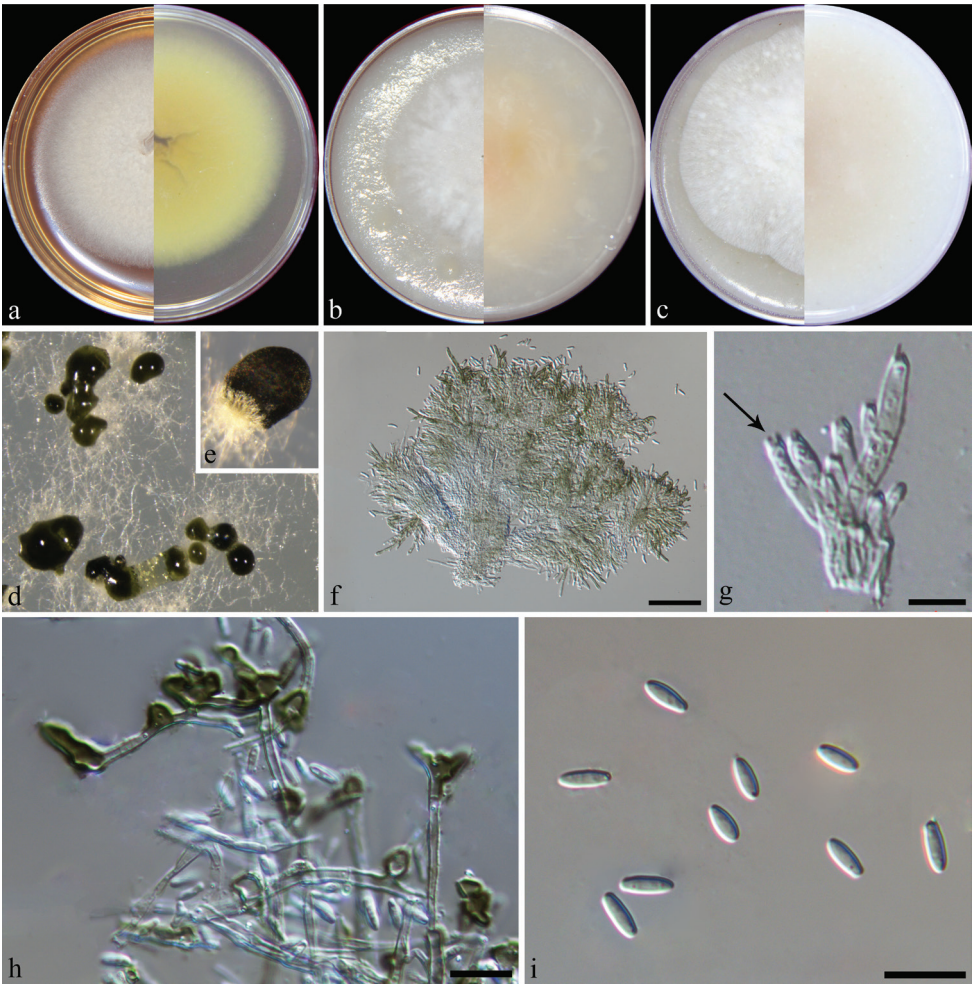

Figure 5. *Alfaria poae* (from ex-type strain CGMCC3.19198) **a–c** colony on PDA, CMA, OA **d–e** conidiomata on SNA **f** synnematous conidioma **g** conidiogenous cells, the arrow showing conspicuous collarette **h** aged conidiophores **i** conidia. Scale bars: 50 µm (**f**); 5 µm (**g**); 10 µm (**h, i**).

reverse on PDA sienna. *Hyphae* hyaline, smooth, branched, 1–2 µm wide. *Conidiomata* synnematous, solitary, 60–250 µm high, 30–80 µm wide at the base, 60–150 µm at the apex, with setose hyphae surrounding a green agglutinated mass of conidia. *Stroma* well developed, hyaline, of textura angularis. *Setae* absent. *Conidiophores* arising from the basal stroma, branched, initially hyaline and becoming pigmented and verrucose with age covered by an olivaceous green mucoid layer, up to 30 µm long. *Conidiogenous cell* phialidic, clavate to cylindrical, hyaline, smooth, 5–10 × 1–2 µm, becoming pigmented and verrucose with age, with conspicuous collarettes and periclinal thickenings. *Conidia* aseptate, smooth, hyaline, ellipsoidal to fusiform, 6–8 × 2–3 µm (av. 7 ± 0.4× 2 ± 0.2 µm, n = 50).

Distribution. China.

Etymology. Name refers the host, *Poa* sp., from which this fungus was isolated.

Additional isolate examined. China, Hainan, from leaves of *Imperata cylindrica*, 10 Mar 2018, J.M. Liang & Lei Cai, LC12141, LC12142.

Notes. *Alfaria poae* formed a well-supported clade in *Alfaria* (Fig. 1). Similar to *Alf. ossiformis* and *Alf. terrestris*, *Alf. poae* does not produce setae surrounding the sporodochia, distinguishing it from *Alf. caricicola* and *Alf. thymi*. *Alfaria poae* produces ellipsoidal to fusiform conidia, which are different from the ossiform conidia produced by *Alf. ossiformis* (Lombard et al. 2016). The conidia of *Alf. terrestris* have basal hilum which was not observed in *Alf. poae*. In addition, *Alf. poae* shares morphological characters with several un-sequenced *Myrothecium* taxa, such as *M. atrocarneum* (Berkeley & Broom, 1877), *M. conicum* (Fuckel, 1870), *M. ellipsosporum* (Fuckel, 1866) and *M. leucomelas* (Höhnel, 1925). Because the descriptions of *M. atrocarneum*, *M. conicum* and *M. ellipsosporum* were not elaborate enough, these old species are not distinct from *Alf. poae* yet. Future comparisons should be made when these old species are epitypified by fresh collections. Although *M. leucomelas* (host: *Sumbaviae rotttleroidis*; location: Bulacan, Luzon) had a detailed description, it cannot be epitypified by *Alf. Poae,* because *Alf. poae* was collected from a distinct location and plant host. Taking the above special characters into account, we considered introducing a new species, *Alfaria poae*.

Paramyrothecium sinense **J.M. Liang, G.S. Li & L. Cai, sp. nov.**
MycoBank MB 829698
Fig. 6

Type. China, Beijing, Olympic Park, from rhizosphere soil of *Poa* sp., 13 Dec 2017, S.Y. Zhou, holotype HMAS 247956, ex-holotype culture CGMCC3.19212 = LC12136.

Description. *Colonies* on PDA, CMA and OA approx. 5–6 cm diam. after 7 d at 25 °C. *Hyphae* white, hyaline, smooth, branched, 1–2 µm wide, reverse on PDA pale luteous. *Conidiomata* sporodochial, stromatic, cupulate, superficial, scattered or gregarious, oval or irregular in outline, 80–600 µm diam., 50–150 µm deep, with a white setose fringe surrounding an olivaceous green to black agglutinated slimy mass

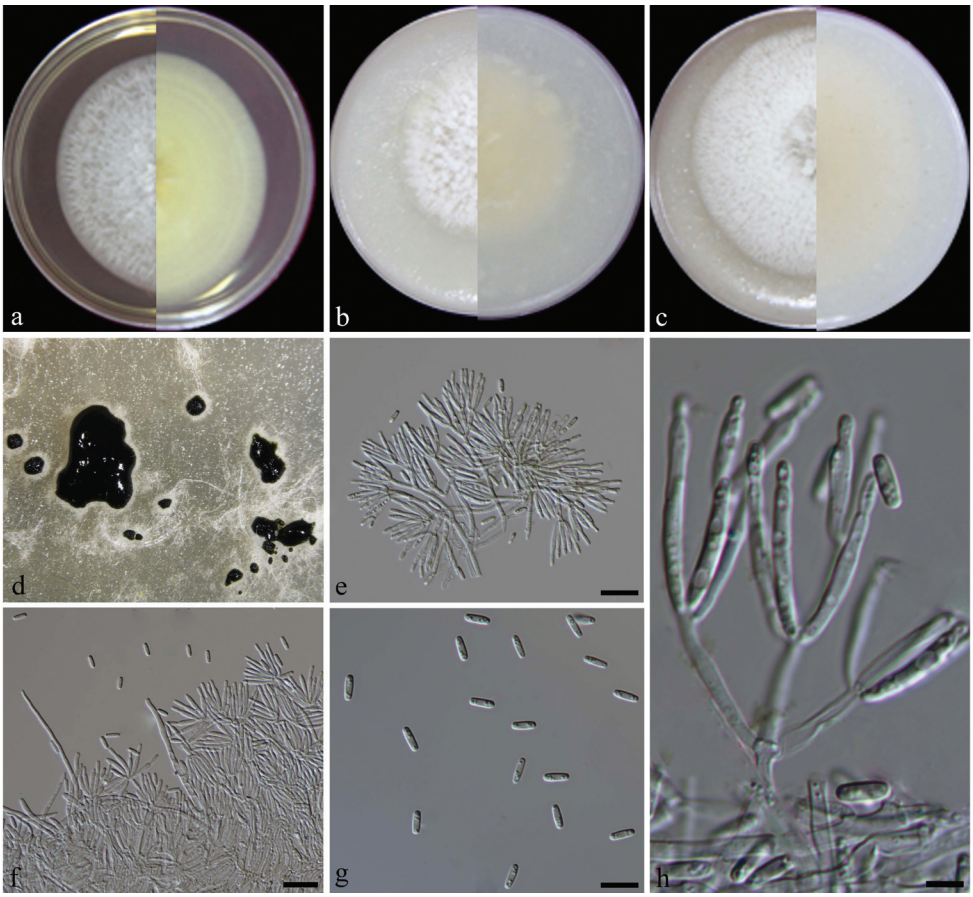

Figure 6. *Paramyrothecium sinense* (from ex-type CGMCC3.19212) **a–c** colony on PDA, CMA, OA **d** conidiomata on SNA **e** sporodochial conidioma **f** setae **g** conidia **h** conidiogenous cells. Scale bars: 20 μm (**e, f**); 10 μm (**g**); 5 μm (**h**).

of conidia. *Stroma* poorly developed, hyaline, of textura angularis. *Setae* arising from stroma, thin-walled, hyaline, 1–3-septate, straight to flexuous, 45–90 μm long, 1–3 μm wide, tapering to an acutely rounded apex. *Conidiophores* arising from the basal stroma, consisting of a stipe and a penicillately branched conidiogenous apparatus; stipes unbranched, hyaline, septate, smooth, 20–30 × 2–3 μm; primary branches aseptate, unbranched, smooth, 13–40 × 2–3 μm; secondary branches aseptate, unbranched, smooth, 8–15 × 2–3 μm; terminating in a whorl of 3–6 conidiogenous cells; conidiogenous cell phialidic, cylindrical to subcylindrical, hyaline, smooth, straight to slightly curved, 7–16 × 1–3 μm, with conspicuous collarettes and periclinal thickenings. *Conidia* aseptate, hyaline, smooth, cylindrical, 6–7 × 2–3 μm (av. 7 ± 0.3 × 2 ± 0.2 μm, n = 40), rounded at both ends.

Distribution. China.

Etymology. Named after the country of collection, China.

Additional isolate examined. China, Beijing, Olympic Park, from rhizosphere soils of *Poa* sp., 13 Dec 2017, S.Y. Zhou, LC12137, LC12138, LC12139.

Notes. Lombard et al. (2016) introduced a new genus, *Paramyrothecium*, based on an epitype of *Myrothecium roridum* Tode, 1790. Gams (2016) pointed out that *Myrotheciella catenuligera*, the type species of *Myrotheciella* was listed as a synonym of *P. roridum* by Lombard et al. (2016), thus *Paramyrothecium* is illegitimate and *Myrotheciella* should be the correct name for *Paramyrothecium*. However, the original description of *Myrotheciella catenuligera* suggested that it lacks seta (Spegazzini 1911), thus is clearly different from the morphological circumscription of *P. roridum*. Therefore, we do not agree with the treatment of Lombard et al. (2016) of listing *Myrotheciella catenuligera* as a synonym of *P. roridum*.

Paramyrothecium sinense formed a highly supported distinct clade closely related to *P. humicola*. The setae of this species are terminated with obtuse apices, dissimilar to the acute apices in *P. humicola.* In addition, the conidiophore stipes (20–30 μm long) and primary branches (13–40 μm long) of *P. sinense* are much longer than those of *P. humicola* (stipe, 12–22 μm long; primary branches, 7–17 μm long) (Lombard et al. 2016). Among old un-sequenced taxa in *Myrothecium*, only *M. biforme* and *M. dimorphum* show seta with obtuse apices, but both taxa produce two types of conidia (Jiang et al. 2014; Watanabe et al. 2003).

Discussion

The ITS has been shown to be insufficient to delineate the myrothecium-like species. With the additions of partial sequences of *rpb2*, *cmdA* and *tub2*, phylogenetic relationships within Stachybotryaceae could be better resolved (Lombard et al. 2016). In this study, we isolated fungi from rhizosphere soils, leaves and roots of several turfgrasses, and our phylogenetic analyses based on concatenated four loci together with the morphological characters supported the recognition of five novel species in Stachybotryaceae.

By comparing the topologies of the four single-locus trees, incomplete lineage sorting was discovered in *Dimorphiseta*. Based on the single-locus trees of ITS and *rpb2*, *D. acuta*, *D. obtusa* and *D. terrestris* grouped together (Supp. materials 1, 4). Whereas in the single-locus phylogenetic analyses based on *tub2* and *cmdA*, *D. obtusa* grouped distantly from *D. acuta* and *D. terrestris*, but close to *Myxospora* and *Albifimbria* species (Supp. materials 2, 3). Three *Dimorphiseta* species are similar in the conidial shape and size (7–19 μm long), which are distinct from the shorter conidia in *Albifimbria* (4–8 μm long) and *Myxospora* (4–6 μm long) species (Tulloch 1972; Lombard et al. 2016). Conidia with a funnel-shaped apical appendage are a distinct feature of three *Dimorphiseta* species, but they are absent in all *Myxospora* species and most *Albifimbria* species (Lombard et al. 2016). Furthermore, the *rpb2* and 28S ribosomal DNA combined dataset, which was suggested to delimit generic boundaries of myrothecium-like

species (Lombard et al. 2016) revealed that the three *Dimorphiseta* species clustered together (Supp. material 6: Table S1, Supp. material 5).

In the multi-locus sequence analysis of *Myrothecium* s.l. by Lombard et al. (2016), thirteen new genera were introduced including several monotypic genera, such as *Dimorphiseta*, *Capitofimbria*, *Gregatothecium* and *Neomyrothecium*. In this study, we reported two new species in *Dimorphiseta* (*D. acuta* and *D. obtusa*). With this addition, the generic concept of *Dimorphiseta* is slightly expanded for including a third type of setae. Hereto, *Dimorphiseta* is the genus with the most variable types of seta among *Myrothecium* s.l., which might be useful in the generic delimitation in *Myrothecium* s.l. (Lombard et al. 2016).

Lombard et al. (2016) narrowed the concept of *Myrothecium* s.s. to only include species with sporodochia or mononematous conidiophores producing conidia shorter than 5 μm in green slimy masses without mucoid appendages. Whether or not a conidial size should be defined in the generic concept remained debatable. Because many *Myrothecium* published recently produced much longer conidia, e.g. *M. chiangmaiense* (4–7 μm) (Dai et al. 2017), *M. uttaraditense* (10–15 μm) (Dai et al. 2017), *M. thailandicum* (6.5–10 μm) (Dai et al. 2017), *M. septentrionale* (8.5–12 μm) (Tibpromma et al. 2017), *M. variabile* (12.5–16.5 μm) (Wu et al. 2014) and *M. xigazense* (2.5–15 μm) (Wu et al. 2014). These above species were identified, either based on morphology only or with a single molecular locus (ITS), and should be better confirmed for their generic placement when more data are available. Currently, there are 90 records of *Myrothecium* in Index Fungorum (Jan 10, 2019), and 25 names have been successively transferred to other genera, i.e., *Capitofimbria*, *Melanconis*, *Striaticonidium*, *Xepicula* (Lombard et al. 2016), *Digitiseta* (Gordillo and Decock 2018). Only a limited number of the remaining species in *Myrothecium* have available molecular data (Dai et al. 2017; Tibpromma et al. 2017), as most of these taxa have no living cultures. We agree with Gams (2016) that these unvisited taxa are still important when the original descriptions are sufficiently clear to recognize a species. They should be epitypified in future studies when fresh collections with living cultures are available, and before that, descriptions of new taxa in this group should be made carefully with the inclusion of these un-sequenced taxa in morphological comparisons.

Acknowledgements

This study was financially supported by National Natural Science Foundation of China (NSFC 31600405).

References

Alves JL, Barreto RW, Pereira OL, Soares DJ (2010) Additions to the mycobiota of the invasive weed *Miconia calvescens* (Melastomataceae). Mycologia, 102(1):69–82. https://doi.org/10.3852/09-070

Berkeley MJ, Broome CE (1877) Supplement to the enumeration of fungi of Ceylon. Botanical Journal of the Linnean Society. 15: 82–86. https://doi.org/10.1111/j.1095-8339.1876.tb00225.x

Carbone I, Kohn LM (1999) A method for designing primer sets for speciation studies in filamentous ascomycetes. Mycologia 91: 553–556. https://doi.org/10.2307/3761358

Chen Q, Zhang KE, Zhang G, Cai L (2015) A polyphasic approach to characterise two novel species of *Phoma* (Didymellaceae) from China. Phytotaxa 197: 267–281. https://doi.org/10.11646/phytotaxa.197.4.4

Dai DQ, Phookamsak R, Wijayawardene NN (2017) Bambusicolous fungi. Fungal Diversity 82: 1–105. https://doi.org/10.1007/s13225-016-0367-8

Decock C, Huret S, Bivort C (2008) Anamorphic fungi from French Guyana. *Septomyrothecium* sp. nov. and *S. setiramosum* comb. nov. (anamorphic Hypocreales, Ascomycota). Cryptogamie Mycologie 29: 321–331. https://doi.org/10.1093/ml/gcm091

Ellis MB, Ellis JP (1985) Microfungi on Land Plants-An Identification Handbook. Bulletin of the Torrey Botanical Club 113: 61. https://doi.org/10.2307/2996241

Fuckel L (1866) Fungi Rhenani exsiccati Cent. 12–17 (2), no 1450–1632. Hedwigia. 5: 23–30.

Fuckel L (1870) Symbolae mycologicae. Beiträge zur Kenntniss der Rheinischen Pilze. Jahrbücher des Nassauischen Vereins für Naturkunde. 23–24: 1–459.

Glass NL, Donaldson G (1995) Development of primer sets designed for use with PCR to amplify conserved genes from filamentous ascomycetes. Applied and Environmental Microbiology 61: 1323–1330. https://doi.org/10.0000/PMID7747954

Gams W (2016) Are old taxa without living authenticated cultures losing their status? IMA Fungus. 7(2): 72–73.

Gordillo A, Decock C (2018) *Myrothecium*-like (Ascomycota, Hypocreales) species from tropical areas: *Digitiseta* gen. nov. and additions to *Inaequalispora* and *Parvothecium*. Mycological Progress 17: 179–190. https://doi.org/10.1007/s11557-017-1302-4

Groenewald JZ, Nakashima C, Nishikawa J, Shin HD, Park JH, Jama AN, Groenewald M, Braun U, Crous PW (2013) Species concepts in *Cercospora*: spotting the weeds among the roses. Studies in Mycology 75: 115–170. https://doi.org/10.3114/sim0012

Hall TA (1999) BioEdit: a user-friendly biological sequence alignment editor and analysis for Windows 95/98/NT. Nucleic Acids Symppsium Series 41: 95–98. https://doi.org/10.1021/bk-1999-0734.ch008

Höhnel (1925) Mitt. Bot. Inst. Techn. Hochsch. Wien 2(3): 96.

Jiang YL, Wang HF, Pan HQ, Zhang TY (2014) *Myrothecium* (Hyphomycetes): three new species, one new variety and a key to species and varieties of the genus known from soils in China. Mycosystema, 33(1): 7–14.

Kazutaka K, Standley DM (2013) MAFFT Multiple Sequence Alignment Software Version 7: Improvements in Performance and Usability. Molecular Biology and Evolution 30: 772–780. https://doi.org/10.1093/molbev/mst010

Kobayashi M, Sato I, Abe F, Nitta K, Hashimoto M, Fujie A, Hino M (2004) FR227244, a novel antifungal antibiotic from *Myrothecium cinctum* No. 002 I. Taxonomy, fermentation, isolation and physio-chemical properties. Journal of Antibiotics 57: 780–787. https://doi.org/10.7164/antibiotics.57.788

Kornerup A, Wanscher JH (1978) Methuen Handbook of Colour. Methuen.

Krisai-Greilhuber I, Chen Y, Jabeen S, ... Yu JY (2017) Fungal systematics and evolution: FUSE 3. Sydowia, 69: 229–264. https://doi.org/10.12905/0380.sydowia69-2017-0229

Link HF (1809) Observationes in ordines plantarum naturales. Dissertatio I.3: 3–42.

Liu JY, Huang LL, Ye YH, Zou WX, Guo ZJ, Tan RX (2006) Antifungal and new metabolites of *Myrothecium* sp. Z16, a fungus associated with white croaker *Argyromosum argentatus*. Journal of Applied Microbiology 100: 195–202. https://doi.org/10.1111/j.1365-2672.2005.02760.x

Lombard L, Houbraken J, Decock C, Samson R.A, Meijer M, Réblová M, Groenewald JZ, Crous PW (2016) Generic hyper-diversity in Stachybotriaceae. Persoonia 36: 156–246. https://doi.org/10.3767/003158516X691582

Murakami R, Kobayashi T, Takahashi K (2005) Myrothecium leaf spot of mulberry caused by *Myrothecium verrucaria*. Journal of General Plant Pathology 71: 153–155. https://doi.org/10.1007/s10327-004-0178-8

Nirenberg HI (1981) A simplified method for identifying *Fusarium* spp. occurring on wheat. Canadian Journal of Botany 59: 1599–1609. https://doi.org/10.1139/b81-217

Nylander JAA (2004) MrModelTest (program distributed by the author). Evolutionary Biology Centre, Uppsala University.

O'Donnell K, Sarver BA, Brandt M, Chang DC, Noble-Wang J, Park BJ, Sutton DA, Benjamin L, Lindsley M, Padhye A, Geiser DM, Ward TJ (2007) Phylogenetic diversity and microsphere array-based genotyping of human pathogenic Fusaria, including isolates from the multistate contact lens-associated U.S. keratitis outbreaks of 2005 and 2006. Journal of Clinical Microbiology 45: 2235–2248. https://doi.org/10.1128/JCM.00533-07

Okunowo WO, Gbenle GO, Osuntoki AA, Adekunle AA, Ojokuku SA (2010) Production of cellulolytic and xylanolytic enzymes by a phytopathogenic *Myrothecium roridum* and some avirulent fungal isolates from water hyacinth. African Journal of Biotechnology 9: 1074–1078. https://doi.org/10.5897/AJB09.1598

Pidoplichko NM, Kirilenko TS (1971) On the taxonomy of the genus *Myrothecium*. In: Pidoplichko NM (Ed.) Metabolites of soil micromycetes. Dumka, Naukova, Kiev, Ukrain, 157–171.

Pope S (1944) A new species in *Metarrhizium* active in decomposing cellulose. Mycologia 36: 343–350. https://doi.org/10.2307/3754750

Rogers SO, Bendich AJ (1994) Extraction of total cellular DNA from plants, algae and fungi. In: Gelvin SB, Schilperoort RA (Eds) Plant Molecular Biology Manual. Springer, Dordrecht, 183–190. https://doi.org/10.1007/978-94-011-0511-8_12

Ronquist F, Huelsenbeck JP (2003) MrBayes 3: Bayesian phylogenetic inference under mixed models. Bioinformatics, 19: 1572–1574. https://doi.org/10.1093/bioinformatics/btg180

Ruma K, Sunil K, Kini KR, Prakash HS (2015) Genetic diversity and antimicrobial activity of endophytic *Myrothecium* spp. isolated from *Calophyllum apelatum* and *Garcinia morella*. Molecular Biology Reports 42: 1533–1543. https://doi.org/10.1007/s11033-015-3884-8

Saccardo PA (1917) Notae mycologicae series XXIII. Fungi Philippinenses. Atti della Accademia Scientifica Veneto-Trentino-Istriana. 10: 57–94.

Spegazzini C (1911) Mycetes Argentinenses (Series V). Anales del Museo Nacional de Historia Natural Buenos Aires. ser. 3, 13: 329–467.

Stamatakis A (2006) RAxML-VI-HPC: maximum likelihood-based phylogenetic analyses with thousands of taxa and mixed models. Bioinformatics 22: 2688. https://doi.org/10.1093/bioinformatics/btl446

Tibpromma S, Hyde KD, Jeewon R, Maharachchikumbura SSN, Liu JK, Bhat DJ et al. (2017) Fungal diversity notes 491–602: taxonomic and phylogenetic contributions to fungal taxa. Fungal Diversity 83: 1–261 https://doi.org/10.1007/s13225-017-0378-0

Tulloch M (1972) The genus *Myrothecium* Tode ex Fr. Mycological Papers 130: 1–42.

Von Höhnel FV (1905) Über *Myrothecium* und Formverwandte Gattungen. Annales Mycologici 3: 559–560.

Wagenaar MM, Clardy J (2001) Two new roridins isolated from *Myrothecium* sp. The Journal of Antibiotics 54: 517. https://doi.org/10.7164/antibiotics.54.517

Watanabe T, Watanabe Y, Nakamura K (2003) *Myrothecium dimorphum* sp. nov. a soil fungus from beach sand in the Bonin (Ogasawara) Islands, Japan. Mycoscience, 44(4):283–286. https://doi.org/10.1007/s10267-003-0112-5

White TJ, Burns T, Lee S, Taylor F, White TJ, Lee S-H, Taylor L, Shawe-Taylor J (1990) Amplification and direct sequencing of fungal ribosomal RNA genes for phylogenetics. In: Innis MA, Gelfand DH, Sninsky JJ et al. (Eds) PCR protocols: a guide to methods and applications: 282–287. https://doi.org/10.1016/B978-0-12-372180-8.50042-1

Wu YM, Jiang YL, Ma YN Zhang TY (2014) Two new species of *Myrothecium* from the Qinghai-Tibet Plateau Area, China. Mycotaxon 129: 403–406. https://doi.org/10.5248/122.171

Zhang ZF, Liu F, Zhou X, Liu X.Z, Liu S.J, Cai L (2017) Culturable mycobiota from Karst caves in China, with descriptions of 20 new species. Persoonia 39: 1–31. https://doi.org/10.3767/persoonia.2017.39.01

Supplementary material 1

Figure S1. The ML consensus tree inferred based on *ITS* partial sequence with bootstrap values for ML (> 70%) and posterior probability (PP) (PP > 0.95) labeled to the left of a node (ML/PP)

Authors: Junmin Liang, Guangshuo Li, Shiyue Zhou, Meiqi Zhao, Lei Cai

Data type: phylogenetic data

Explanation note: The type strains were labeled with “T”. Strains obtained from this study are in red.

Link: https://doi.org/10.3897/mycokeys.51.31957.suppl1

Supplementary material 2

Figure S2. The ML consensus tree inferred based on *tub2* partial sequence with bootstrap values for ML (> 70%) and posterior probability (PP) (PP > 0.95) labeled to the left of a node (ML/PP)

Authors: Junmin Liang, Guangshuo Li, Shiyue Zhou, Meiqi Zhao, Lei Cai

Data type: phylogenetic data

Explanation note: The type strains were labeled with "T". Strains obtained from this study are in red.

Link: https://doi.org/10.3897/mycokeys.51.31957.suppl2

Supplementary material 3

Figure S3. The ML consensus tree inferred based on *cmdA* partial sequence with bootstrap values for ML (> 70%) and posterior probability (PP) (PP > 0.95) labeled to the left of a node (ML/PP)

Authors: Junmin Liang, Guangshuo Li, Shiyue Zhou, Meiqi Zhao, Lei Cai

Data type: phylogenetic data

Explanation note: The type strains were labeled with "T". Strains obtained from this study are in red.

Link: https://doi.org/10.3897/mycokeys.51.31957.suppl3

Supplementary material 4

Figure S4. The ML consensus tree inferred based on *rpb2* partial sequence with bootstrap values for ML (> 70%) and posterior probability (PP) (PP > 0.95) labeled to the left of a node (ML/PP)

Authors: Junmin Liang, Guangshuo Li, Shiyue Zhou, Meiqi Zhao, Lei Cai

Data type: phylogenetic data

Explanation note: The type strains were labeled with "T". Strains obtained from this study are in red.

Link: https://doi.org/10.3897/mycokeys.51.31957.suppl4

Supplementary material 5

Figure S5. The ML consensus tree inferred based on LSU and *rpb2* partial sequences with bootstrap values for ML (> 70%) and posterior probability (PP) (PP > 0.95) labeled to the left of a node (ML/PP)

Authors: Junmin Liang, Guangshuo Li, Shiyue Zhou, Meiqi Zhao, Lei Cai

Data type: phylogenetic data

Explanation note: The type strains were labeled with "T". Strains obtained from this study are in red.

Link: https://doi.org/10.3897/mycokeys.51.31957.suppl5

Supplementary material 6

Table S1. NCBI GenBank accessions of *28S* ribosomal DNA large-subunit sequences (LSU) used in the phylogenetic analyses

Authors: Junmin Liang, Guangshuo Li, Shiyue Zhou, Meiqi Zhao, Lei Cai

Data type: phylogenetic data

Link: https://doi.org/10.3897/mycokeys.51.31957.suppl6

MycoKeys 51: 55–64 (2019)
doi: 10.3897/mycokeys.51.30798
http://mycokeys.pensoft.net

RESEARCH ARTICLE

A peer-reviewed open-access journal
MycoKeys
Launched to accelerate biodiversity research

Blastosporium persicolor gen. et sp. nov., a new helotialean fungus

Hua Zheng[1,*], ZhenNa Zhang[2,*], ZhiJia Wen[2], Rafael F. Castañeda-Ruiz[3], ZeFen Yu[1]

1 *Laboratory for Conservation and Utilization of Bio-resources, Key Laboratory for Microbial Resources of the Ministry of Education, Yunnan University, Kunming, Yunnan, 650091, China* **2** *Xiamen Tobacco Industrial CO., LTD, Xiamen, Fujian, China* **3** *Associate Research of Instituto de Investigaciones Fundamentales en Agricultura Tropical Alejandro de Humboldt (INIFAT), Calle 1 Esq. 2, Santiago de Las Vegas, C. Habana, C.P. 17200, Cuba*

Corresponding author: *ZeFen Yu* (zfyuqm@hotmail.com)

Academic editor: *T. Lumbsch* | Received 24 October 2018 | Accepted 9 April 2019 | Published 22 April 2019

Citation: Zheng H, Zhang ZN, Wen Z, Castañeda-Ruiz RF, Yu ZF (2019) *Blastosporium persicolor* gen. et sp. nov., a new helotialean fungus. MycoKeys 51: 55–64. https://doi.org/10.3897/mycokeys.51.30798

Abstract

A new genus and species, *Blastosporium persicolor*, is described and illustrated from leaves of mildewed tobacco. It is characterised by branched, septate hyphae from which arise macronematous, unbranched or spaced branched conidiophores and mono- or polyblastic conidiogenous cells that produced solitary and blastocatenate, obovoid, oblong, ellipsoidal, allantoid, broad fusiform to irregular, unicellular, hyaline conidia. The phylogenetic analyses, based on the combined sequence data from the small and large nuclear subunit ribosomal DNA (SSU and LSU), placed *B. persicolor* in the Leotiomycetes class, Helotiales order.

Keywords

Ascomycota, Pezizomycotina, phylogeny, *Nicotiana tabacum*

Introduction

The Kingdom Fungi contains a huge number of species, which continues to rise with more collections. With the advance in the studies of DNA sequence data, the fungal classification system has been updated over the years. Many described species obtained

* These authors contributed equally to this work

new taxonomic status after the molecular data and have been processed. Leotiomycetes is a large class in Ascomycota and has potential taxonomic value relating to the ecology and biology. The traditional classification of Leotiomycetes at high levels has experienced considerable challenges with the inclusion of the molecular techniques in systematics studies. For example, early research accepted five orders, 21 families and about 510 genera in the Leotiomycetes on the basis of both traditional classification and molecular phylogenetic studies (Eriksson 2005, Kirk et al. 2001), but a recent study reported a new classification of Leotiomycetes, including 11 orders, 44 families and about 590 genera (Wijayawardene et al. 2018) and this classification also lacks sufficient DNA sequence data. In Leotiomycetes, the order Helotiales, one of the largest non-lichen-forming ascomycetous groups, is composed of fungi of diverse morphology and ecology. Of these, members of the Helotiales thrive in various ecosystems and cover a broad range of niches and helotialean fungi have been found as plant pathogens, endophytes, nematode-trapping fungi, mycorrhizae, ectomycorrhizal parasites, fungal parasites, terrestrial saprobes, aquatic saprobes, root symbionts and wood rot fungi (Wang et al. 2006).

During a survey of fungi growing on mildewed tobacco leaves, an unknown fungus was found. Based on its morphological characters and DNA sequence data, it is proposed as a new asexual genus and species, *Blastosporium persicolor*.

Materials and methods

Isolation and morphological study of strain

Samples of the mildewed tobacco leaves were collected from Xiamen Logistics Warehousing Center. Samples were preserved in zip-locked plastic bags, labelled and transported to the laboratory. The procedure was as follows: samples (5g) were placed in PDA liquid medium (200 g potato, 20 g glucose, 1000 ml distilled water), shaken at 140 rpm/min for 1 h and the filtrate was collected. The filtrate was coated on a CMA plate (20 g cornmeal, 10 g agar, 1000 ml distilled water) at 28 °C, supplemented with two antibiotics (penicillin G, 0.5 g/l; and streptomycin, 0.5 g/l; Gams et al. 1998). After 3–5 days, single colonies were isolated into pure culture, grown on potato dextrose agar plates (PDA). The characteristics of the colonies were from PDA, CMA and SNA (synthetic low nutrient agar). Microscopic characteristics were made from cultures growing on CMA after incubation at room temperature for one week.

The pure cultures and dried cultures were deposited in the Herbarium of the Laboratory for Conservation and Utilization of Bio-resources, Yunnan University, Kunming, Yunnan, P.R. China (YMF, formerly Key Laboratory of Industrial Microbiology and Fermentation Technology of Yunnan).

DNA extraction, polymerase chain reaction (PCR) amplification and sequencing

Pure cultures were grown on PDA for 5 days at 25 °C. Actively growing mycelium was scraped off the surface of a culture and transferred to 2 ml Eppendorf micro-centrifuge tubes. Total genomic DNA was extracted according to the procedures in Turner et al. (1997). Primers used for PCR amplification and sequencing of nucSSU rDNA, nucLSU rDNA and ITS rDNA were NS1-NS4, LROR-LR7 and ITS1-ITS4, respectively (White et al. 1990, Vilgalys and Hester 1990). Detailed protocols and PCR conditions for the amplification were fully described by Su et al. (2015). PCR products were then purified using a commercial Kit (Bioteke Biotechnology Co, Ltd, China) and forward and reverse sequences with a LI-COR 4000L automatic sequencer, using a Thermo Sequenase-kit, as described by Kindermann et al. (1998). The sequences were deposited in the National Center for Biotechnology Information (NCBI) and the accession numbers are listed in Table 1.

Sequence alignment and phylogenetic analysis

Other fungal sequences were obtained from the GenBank nucleotide database. DNA sequence data were aligned using ClustalX 1.83 (Higgins 1994) with default parameters and the consensus sequences were manually adjusted and linked in BioEdit v.7.0 (Hall 1999). Manual gap adjustments were made to improve the alignment and ambiguously aligned regions were also excluded. Portions of the 5'- and 3'-ends of the nuclear small and large subunits ribosomal DNA (nucSSU and nucLSU) were excluded from all analyses and coded by a question mark (?). MrBayes (Ronquist and Huelsenbeck 2003) was used to calculate the SSU rRNA and LSU rRNA sequence-based Bayesian inference of the phylogeny tree, with the following parameters: ngen=1,000,000; samplefr=1,000; printfr=1,000. The GenBank accession numbers of sequences used in the phylogenetic analysis are shown in Table 1 including the classes of Leotiomycetes, Arthoniomycetes, Dothideomycetes, Eurotiomycetes, Orbiliomycetes, Pezizomycetes and Sordariomycetes. *Candida albicans* (C.P. Robin) Berkhout (Saccharomycetes) was used as outgroup.

Results

Sequence analyses

In BLAST searches, the ITS sequence *B. persicolor*, MH992518, had the highest similarity of 88% with *Tetracladium* and 87% with *Chalara* (Corda) Rabenh., both belonging to Leotiomycetes. Therefore, most sequences are mainly from Leotiomycetes in the dataset. The dataset comprised 57 taxa representing 7 classes, 11 orders, 22

Table 1. Strains and the GenBank accession numbers of sequences used in the molecular phylogenetic analyses in this study.

Name	Strain	GenBank accession number	
		LSU	SSU
Arthonia caesia (Flot) Körb.	AFTOL-ID 775	FJ469668	–
Arthrobotrys elegans (Subram & Chandrash) Seifert & W.B. Kendr.	AFTOL-ID 1252	FJ176864	FJ176810
Arthrocladiella mougeotii (Lév) Vassilkov	–	AB022379	AB033477
Blastosporium persicolor Z. F. Yu & H. Zheng	**YMF1.05546**	**MH992517**	**MH992516**
Blumeria graminis (DC.) Speer	–	AB022362	AB033476
Brasiliomyces trinus (Harkn) R.Y. Zheng	–	AB022350	–
Bryoglossum gracile (P. Karst.) Redhead	MBH52481	AY789420	AY789419
Bulgaria inquinans (Pers.) Fr.	ZW-Geo52-Clark	AY789344	AY789343
Candida albicans (C.P. Robin) Berkhout	WO1	L28817	X53497
Capnodium coffeae Pat.	CBS 147.52	DQ247800	DQ247808
Chlamydotubeufia huaikangplaensis Boonmee & K.D. Hyde	MFLUCC10-0926	JN865198	–
Ciboria batschiana (Zopf) N. F. Buchw.	WZ-JXD-22	AY789322	–
Cudonia circinans (Pers.) Fr.	OSC56399	AF279379	AF107343
Cyttaria darwinii Berk.	14	EU107208	EU107181
Dermea acerina (Peck) Rehm	CBS 161.38	DQ247801	DQ247809
Disciotis venosa (Pers.) Arnould	AFTOL-ID 179	AY544667	AY544711
Dothidea sambuci (Pers.) Fr.	AFTOL-ID 274	AY544681	AY544722
Erysiphe australiana (McAlpine) U. Braun & S. Takam.	–	AB022407	–
Erysiphe cornicola Meeboon & S. Takam.	–	AB022389	–
Erysiphe glycines F. L. Tai	MUMH52	AB022397	AB120748
Erysiphe gracilis R. Y. Zheng & G. Q. Chen	–	AB022357	–
Erysiphe mori (I. Miyake) U. Braun & S. Takam.	–	AB022418	AB033484
Erysiphe simulans (E. S. Salmon) U. Braun & S. Takam.	–	AB022395	–
Eupenicillium limosum S. Ueda	AFTOL-ID 2014	EF411064	EF411061
Fabrella tsugae (Farl) Kirschst.	–	AF356694	–
Geoglossum glabrum Pers.	OSC60610	AY789317	AY789316
Geoglossum umbratile Sacc.	Mycorec1840	AY789303	AY789302
Helicoma chlamydosporum Shearer	CBS 160.69	AY856875	AY856923
Helicoma vaccinii Carris	CBS 216.90	AY856879	AY856926
Helicomyces roseus Link	CBS 283.51	AY856881	AY856928
Helicosporium guianense Linder	CBS 269.52	AY856893	AY856938
Holwaya mucida (Schulzer) Korf & Abawi	B 70 0009352	DQ257356	DQ257355
Lachnum bicolor (Bull.) P. Karst.	AFTOL-ID 177	AY544674	AY544690
Lachnum virgineum (Batsch) P. Karst.	AFTOL-ID 49	AY544646	AY544688
Leotia lubrica (Scop.) Pers.	ZW-Geo59-Clark	AY789359	AY789358
Monascus purpureus Went	AFTOL-ID 426	DQ782908	DQ782881
Morchella esculenta (L.) Pers.	AFTOL-ID 60	AY544664	AY544708
Mycosphaerella punctiformis (Pers.) Starbäck	AFTOL-ID 942	DQ470968	DQ471017
Neoerysiphe galeopsidis (DC.) U. Braun	–	AB022369	–
Neofabraea malicorticis (Cordley) H.S. Jacks.	AFTOL-ID 149	AY544662	AY544706
Orbilia vinosa (Alb. & Schwein.) P. Karst.	AFTOL-ID 905	DQ470952	DQ471000
Penicillium freii Frisvad & Samson	DAMO 216705	AY640958	AY640998
Phyllactinia moricola (Henn.) Homma	–	AB022401	AB033481
Piceomphale bulgarioides (P. Karst.) Svrček	1589.P	Z81415	–
Pleochaeta shiraiana (Henn.) Kimbr. & Korf	MUMH36	AB022403	AB120750
Podosphaera tridactyla (Wallr.) de Bary	–	AB022393	–
Roccellographa cretacea J. Steiner	AFTOL-ID 93	DQ883696	DQ883705
Rutstroemia bolaris (Batsch) Rehm	1526.P	Z81419.1	–
Sawadaea polyfida (C.T. Wei) R.Y. Zheng & G.Q. Chen	–	AB022364	–
Schismatomma decolorans (Erichsen) Clauzade & Vězda	DUKE 0047570	NG_027622	NG_013155
Scleromitrula shiraiana (Henn.) S. Imai	Hirayama062001	AY789407	AY789406
Sclerotinia sclerotiorum (Lib.) de Bary	WZ0067	AY789347	AY789346
Spathularia flavida Pers.	wz138	AF433142	AY789356
Thaxteriella inthanonensis Boonmee & K.D. Hyde	MFLUCC11-0003	JN865199	–
Trichoglossum hirsutum (Pers.) Boud.	AFTOL-ID 64	AY789313	AY789312
Vibrissea flavovirens (Pers.) Korf & J.R. Dixon	MBH39316	AY789426	AY789425
Vibrissea truncorum (Alb. & Schwein) Fr.	CUP-62562	AY789402	AY789401

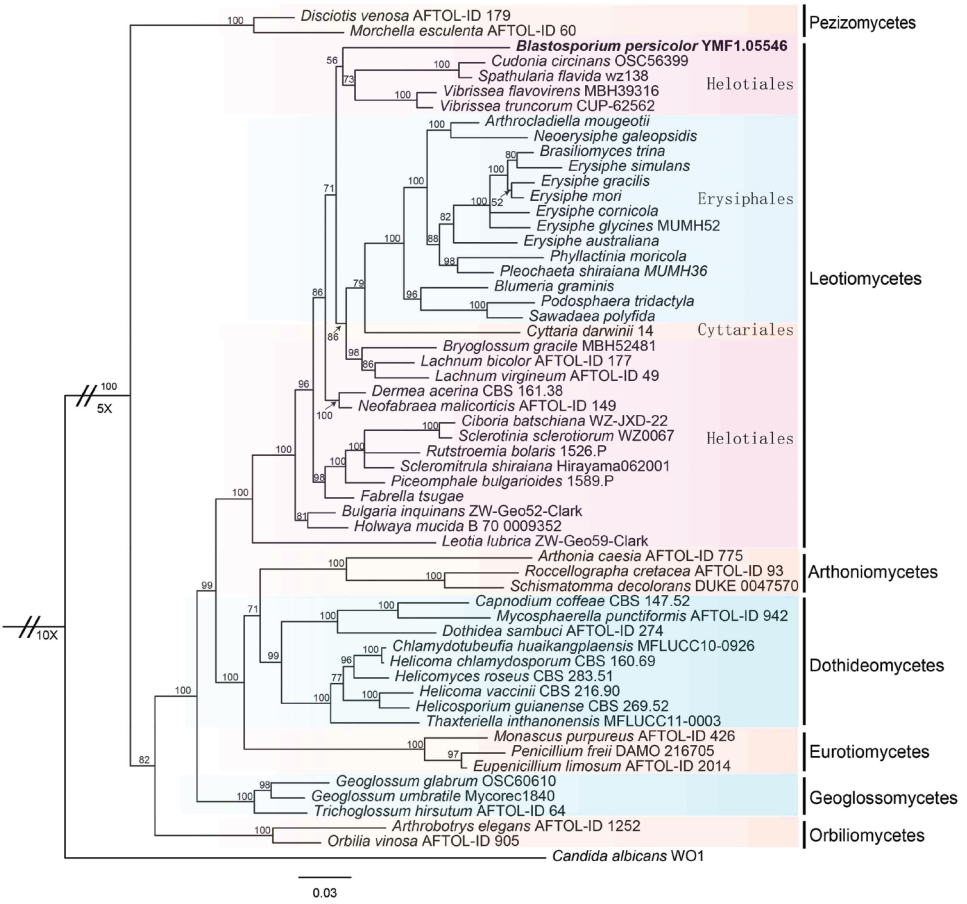

Figure 1. Phylogenetic tree based on Bayesian analysis of the combined LSU and SSU sequences. *Candida albicans* is used as outgroup. Bayesian bootstraps were indicated by the nodes and the scale bar shows the expected changes per site. The new genus proposed is in boldface.

families and 57 species with *Candida albicans* as outgroup. Other DNA sequences were obtained from the GenBank. The final alignment comprised a total of 1635 base pairs (TreeBASE accession number: 23451), which combined the SSU rRNA and LSU rRNA sequences and the dataset was analysed by the Bayesian Inference method. The topologies of the tree are shown with the Bayesian posterior probabilities values for clades of analyses (Figure 1). In this tree, the new genus is phylogenetically placed in the Leotiomycetes. This monophyletic group formed a close relationship with several genera, which are grouped in this class, e.g. *Vibrissea flavovirens* and *Vibrissea truncorum* (Vibrisseaceae), *Cudonia circinans* and *Spathularia flavida* (Cudoniaceae) that are grouped with the new genus in the same clade. Therefore, analysis of partial LSU and SSU nuc rDNA sequences placed the new genus in the Leotiomycetes. Additionally, the tree also supports the fact that the Helotiales is not monophyletic.

Taxonomy

Blastosporium Z. F. Yu & H. Zheng, gen. nov.

MycoBank MB828280

Etymology. Latin, *Blasto-*, referring to the blastic conidial ontogeny, + Latin, *sporium*, referring to the conidia.

Type species. *Blastosporium persicolor* Z. F. Yu & H. Zheng

Diagnosis. Characterised by mono- and polyblastic, integrated or discrete conidiogenous cells, solitary or blastocatenate, unicellular, obovoid, oblong, ellipsoidal, allantoid conidia (5–8 × 2.3–4.1 μm). Differs from the genus *Tetracladium* De Wild. by macronematous or semi-macronematous conidiophores and mono- and polyblastic conidiogenous cells.

Description. Mycelium partly superficial and partly immersed, composed of branched, septate, smooth, hyaline hyphae. *Conidiophores* macronematous or semi-macronematous, erect or prostrate, smooth, hyaline, sometimes reduced to conidiogenous cells. *Conidiogenous cells* mono- and polyblastic, terminal, integrated or discrete, determinate, sometimes with sympodial elongations, smooth, hyaline. *Conidia* solitary or blastocatenate, acrogenous, unicellular, obovoid, oblong, ellipsoidal, allantoid, broad fusiform to irregular, smooth, hyaline.

Distribution. China.

Notes. *Blastosporium* is superficially similar to the genera, *Acaromyces* Boekhout et al. and *Meira* Boekhout et al. Their conidiophores are reduced to conidiogenous cells, which produce solitary or sometimes blastocatenate, unicellular, hyaline conidia by blastic conidial ontogeny. These genera are yeast-like hyphomycetes that have been connected phylogenetically with Exobasidiomycetidae (Ustilaginomycetes, Basidiomycota) (Boekhout et al. 2003, Seifert et al. 2011).

Hyphozyma de Hoog & M.T.Sm. also superficially resembles *Blastosporium*, but *Hyphozyma* is a typical yeast-like hyphomycete, characterised by undifferentiated conidiophores and conidia are unicellular, hyaline, solitary or produced in basipetal chains (de Hoog and Smith 1981, Seifert et al. 2011).

Blastosporium persicolor Z. F. Yu & H. Zheng, sp. nov.

MycoBank MB828281
Figure 2

Etymology. Latin, *persicolor*, referring to the apricot colour of the colonies on PDA medium.

Description. Colonies on CMA with 1–2 concentric rings slightly curled, entire at the margin, light orange-yellowish-pinkish colour. Reverse yellowish-orange. Mycelium partly superficial and partly immersed, composed of branched, septate, smooth-walled, creeping, 2.0–3.3 μm wide hyphae. *Conidiophores* macronematous or semi-

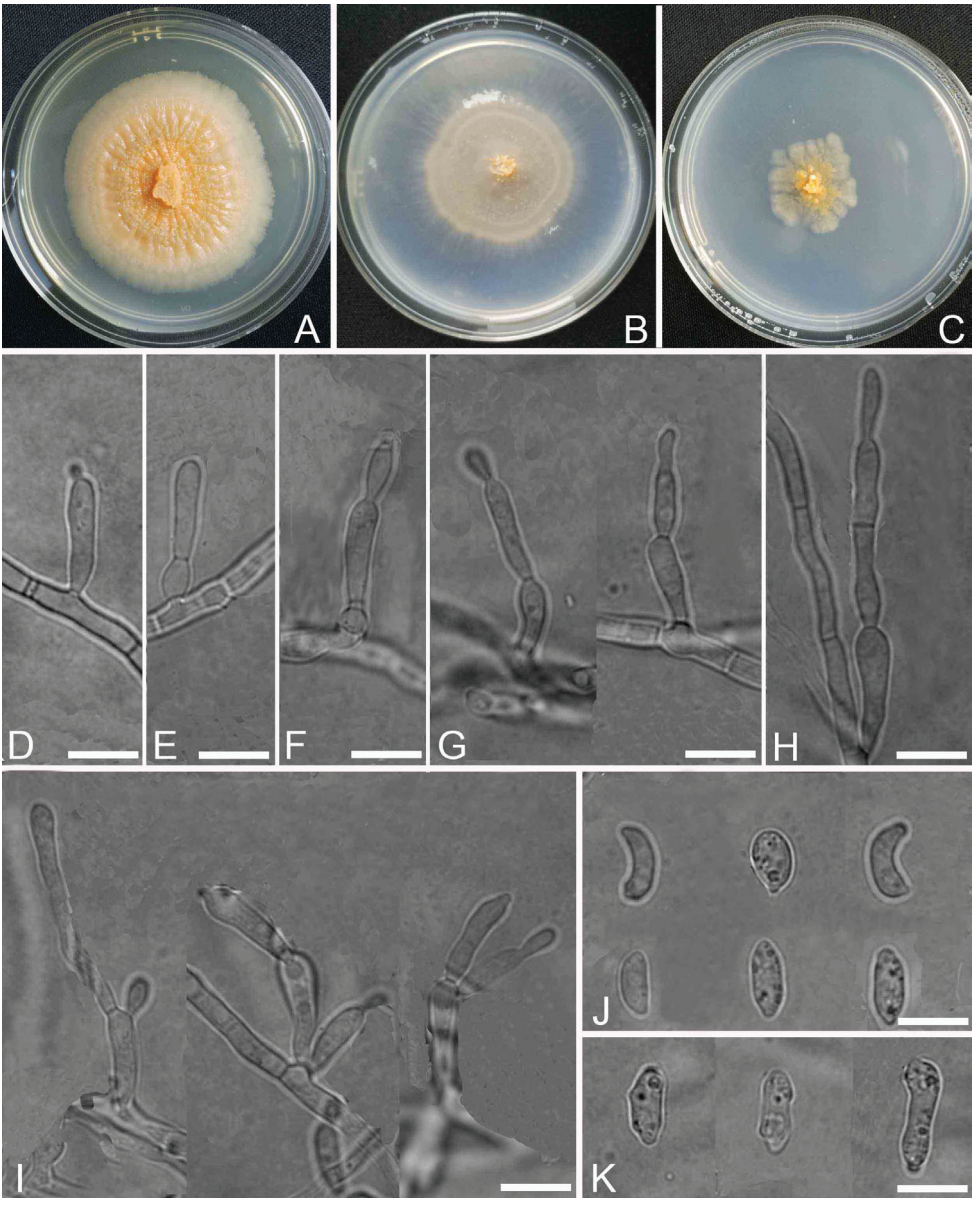

Figure 2. Cultures and anamorph of *Blastosporium persicolor* (YMF 1.05546). **A–C** Cultures (**A** on PDA **B** on CMA **C** on SNA) at 25 °C after 12 days **D–H** conidiophores and monoblastic conidiogenous cells **I** conidiophores and polyblastic conidiogenous cells **J, K** conidia (**J** one scar on conidia **K** multi-scars on conidia); Scale bar: 10 μm (**D–K**).

macronematous, mononematous, erect or prostrate, straight or flexuous, unbranched or slightly branched, hyaline, smooth-walled, 35–14.4 × 1.8–3.5 μm. *Conidiogenous cells* mostly monoblastic, sometime polyblastic after several sympodial elongations,

integrated or discrete, terminal or intercalary, 7.0–13.1× 2.6–3.3 μm, clavate or cylindrical, with a distinct or inconspicuous denticle at the conidiogenous loci. *Conidia* solitary or blastocatenate, acrogenous, obovoid, oblong, ellipsoidal, subcylindrical, allantoid, broad fusiform to irregular, slightly attenuated, truncate at the base or at the ends, unicellular, smooth, hyaline, 5–8 × 2.3–4.1 μm. Sexual form unknown.

Culture characteristics. (in darkness, at 25 °C after 10 d). Colonies attaining 1.5–1.7 cm diam. on PDA, 1.0–1.2 cm diam. on SNA, 1.5–1.7 cm on CMA. On PDA, colonies plicated, orange, reverse pale yellow, margin smooth and entire; sporulation abundant. On SNA, colonies flat, white to cream-coloured, flocculent, reverse white, growing slowly, sporulation abundant. The fungus does not grow at 35 °C on PDA, CMA and SNA.

Type. CHINA. Xiamen, Fujian Province, 24°33'9.6"N, 117°55'7.4"E, 23 m alt., from mildewed tobacco (*Nicotiana tabacum* L.) leaves, June 2018, Z.N. Zhang (dried slide YMFT 1.05546, holotype; ex-type YMF 1.05546).

Discussion

To determine the phylogenetic placement of this species, *Blastosporium persicolor* was analysed with species from 7 classes, Leotiomycetes, Arthoniomycetes, Dothideomycetes, Eurotiomycetes, Orbiliomycetes, Pezizomycetes and Geoglossomycetes (Wang et al. 2006). By Bayesian analysis, the new genus was placed in the Helotiales, Leotiomycetes. In the tree, *B. persicolor* grouped with the *Cudonia-Spathularia* clade and *Vibrissea* clade, but the placement did not receive strong support. Therefore, we have temporarily designated this species as a new genus and family *incertae sedis*.

In the Helotiales, many genera, such as *Bulgaria* Fr. (Bulgariaceae), *Rutstroemia* P. Karst. (Rutstroemiaceae) and *Hegermila* Raitv. (Hyaloscyphaceae), were only observed as sexual morphs, but *Neofabraea* H.S. Jacks (Dermateaceae) and *Articulospora* Ingold (Helotiaceae) were observed as having asexual and sexual morphs (Chen et al. 2015, Wijayawardene et al. 2018, Wang et al. 2015a). In this study, we just observed the asexual morph of *B. persicolor*.

Based on ITS sequence data, *B. persicolor* is 88% similar to the genus *Tetracladium* De Wild. (*T. marchalianum* De Wild. as the type species), which was placed in the Helotiales and family incertae sedis. Moreover, *Blastosporium* shares some morphological features with *Tetracladium* as pale yellow and compact colonies and hyphae branched, septate and hyaline and both *Blastosporium* and *Tetracladium* sporulated abundantly on natural substrates (Sati et al. 2009, Wang et al. 2015b). However, *B. persicolor* is obviously distinct from the genus *Tetracladium* by the size and shape of conidia.

By molecular phylogeny analysis, *Blastosporium* belongs to the order Helotiales that currently contains 27 families (Wijayawardene et al. 2018). Moreover, members of the Helotiales cover a broad range of niches, such as plant pathogens, endophytes and aquatic hyphomycetes. *Blastosporium persicolor* was discovered from mildewed tobacco; therefore, it may be a plant pathogen.

Acknowledgements

This work was financed by the National Natural Science Foundation Program of PR China (31570023, 31770026). We are grateful to two reviewers for critically reviewing the manuscript and for providing helpful suggestions to improve this paper.

References

Boekhout T, Theelen B, Houbraken J, Robert V, Scorzetti G, Gafni A, Gerson U, Sztejnberg A (2003) Novel anamorphic mite-associated fungi belonging to the Ustilaginomycetes: *Meira geulakonigii* gen. nov., sp. nov., *Meira argovae* sp. nov. and *Acaromyces ingoldii* gen. nov., sp. nov. International Journal of Systematic and Evolutionary Microbiology 53(5): 1655–1664. https://doi.org/10.1099/ijs.0.02434-0

Chen C, Verkley GJ, Sun G, Groenewald JZ, Crous PW (2015) Redefining common endophytes and plant pathogens in *Neofabraea*, *Pezicula*, and related genera. Fungal Biology 120: 1291–1322. https://doi.org/10.1016/j.funbio.2015.09.013

de Hoog GS, Smith MT (1981) *Hyphozyma*, a new genus of yeast-like hyphomycetes. Antonie van Leeuwenhoek 47: 339–352. https://doi.org/10.1007/BF02350784

Eriksson OE (2005) Outline of Ascomycota-2005. Myconet 11: 1–113.

Gams W, Hoekstra ES, Aptroot A (1998) CBS course of mycology, 4th edn. Centraalbureau voor Schimmelcultures, Baarn.

Hall TA (1999) BioEdit: a user-friendly biological sequence alignment editor and analysis program for Windows 95/98/NT. Nucleic Acids Symposium Series 41: 95–98. https://doi.org/10.1007/978-1-4757-0905-6_31

Higgins DG (1994) CLUSTAL V: multiple alignment of DNA and protein sequences. Methods in Molecular Biology 25: 307–318. https://doi.org/10.1385/0-89603-276-0:307

Kindermann J, El-Ayouti Y, Samuels GJ, Kubicek CP (1998) Phylogeny of the genus *Trichoderma* based on sequence analysis of the internal transcribed spacer region 1 of the rDNA clade. Fungal Genetics and Biology 24(3): 298–309. https://doi.org/10.1006/fgbi.1998.1049

Kirk PM, Cannon PF, David JC, Stalpers JA (2001) Ainsworth and Bisby's dictionary of the fungi (9th edn). CAB International, Wallingford.

Ronquist F, Huelsenbeck JP (2003) MrBayes 3: Bayesian phylogenetic inference under mixed models. Bioinformatics 19: 1572–1574. https://doi.org/10.1093/bioinformatics/btg180

Sati SC, Arya P, Belwal M (2009) *Tetracladium nainitalense* sp. nov. a root endophyte from Kumaun Himalaya, India. Mycologia 101(5): 692–695. https://doi.org/10.3852/08-192

Seifert KA, Morgan-Jones G, Gams W, Kendrick B (2011) The genera of hyphomycetes. CBS Biodiversity Series 9.

Su HY, Udayanga D, Luo ZL, Manamgoda DS, Zhao YC, Yang J, Liu XY, Mckenzie EH, Zhou DQ, Hyde KD (2015) Hyphomycetes from aquatic habitats in Southern China: species of *Curvularia* (Pleosporaceae) and *Phragmocephala* (Melannomataceae). Phytotaxa 226(3): 201–216. https://doi.org/10.11646/phytotaxa.226.3.1

Turner D, Kovacs W, Kuhls K, Lieckfeldt E, Peter B, Arisan-Atac I, Strauss J, Samuels GJ, Börner T, Kubicek CP (1997) Biogeography and phenotypic variation in *Trichoderma* sect. *Longibrachiatum* and associated *Hypocrea* species. Mycological Research 101(4): 449–459. https://doi.org/10.1017/S0953756296002845

Vilgalys R, Hester M (1990) Rapid genetic identification and mapping of enzymatically amplified ribosomal DNA from several *Cryptococcus* species. Journal of Bacteriology 172: 4238–4246. https://doi.org/10.1128/jb.172.8.4238-4246.1990

Wang L, Sun X, Wei JG, Lou JF, Guo LD (2015a) A new endophytic fungus *Neofabraea illicii*, isolated from *Illicium verum*. Mycoscience 56(3): 332–339. https://doi.org/10.1016/j.myc.2014.10.002

Wang M, Jiang X, Wu W, Hao Y, Su Y, Cai L, Xiang M, Liu X (2015b) Psychrophilic fungi from the world's roof. Persoonia 34: 100–112. https://doi.org/10.3767/003158515X685878

Wang Z, Johnston PR, Takamatsu S, Spatafora JW, Hibbett DS (2006) Toward a phylogenetic classification of the Leotiomycetes based on rdna data. Mycologia, 98(6): 1065–1075. https://doi.org/10.3852/mycologia.98.6.1065

White TJ, Bruns T, Lee S, Taylor J (1990) Amplification and direct sequencing of fungal ribosomal RNA genes for phylogenetics. PCR Protocols: a guide to methods and applications 18(1): 315–322. https://doi.org/10.1016/B978-0-12-372180-8.50042-1

Wijayawardene NN, Hyde KD, Lumbsch HT, Liu JK, Maharachchikumbura SS, Ekanayaka AH, Tian Q, Phookamsak R (2018) Outline of ascomycota: 2017. Fungal Diversity 88(1): 167–263. https://doi.org/10.1007/s13225-018-0394-8

MycoKeys 51: 65–83 (2019)
doi: 10.3897/mycokeys.51.33513
http://mycokeys.pensoft.net

RESEARCH ARTICLE

A peer-reviewed open-access journal
MycoKeys
Launched to accelerate biodiversity research

A new record of *Ganoderma tropicum* (Basidiomycota, Polyporales) for Thailand and first assessment of optimum conditions for mycelia production

Thatsanee Luangharn[1,2,3,4], Samantha C. Karunarathna[1,3,4], Peter E. Mortimer[1,4], Kevin D. Hyde[3,5], Naritsada Thongklang[5], Jianchu Xu[1,3,4]

1 *Key Laboratory for Plant Diversity and Biogeography of East Asia, Kunming Institute of Botany, Chinese Academy of Sciences, Kunming 650201, Yunnan, China* **2** *University of Chinese Academy of Sciences, Beijing 100049, China* **3** *East and Central Asia Regional Office, World Agroforestry Centre (ICRAF), Kunming 650201, Yunnan, China* **4** *Centre for Mountain Ecosystem Studies (CMES), Kunming Institute of Botany, Kunming 650201, Yunnan, China* **5** *Center of Excellence in Fungal Research, Mae Fah Luang University, Chiang Rai 57100, Thailand*

Corresponding author: *Jianchu Xu* (jxu@mail.kib.ac.cn); *Peter E. Mortimer* (peter@mail.kib.ac.cn)

Academic editor: *María P. Martín* | Received 30 January 2019 | Accepted 12 March 2019 | Published 7 May 2019

Citation: Luangharn T, Karunarathna SC, Mortimer PE, Hyde KD, Thongklang N, Xu J (2019) A new record of *Ganoderma tropicum* (Basidiomycota, Polyporales) for Thailand and first assessment of optimum conditions for mycelia production. MycoKeys 51: 65–83. https://doi.org/10.3897/mycokeys.51.33513

Abstract

In this study a new record of *Ganoderma tropicum* is described as from Chiang Rai Province, Thailand. The fruiting body was collected on the base of a living *Dipterocarpus* tree. The sample is described on the basis of morphological characteristics and phylogenetic analyses, and compared with closely related taxa. Multigene phylogenetic analyses of LSU, ITS, and RPB2 highly support the placement of the *G. tropicum* group with isolates from China and Taiwan (Maximum likelihood 100%, Maximum parsimony 100%, and Bayesian posterior probabilities 1.00). The optimal media, pH, and temperature for mycelial growth of the *G. tropicum* strain KUMCC18-0046 was also investigated and is reported as: PDA, MEA, and YPD, at pH 7–8 and 25–28 °C, respectively. This is the first report on the successful growing conditions for mycelial production, but unfortunately fruiting could not be achieved.

Keywords

Cultivation, medicinal mushroom, morphological characteristics, phylogeny, taxonomy

Introduction

Ganoderma P. Karst. was established as a white rot fungus (Ryvarden 2004), showing parasitic or pathogenic behavior on wide range of tree species (Ryvarden 2004; Pilotti 2005; Dai et al. 2007). *Ganoderma* is more frequently distributed in tropical and temperate regions worldwide (Cao and Yuan 2013), and the distribution of *G. tropicum* is limited to the tropics (Cao et al. 2012). *Ganoderma* is characterized by distinctive laccate or non-laccate, sessile to stipitate basidiomata, double-walled basidiospores, and interwall pillars (Karsten 1881; Moncalvo and Ryvarden 1997). *Polyporus lucidus* (Curtis) Fr. is the original type species of the genus (Moncalvo and Ryvarden 1997). There are 449 records in the Index Fungorum (http://www.indexfungorum.org/; accessed date: 25 January 2019) and 384 records of taxa in MycoBank (http://www.mycobank.org/; accessed date: 25 January 2019).

Ganoderma produces a high number of natural bioactive compounds, such as polysaccharides, triterpenoids, sterols, and secondary metabolites (i.e. ganoderic acid, ganodermanondiol, ganodermanontriol, and ganodermadiol), which can be used to remedy a wide range of diseases (Richter et al. 2015; Hapuarachchi et al. 2018b). Many compounds have been found in different species of *Ganoderma*, and extracts derived from *G. tropicum* contain phenolic compounds such gano-dermatropins A (1) and B (2), as well as compounds with antimicrobial activity (Hu et al. 2013). *Ganoderma tropicum* is recognized as a medicinal mushroom and has been recorded in the Chinese Pharmacopeia (Wu et al. 2013). The fruiting bodies contain natural triterpenes, primarily lanostanoid-type triterpenes, with potential use in chemotaxonomy (Ríos et al. 2012; Da Silva et al. 2013; Zhang et al. 2015).

The taxonomy of *Ganoderma* has been a constant topic of debate due to the high levels of phenotypic plasticity in species such as *G. lingzhi*, *G. lucidum*, and *G. sichuanense* (Pilotti et al. 2004; Wang et al. 2009; Cao et al. 2012; Dai et al. 2017; Loyd et al. 2018; Hapuarachchi et al. 2019). In an attempt to further our knowledge of the taxonomy this genus, we describe a specimen of *Ganoderma tropicum* as a new record for Thailand based on morphological characteristics and phylogenetic analyses, and the optimal conditions for mycelial growth of *G. tropicum* are also reported.

Methods

Sample collection and isolation

In October 2017, a single fresh basidiocarp of *Ganoderma tropicum* was collected on a living *Dipterocarpus* tree in a deciduous mixed rainforest dominated by *Castanopsis* and *Dendrocalamus strictus* during the dry season. The coordinates of the described area in Chiang Rai Province, Thailand are 19°49'23"N; 100°01'41"E, 41 m. The sample was then photographed and transported back to the laboratory where its

fresh macroscopic details were described. The culture was aseptically isolated by using heat sterilized forceps, transferring sections of internal tissue from fruiting bodies onto potato dextrose agar (PDA) and incubated at 25 °C, for 21 days, under dark conditions (Luangharn et al. 2017). After incubation, the agar surface was fully covered with white mycelium. The pure stock culture was then covered with mineral oil and deposited in the voucher culture collection of the Kunming Institute of Botany culture collection under the accession number KUMCC18-0046. The cultures are being maintained at 4 °C for further studies. The sample was then air dried at 45 °C for 48 hours until it was completely dehydrated. Finally, the herbarium material was deposited in the Herbarium of Mae Fah Luang University, Chiang Rai, Thailand (voucher number MFLU Herb. 17-1934) with duplicates in the Herbarium of Kunming Institute of Botany, Academia Sinica (HKAS), Yunnan Province, China (voucher number HKAS 97486).

Morphological study

Macro-morphological characteristics were described following the method by Lodge et al. (2004), while colors were recorded following (Ridgeway 1912). Macroscopic characteristics were determined according to the methodology described by Largent (1986). To observe microscopic characteristics, free-hand sections were made under a dissecting microscope (OLYMPUS SZ61) and mounted on a glass slide in 3–5% KOH, 1–3% Congo red, and Melzer's reagent for highlighting all tissues (Kreisel and Schauer 1987). Microphotography was done with a Nikon ECLIPSE Ni (Nikon, Tokyo, Japan) compound microscope, with a Canon EOS 600D (Tokyo, Japan) digital camera fitted on the top of the microscope. Basidiospores and hyphal system sizes, colour, and shapes were recorded and photographed. Measurements were taken using the Tarosoft® Image Framework program v. 0.9.0.7. The size and shape of basidiospores were followed [$Q = L/W$] and calculated considering the mean value of the lengths and widths in side view. The calculation was done by using at least 50 basidiospores from each basidiomata (Miettinen and Larsson 2006). The photographs were edited in Adobe Illustrator CS v. 3.

DNA extraction, PCR amplification, and sequencing

Dried internal tissues of the basidiocarp were ground and total DNA was extracted using the Biospin Fungus Genomic DNA Extraction Kit (BioFlux). The ITS, LSU, and RPB2 genes were amplified by Polymerase Chain Reaction (PCR). The PCR amplifications were performed in a total volume of 25 µL of PCR mixtures containing 9.5 µL ddH_2O, 12.5 µL of PCR master mix, 1 µL of DNA template, and 1 µL of each primer (10 µM). PCR amplification was carried out using primer pairs LROR/

LR5 for the nuclear ribosomal large subunit 28S rDNA gene (LSU), ITS5/ITS4 for internal transcribed spacer rDNA region (ITS1, 5.8S rDNA and ITS2), and fRPB2-5F/fRPB2-7cR for the partial RNA polymerase second largest subunit region (RPB2) (Vilgalys and Hester 1990; White et al. 1990; Liu et al. 1999). The PCR cycling amplification conditions incorporated the following modifications: LSU initial denaturation was at 95 °C for 3 min, followed by 35 cycles at 95 °C for 30 s, 56 °C for 45 s, 72 °C for 1 min, and a final extension of 72 °C for 10 min. The PCR cycling for ITS was as follows: initial denaturation at 95 °C for 3 min, followed by 35 cycles at 95 °C for 30 s, 55 °C for 1 min and 72 °C for 1 min and a final extension of 72 °C for 10 min. The PCR cycling for RPB2 was as follows: initial denaturation at 96 °C for 3 min, followed by 35 cycles at 95 °C for 35 s, 54 °C for 10 s, 72 °C for 10 s, and a final extension of 72 °C for 5 min. The sequencing of PCR products was carried out by Sangon Biotech Co., Shanghai, China. The nuclear ribosomal Internal Transcribed Spacer region (nrITS) of the fungi was amplified and the sequence was deposited in GenBank to obtain the accession number.

Sequence alignment and phylogenetic analyses

The sequence of the new record was subjected to standard BLAST searches of GenBank to determine the primary identity of the fungal isolate. All the other sequences of this study were retrieved from GenBank. All the sequences used to construct the phylogenetic tree are listed in Table 1; *Amauroderma calcitum* D.H. Costa Rezende & E.R. Drechsler-Santos (FLOR:50931) (Costa-Rezende et al. 2017) was used as the outgroup taxon. Sequences were aligned with MAFFT online server (Katoh and Standley 2013), and manually adjusted using Bioedit v. 7.2.5 (Hall 1999). Alignments were checked and optimized manually when necessary. Maximum parsimony (MP) analysis was performed with PAUP v. 4.0b10 (Swofford 2002). Maximum likelihood analyses (ML) were executed on the CIPRES webportal (Miller et al. 2010), performed using RAxML-HPC2 on XSEDE v. 8.2.8 (Stamatakis 2014), and carried out using raxmlGUI v. 1.3.1 (Silvestro and Michalak 2011). The best fitting substitution model for each single gene partition and the concatenated data set were determined in MrModeltest 2.3 (Nylander 2004). Bayesian inference posterior probabilities (PP) with GTR+I+G model was used for each partition. Bayesian Markov Chain Monte Carlo (MCMC) analyses were conducted in MrBayes v. 3.2.2 (Huelsenbeck and Ronquist 2001). The number of generations was set at 1,000,000, with trees being sampled every 100 generations (a total of 10,000 trees), resulting in an average standard deviation of split frequencies below 0.01. Based on the tracer analysis, the first sampled topologies of 2000 trees representing 20% of burn-in phase were discarded. The remaining 8000 trees were used for calculating posterior probabilities (PP) in the majority rule consensus tree (Larget and Simon 1999).

Phylogenetic trees and data files were figured in FigTree v. 1.4.0 (Rambaut 2012) and edited using Microsoft Office PowerPoint 2010 and exported to Adobe Illustrator

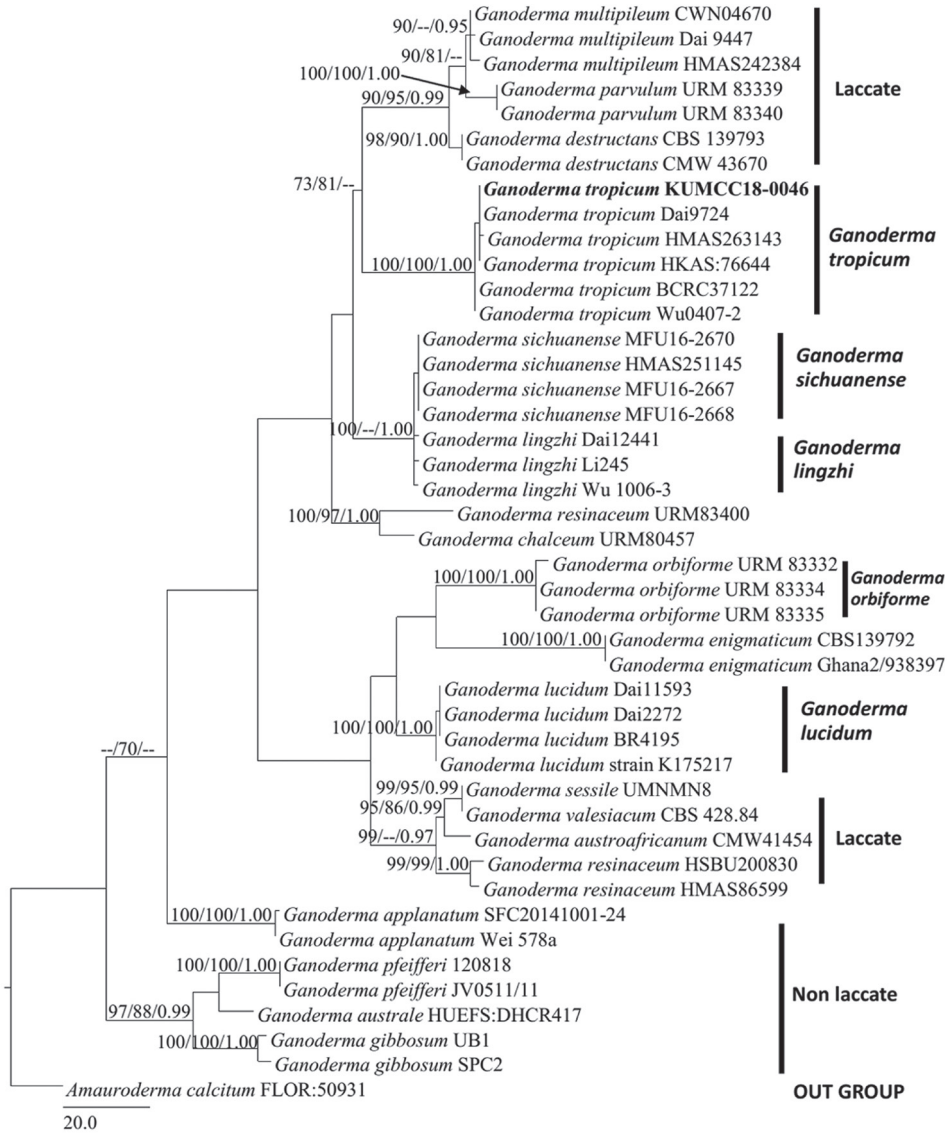

Figure 1. Phylogenetic tree (RAxML) obtained from the DNA sequence data of LSU, ITS, and RPB2 datasets. Bootstrap values (BS) from maximum likelihood (ML, left), Maximum parsimony (MP, middle) greater than 70% and Bayesian posterior probabilities (PP) greater than 0.95 are indicated above the nodes as MLBS/MPBS/PP. The tree is rooted with *Amauroderma calcitum* FLOR:50931. Newly recorded species are indicated in black bold.

CS v. 3. Maximum likelihood (ML) and Maximum parsimony (MP) bootstrap values, equal to or greater than 70%, and Bayesian Posterior Probabilities (BP) equal to or greater than 0.95, are presented above each node (Fig. 1).

Table 1. Fungal species and GenBank accession number of sequences used in this study.

Fungal species	Voucher	GenBank accession no.			References
		ITS	LSU	RPB2	
Ganoderma applanatum	Wei 5787a	KF495001	KF495011	–	GenBank
G. applanatum	SFC20141001–24	KY364255	–	KY393273	Jargalmaa et al. 2017
G. australe	HUEFS: DHCR 417	MF436676	MF436673	–	Costa–Rezende et al. 2017
G. austroafricanum	CMW 41454	KM507324	KM507325	–	Coetzee et al. 2015
G. chalceum	URM 80457	JX310812	JX310826	–	GenBank
G. destructans	CBS 139793	NR_132919	NG_058157	–	Coetzee et al. 2015
G. destructans	CMW 43670	KR183856	KR183860	–	Coetzee et al. 2015
G. enigmaticum	CBS 139792	NR_132918	NG_058156	–	Coetzee et al. 2015
G. enigmaticum	Ghana2/938397	KR014265	KR014266	–	GenBank
G. gibbosum	UB1	KU569556	KU570954	–	Bolaños et al. 2016
G. gibbosum	SPC2	KU569547	KU570946	–	Bolaños et al., 2016
G. lingzhi	Dai12441	JQ781869	–	–	Cao et al. 2012
G. lingzhi	Li245	JQ781863	–	–	Cao et al. 2012
G. lingzhi	Wu 1006–3	JQ781858	–	–	Cao et al. 2012
G. lucidum	K175217	KJ143911	–	–	Zhou et al. 2015
G. lucidum	Dai11593	JQ781852	–	–	Cao et al. 2012
G. lucidum	Dai2272	JQ781851	–	–	Zhou et al., 2015
G. lucidum	Rivoire 4195	KJ143909	–	–	Zhou et al. 2015
G. multiplicatum	CWN 04670	KJ143913	KJ143972	KJ143972	Zhou et al. 2015
G. multiplicatum	HMAS 242384	JF915409	–	JF915432	Wang et al. 2012
G. multiplicatum	Dai 9447	KJ143914	–	KJ143973	Zhou et al. 2015
G. orbiforme	URM 83332	JX310813	JX310827	–	Lima Júnior et al. 2014
G. orbiforme	URM 83334	JX310814	JX310828	–	Lima Júnior et al. 2014
G. orbiforme	URM 83335	JX310815	JX310829	–	Lima Júnior et al., 2014
G. parvulum	URM 83339	JX310817	JX310831	–	Lima Júnior et al. 2014
G. parvulum	URM 83340	JX310818	JX310832	–	Lima Júnior et al. 2014
G. pfeifferi	120818	AY884185	–	–	GenBank
G. pfeifferi	JV 0511/11	KF605660	–	–	GenBank
G. resinaceum	URM 83400	JX310824	JX310838	–	Lima Júnior et al. 2014
G. resinaceum	HSBU 200830	KT343303	–	–	GenBank
G. resinaceum	HMAS 86599	AY884177	–	JF915435	GenBank
G. sessile	UMNMN8	MG654281	–	–	GenBank
G. sichuanense	MFU16–2670	KY404119	–	–	Thawthong et al. 2017
G. sichuanense	HMAS 251145	JF915400	–	–	Wang et al. 2012
G. sichuanense	MFU16–2667	KY244061	–	–	Thawthong et al. 2017
G. sichuanense	MFU16–2668	KY244062	–	–	Thawthong et al. 2017
G. tropicum	HKAS: 76644	KC222317	–	–	Yang and Feng 2013
G. tropicum	Dai9724	JQ781879	–	–	Cao et al. 2012
G. tropicum	HMAS 263143	JF915410	–	–	Wang et al. 2012
*G. tropicu*m	Wu 0407–2	EU021458	–	–	Wang et al. 2009
G. tropicum	BCRC 37122	EU021457	–	–	Wang et al. 2009
G. tropicum	KUMCC 18–0046	**MH823539**	**MH823540**	**MH883621**	This study
G. valesiacum	CBS 428.84	JQ520218	–	–	Park et al. 2012
Amauroderma calcitum	FLOR: 50931	KR816528	KU315207	–	Costa–Rezende et al. 2017

Optimal conditions for mycelial growth

Seven different solid culture media were evaluated to determine the optimal media for the mycelial growth of the *G. tropicum* strain KUMCC18-0046, namely Czapek's agar (CZA), malt extract agar (MEA), potato dextrose agar (PDA), rose Bengal agar (RBA), yeast extract agar (YEA), yeast malt extract agar (YMA), and yeast extract peptone dextrose agar (YPD). The media formulae used are shown in Table 2. All media petri dishes were incubated at 25 °C under dark conditions. In order to discover the mycelial growth rate, colony diameter (mm) was measured; and colony averages calculated by averaging the vertical and horizontal lengths. Mycelial characteristics on the agar surfaces were recorded. Mycelial density was determined by following Kadiri (1998) as very scanty (+), scanty (2+), moderate (3+), somewhat abundant (4+), and abundant (5+). The optimal conditions, growth rate, and mycelial density were carried out in five replicates.

The optimal media shown for mycelial growth was then used to determine the optimal pH for mycelial growth. pH was adjusted to 4, 5, 6, 7, 8, and 9 with 1N HCl and 1N NaOH. The optimal temperature for mycelial growth was determined by using the highest growth rates of media and pH conditions under different dark conditions; including 15 °C, 20 °C, 25 °C, 28 °C, 30 °C, and 35 °C. After 10 days of incubation, five replicates of colony diameter were measured and calculated. The colony diameter was measured as described above.

Data analysis was carried out using statistical programs (SPSS) with five replicates (n = 5). All data were compared to obtain a mean separation using Tukey's test ($p < 0.05$) followed by post-hoc tests. The results are expressed in a one-way analysis of variance (ANOVA) analysis using the SPSS program (Softonic International SA, Barcelona, Spain).

Table 2. Composition of culture media used in this study.

Agar media reagents	Agar media composition (g/L)						
	CZA	MEA	PDA	RBA	YEA	YMA	YPD
Potato infusion			4				
Malt extract		20				3	
Yeast extract					3	3	10
Peptone		6			5	5	20
Dextrose		20	20				20
Glucose						10	
Saccharose	30						
Sodium nitrate	33						
Di-potassium phosphate	1						
Magnesium sulfate	0.5			0.5			
Potassium chloride	0.5						
Ferrous sulfate	0.01						
Potassium dihydrogen phosphate				1			
Rose bengal				0.033			
Chloramphenicol				0.1			
Agar	15	15	15		15	20	15

Results

Phylogenetic analyses

Phylogenetic analyses were inferred from the combined LSU, ITS, and RPB2 sequences, comprising 44 taxa, including 19 *Ganoderma* species with *Amauroderma calcitum* FLOR: 50931 as the outgroup taxon. The dataset comprised 2223 total characters, of which 1961 were constant, 176 variable characters were parsimony-informative, and 86 characters were parsimony-uninformative. The tree topologies were grouped into nine distinct clades, including five laccate clades of *G. tropicum*, *G. sichuanense*, *G. lingzhi*, *G. orbiforme*, *G. lucidum*, and two other laccate clades with one non-laccate clade, and an outgroup clade. The phylogenetic analyses showed considerably high support for the *G. tropicum* strain KUMCC18-0046 being closely related to the laccate *G. tropicum* isolates of China and Taiwan (MLBS = 100%/ MPBS = 100%/ PP = 1.00).

Taxonomy

Ganoderma tropicum **(Jungh.) Bres., Annales Mycologici 8(6): 586 (1910)**
Fig. 2
FOF number: FoF 05068

Description based on specimen from Thailand. Basidiome. Sessile, dimidiate. ***Pileus shape.*** Semicircular to dimidiate or conks, up to 7–12 cm in length and 4–8 cm in width, up to 1.5 cm thick. ***Pileus surface.*** Dark brown (9F5) at the base, slightly brownish red (10C8) at center, reddish gray (10B8) extending to the margin, light yellow (1A5) to yellow (2A6) under basidiocarp with grayish yellow (4C7) to brown (6D7 to 6F6) close to tube layer on upper surface of pileus glabrous, weakly to strongly laccate, glossy and shiny, smooth, spathulate, shallow sulcate several layers thick, consistency furrows, thicker at the base than the margin, covered by a thin and hard crust, and light in weight when dried. Context trimitic, irregular cuticle cells, mostly light yellow (1A5) to yellow (2A6) close to crust, grayish yellow (4C7), brown (6D7 to 6F6) to dark brown (9F5), near the tubes, dense context layer, thick near the base, tough to break when dried. ***Hymenophore.*** Grayish yellow (4C7). ***Basidiospores.*** Mostly oblong ellipsoid and broadly ellipsoid with double wall (ganodermoid) at maturity, (7.3–)7.6–10.1(10.8) × (10.1)10.6–13.3(13.9) µm ($\bar{x}$ = 9.1 × 12.2 µm, n = 50) (including myxosporium), (5.4–)5.6–8.3(8.6) × (8.3)8.4–12.5(12.9) µm ($\bar{x}$ = 7.1 × 10.6 µm, n = 50) µm (excluding outer myxosporium), light brown (6D6–6D8), reddish brown (9F6) to dark brown (9F8), usually with one end tapering, and usually overlaid by a hyaline myxosporium. ***Tubes.*** 2–7 mm long, up to 80–170 µm wide, and sulcate at different levels. ***Stipe.*** Lateral, up to 1.5 cm thick, dark brown

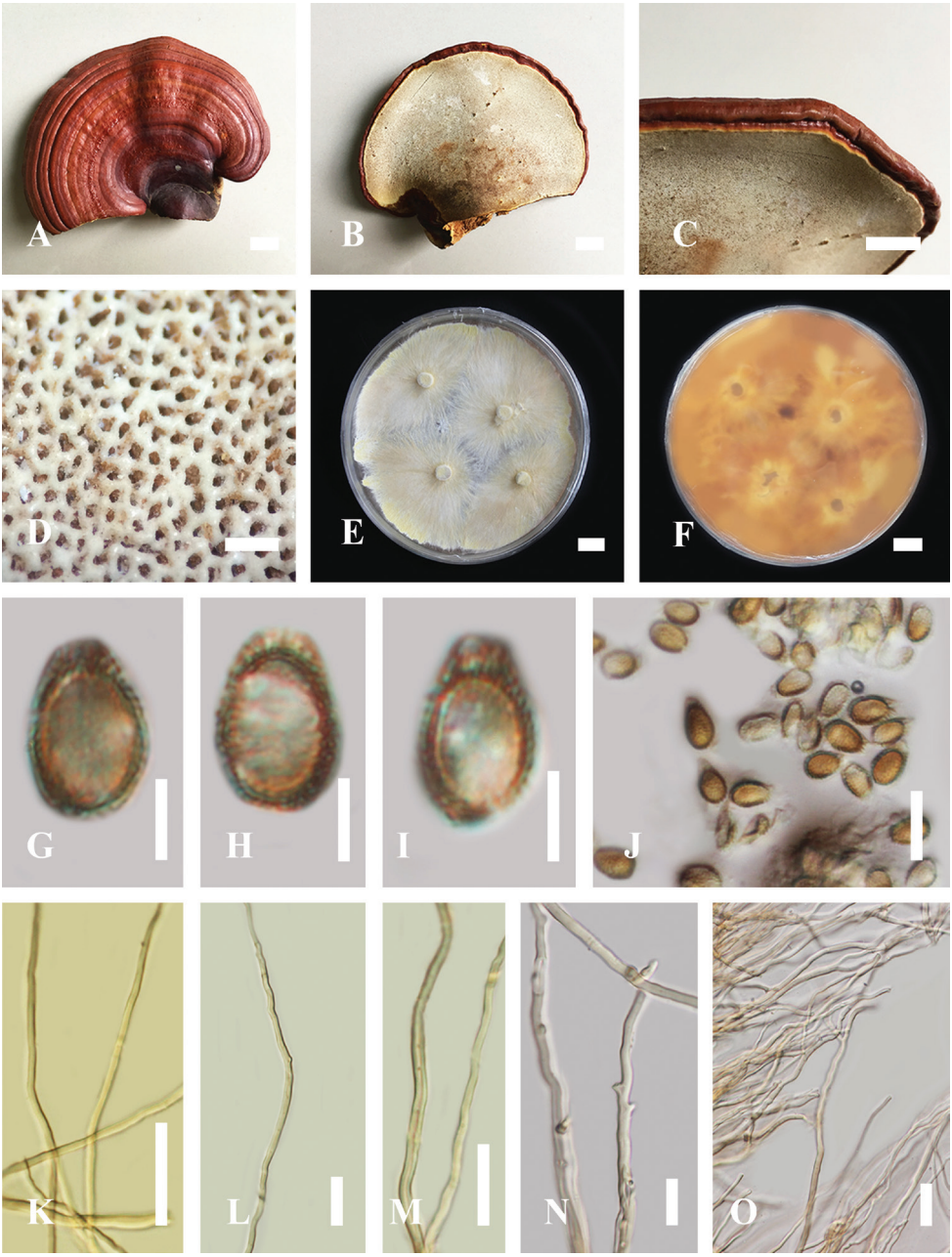

Figure 2. Morphology of *Ganoderma tropicum* strain KUMCC18-0046 **A, B** Mature basidiocarps **C** Margin **D** Pore characteristics **E, F** Culture after incubation at 25 °C for 21 days **G, J** Basidiospore in KOH **K, L** Generative hyphae of context in KOH **M** Skeletal hyphae **N** Skeletal hyphae and binding hyphae **O** Sparing branch hyphae. Scale bars: 1 cm (**A–C**); 500 μm (**D**); 1 cm (**E, F**); 5 μm (**G–I**); 15 μm (**J**); 20 μm (**K, L, O**); 10 μm (**M, N**).

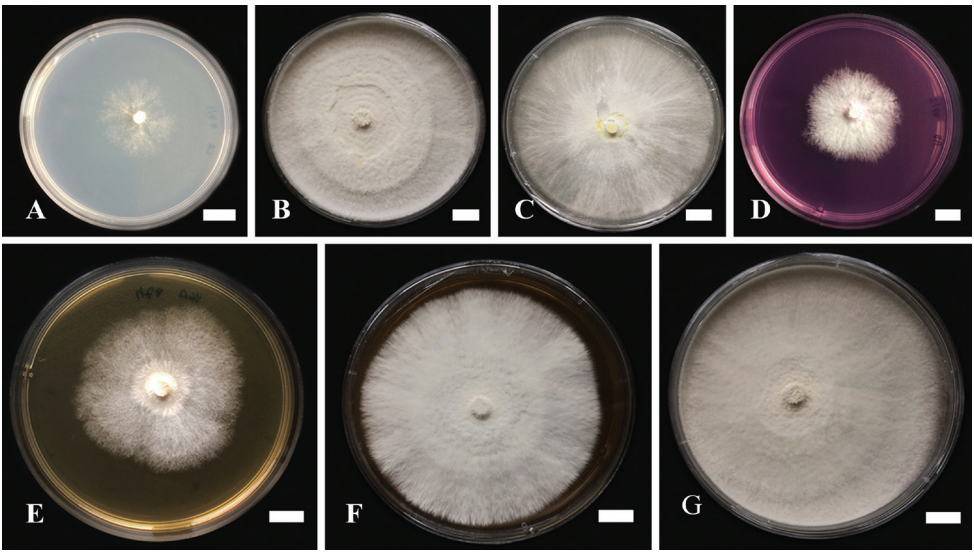

Figure 3. Characteristics of *Ganoderma tropicum* strain KUMCC18-0046 mycelial cultures were incubated at 25 °C for 10 days on different agar media **A** Czapek's agar (CZA) **B** Malt extract agar (MEA) **C** Potato dextrose agar (PDA) **D** Rose Bengal agar (RBA) **E** Yeast extract agar (YEA) **F** Yeast malt extract agar (YMA) **G** Yeast extract peptone dextrose agar (YPD). Scale bars: 1 cm.

(9F5). ***Margin.*** reddish gray (10B8), up to 0.3–0.7 cm thick, round, tough and hard, thicker towards the margin. ***Pore.*** Angular, 4–7 per mm; pore diameter up to 65–120 µm. ***Pore surface.*** Pale yellow (2A3) to light yellow (2A5) and brown (6D7) to dark brown (6F6) when touched. ***Hyphal system.*** Generative hyphae up to 0.80–2.85 µm ($\bar{x}$ = 1.45, n = 50) in diameter, colorless, thin-walled, some thick-walled, branched, with clamp connections; binding hyphae 1.00–3.10 µm ($\bar{x}$ = 2.05, n = 50), colorless, thin-walled, much-branched, clamped; skeletal hyphae up to 1.45–4.25 µm ($\bar{x}$ = 2.35, n = 50), colorless, thick-walled, unbranched or with a few branches in the distal end. ***Culture characteristics.*** Initially white (4A1) to yellowish white (4A2), pale yellow (4A3) when growing, become orange white (5A2), pale orange (5A3), light orange (5A4–6A5) and some reddish yellow (4A6) to dark brown (9F8) around the plugged circle of active mycelium after incubation for 3 weeks. ***Odor.*** Distinctive odor when fresh and dried.

Ganoderma tropicum is diagnosed as having a distinctly dimidiate, smooth, spathulate pileus, with a laccate or glabrous dark brown slightly brownish red upper surface, usually tough when dried; margin usually has a reddish gray surface, round and hard; pore surface pale yellow when young, light yellow when mature, and becoming brown or dark brown when bruised; basidiospores are described as ellipsoid, with size range of (7.3–)7.6–10.1(10.8) × (10.1)10.6–13.3(13.9) µm (including myxosporium), (5.4–)5.6–8.3(8.6) × (8.3)8.4–12.5(12.9) µm (excluding outer myxosporium); context trimitic, abundant generative hyphae with branches; thin-walled, binding hyphae; and skeletal hyphae with clamp connections.

Habitat. Solitary on living *Dipterocarpus* species in deciduous forests.

Specimen examined. Thailand, Chiang Rai Province, 19°48'24"N, 100°03'54"E, 836 m, October, 2017.

Optimal media conditions for mycelial growth and characteristics of mycelial cultures

In our study of the seven different agar media, mycelial growth (mm), growth rates (mm/day), and mycelial density were screened as an indication of favorable growth of Thai *G. tropicum* (Table 3). After 10 days of incubation, the agar surface was fully colonized with a white (6A1) to pale orange (6A2–6A3) mycelium. The best mycelium colony diameter was observed on PDA, MEA, and YPD media, following YMA, RBA, YEA, and CZA, respectively.

Mycelial morphology and colony color characteristics differed on each agar media (Fig. 3). For instance, the morphological characteristics of *G. tropicum* growth on CZA medium were expressed as a very scanty, cotton colony (Fig. 3A). The colony on YEA medium was similar to that of CZA, although YEA exhibited greater density and biomass (Fig. 3E). Mycelial morphological characteristics on MEA and YPD were similar; both were expressed as an abundant (5+) massive cottony colony with orange white to pale orange (6A1–6A3) colony (Fig. 3B, G). The PDA medium, by contrast, showed a somewhat abundant (4+) white cotton colony (Fig. 3C), which was a slightly dark golden yellow (5A7) colony after 18 days of incubation (Fig. 2E, F). Moderate colony growth (3+) was observed on RBA (Fig. 3D). Abundant white massive cottony mycelia, with a radius from the center towards the edge of the petri dish, were observed on the YMA medium (Fig. 3F). Furthermore, filamentous colonies were observed in all media, except for CZA and YEA.

Optimal pH conditions for mycelial growth

All pH values from 4–9 were suitable for promoting mycelium growth of *G. tropicum*, however, the most favorable pH range was shown to be pH 7–8, followed by pH 9 (Table 4).

Table 3. Effect of various agar media on mycelial growth (mm) and mycelial growth rates (mm/day) of *Ganoderma tropicum* strain KUMCC18-0046, incubated at 25 °C for 10 days. Values with the same letter are not significantly different ($p < 0.05$).

Agar media	Colony diameter	Growth rate	Mycelial density
CZA	16.70 ± 0.13^{e}	3.50	+
MEA	41.20 ± 0.12^{a}	8.40	5+
PDA	42.20 ± 0.44^{a}	8.50	4+
RBA	27.70 ± 0.08^{c}	4.20	3+
YEA	21.00 ± 0.08^{d}	5.70	2+
YMA	36.90 ± 0.13^{b}	8.10	5+
YPD	40.40 ± 0.40^{a}	8.40	5+

Table 4. Effect of pH on mycelial growth (mm) and mycelial growth rates (mm/day) of *Ganoderma tropicum* strain KUMCC18-0046, incubated for 10 days. Values with the same letter are not significantly different ($p < 0.05$).

pH	Colony diameter	Growth rate	Mycelial density
4	30.50 ± 0.14[d]	5.50	3+
5	45.90 ± 0.10[c]	7.30	4+
6	46.80 ± 0.10[c]	8.10	4+
7	57.50 ± 0.12[ab]	8.50	5+
8	58.90 ± 0.05[a]	8.50	5+
9	56.10 ± 0.07[b]	8.10	5+

Optimal temperature conditions for mycelial growth

Ganoderma tropicum mycelial growth increased when going up from 15–25 °C and 28 °C, after which it started to decline again, with the most suitable temperature for mycelial growth being between 25 °C and 28 °C. Although the mycelia could grow between 15–35 °C, growth appeared to be drastically suppressed at 15 °C and 35 °C (Table 5).

Table 5. Effect of temperature on mycelial growth (mm) and mycelial growth rates (mm/day) of *Ganoderma tropicum* strain KUMCC18-0046, incubated for 10 days. Values with the same letter are not significantly different ($p < 0.05$).

Temperature (°C)	Colony diameter	Growth rate	Mycelial density
15	17.40 ± 0.07[c]	4.00	1+
20	29.70 ± 0.04[b]	6.30	3+
25	43.50 ± 0.06[a]	8.50	5+
28	43.70 ± 0.04[a]	8.50	5+
30	30.40 ± 0.13[b]	6.40	4+
35	17.90 ± 0.11[c]	4.30	2+

Discussion

In this study, we introduce a new record of *G. tropicum* strain KUMCC18-0046, which was collected from Chiang Rai Province, Thailand. *Ganoderma tropicum* serves as the sister group to *G. multipileum*, *G. parvulum*, and *G. destructans* (ML = 73%, MP = 81%). This finding is consistent with those of Wang et al. (2012), as well as Yang and Feng (2013), whose studies indicated that *G. tropicum* forms a sister clade with *G. multipileum*, exhibiting macro-morphological characteristics of strongly echinulate basidiospores (Wang et al. 2009). *Ganoderma tropicum* and *G. multipileum* were also shown to be the sister groups of *G. lingzhi*, which is in the same clade of species distributed in China (Wang et al. 2012).

Ganoderma tropicum has been widely reported in tropical areas; however, no specimens have been recorded in Thailand prior to this study (Wang et al. 2009; Zhang et

al. 2015). The morphological characteristics of the *G. tropicum* strain from our study are similar to other *G. tropicum* specimens described from other tropical areas, including in mainland China (Cao et al. 2012; Wang et al. 2012; Hapuarachchi et al. 2018a), South America (Gottlieb and Wright 1999), and Taiwan (Wang et al. 2009). Although there is a high degree of variability in the macro-morphological characteristics of *Ganoderma tropicum* specimens found around the world, certain common characteristics can be seen. These common characteristics include a distinct reddish-brown pileal surface, with sessile to dimidiate basidiocarps. Furthermore, there are some similarities between *G. tropicum* and other *Ganoderma* species. According to Cao et al. (2012), among the Chinese *Ganoderma* species, *G. flexipes*, *G. multipileum*, *G. sichuanense*, *G. lingzhi*, and *G. tsugae* are morphologically similar to *G. tropicum*, having a reddish-brown pileus surface, ellipsoid basidiospores, and cuticle cells.

However, *G. flexipesis* can be differentiated from *G. tropicum* by its small basidiocarps and long stipe, while *G. lingzhi* has usually distinctive sessile basidiocarps, a dark brown context, and mostly irregular cuticle cells (Cao et al. 2012; Wang et al. 2012). *Ganoderma multipileum* is distinguished from *G. tropicum* by having mostly concentric growth zones in context, and varying the homogeneous context when maturity (Wang et al. 2012). *Ganoderma sichuanense* is separated from *G. tropicum* by its usually formed flabellate to reniform, concave or convex basidiocarps, and also by its ovoid basidiospores which are truncate at the apexes (Yao et al. 2013). *Ganoderma tsugae* is separated from *G. tropicum* by absence of the melanoid bands, and also thin dissepiments when mature (Wang et al. 2012).

Our morphological analyses show that the Thai *G. tropicum* strain has a semicircular to dimidiate pileus, a pileus size between 4–8 cm in width, 7–12 cm in length, and up to 1.5 cm thick. The basidiospores are mostly oblong ellipsoid and broadly ellipsoid in shape, with double walls, (7.3–)7.6–*8.2*–10.1(–10.8) × (10.1–)10.6–*11.7*–13.3(–13.9) µm ($\bar{x}$ = 9.1 × 12.2 µm, n = 50), and (5.4–)5.6–*7.1*–8.3(–8.6) × (8.3)8.4–*10.8*–12.5(–12.9) µm ($\bar{x}$ = 7.1 × 10.6 µm, n = 50) mm (excluding outer myxosporium); the pore surface is pale yellow (2A3) with pore are 4–7 per mm, and the tubes are 2–7 mm long with a light yellow to dark brown context. The original description of *G. tropicum* has the basidiospores fasciculate, 7–9 × 10–12 µm with 4–5 µm of hymenia hyphae (Tai et al. 1979). These characteristics are in accordance with the basidiospore sizes we recorded for the Thai strain of *G. tropicum*. The strain of *G. tropicum* from South America shares much in common with the Thai strain; however, notable differences in the South American strain include light brown ovoid basidiospores, a pileus of dark to black coloring at the base, and a blunt to slightly round margin. Our results of *G. tropicum* are in accordance with the description of Hapuarachchi et al. (2018a), who described specimens of a Chinese strain of *G. tropicum* collected from Hainan Province. This Hainan strain had the following characteristics: pileus size 4–8 × 2.5–6 cm, up to 1 cm thick at the base, basidiospores were described as (10.8–)11.2–*12.1*–12.8(–13.1) × (8.3–)9.6–*10.1*–10.8(11.1) µm (with myxosporium) and (7.9–)8.8–*9.1*–10.2(–10.8) × (5.8–)6.4–*7.3*–7.8(–9.8) µm (without myxosporium), with shared white to orange pore surface.

The optimal conditions for mycelial growth were investigated based on medium, pH, and temperature. The best growth rates were obtained using PDA, MEA, and YPD media. These three media are composed of high concentrations of dextrose as a carbon source, while various forms of carbon sources have been reported as affecting fungal mycelial growth (Simonic et al. 2008; Dang et al. 2018). Although identical fungal species are able to grow on different agar media, the morphological characteristics of the mycelia can be expressed differently, and we therefore conclude that each ingredient in each agar medium affects the morphological characteristics of the resultant culture. The optimal pH was evaluated by using the PDA media, and pH 7–8 was found to be the optimal pH range. Here, we found that *G. tropicum* grows well in an alkali pH range, as its fruiting body was also collected on the substrate at pH 8 in nature (data not shown). The optimal PDA media at pH 7, incubated within the temperature range at 25–28 °C, were found to be the most suitable for *G. tropicum* mycelial growth, while temperatures lower than 15 °C or higher than 30 °C are not suitable for mycelial growth. Luangharn et al. (2017) reported that the non-laccate Thai strain of *G. australe* grew well on PDA media, at a pH of 7–8 and at temperature range of 25–30 °C. This study revealed similar mycelial growth conditions with other *Ganoderma* species that have been previously evaluated (Lee et al. 2008; Jo et al. 2009; Magday et al. 2014). In light of medicinal mushroom consumption trends, *G. tropicum* has a high potential for commercial production. Further studies will evaluate the best method to optimize the mushroom spawn and growing substrate for bringing Thai *G. tropicum* cultivation into high-yield production, and also establish whether other *Ganoderma* species remain to be discovered in Thailand.

Conclusion

This study confirmed the new record of *Ganoderma tropicum* from Northern Thailand based on morphological characteristics together with phylogenetic analyses. The optimal conditions for promoting the mycelial growth of *G. tropicum* were investigated and the best media and pH for mycelia growth were found to be PDA, MEA, and YPD media at pH 7–8, respectively. The optimal temperature was found to be 25–30 °C.

Acknowledgements

We appreciate the kind support given by the University of Chinese Academy of Sciences, Beijing 100049, China; Key Laboratory for Economic Plants and Biotechnology, Kunming Institute of Botany, Chinese Academy of Sciences, Kunming 650201, Yunnan, China; and Key Laboratory for Plant Diversity and Biogeography of East Asia, Kunming Institute of Botany, Chinese Academy of Sciences, Kunming 650201, Yunnan, China. This research was supported by the Key Research Program of Frontier Sciences, CAS, Grant No. QYZDY-SSW-SMC014. We thank the Germplasm Bank of Wild Species, Kunming Institute of Botany, Kunming 650201, Yun-

nan, China for enabling our molecular laboratory work. Dr Olivier Raspé is thanked for his help with phylogenetic analyses. Dr Saowaluck Tibpromma, Nimali I. de Silva and Subashini Chathumini are thanked for their help and valuable suggestions. Kasiphat Limsakul and Wilawan Punyaboon are acknowledged for their invaluable assistance. Samantha C. Karunarathna thanks CAS President's International Fellowship Initiative (PIFI) for funding his postdoctoral research (No. 2018PC0006) and the National Science Foundation of China (NSFC) for funding this work under the project code 31750110478. Peter E. Mortimer thanks the National Science Foundation of China (NSFC) project codes 41761144055 and 41771063. The authors also thank William A. Julian for his contributions to the English editing. This research is part of the CGIAR-FTA Program.

References

Bolaños AC, Bononi VLR, Gugliotta AM, Muñoz JE (2016) New records of *Ganoderma multiplicatum* (Mont.) Pat. (Polyporales, Basidiomycota) from Colombia and its geographic distribution in South America. Check List 12(4): 1–7. https://doi.org/10.15560/12.4.1948

Cao Y, Yuan HS (2013) *Ganoderma mutabile* sp. nov. from southwestern China based on morphological and molecular data. Mycological Progress 12: 121–126. https://doi.org/10.1007/s11557-012-0819-9

Cao Y, Wu SH, Dai YC (2012) Species clarification of the prize medicinal *Ganoderma* mushroom "Lingzhi". Fungal Diversity 56: 49–62. https://doi.org/10.1007/s13225-012-0178-5

Choeyklin R, Hattori T, Jones EBG (2011) A checklist of aphyllophoraceous fungi in Thailand: Part I. New records. Mycosphere 2(2): 161–177.

Coetzee MPA, Marincowitz S, Muthelo VG, Wingfield MJ (2015) *Ganoderma* species, including new taxa associated with root rot of the iconic *Jacaranda mimosifoliain* Pretoria, South Africa. International Mycological Association 6(1): 249–256. https://doi.org/10.5598/imafun-gus.2015.06.01.16

Costa-Rezende DH, Robledo GL, Góes-Neto A, Reck MA, Crespo E, Drechsler-Santos ER (2017) Morphological reassessment and molecular phylogenetic analyses of *Amauroderma* s. lat. raised new perspectives in the generic classification of the Ganodermataceae family. Persoonia 39: 254–269. https://doi.org/10.3767/persoonia.2017.39.10

Da Silva DD, Rapior S, Sudarman E, Stadler M, Xu JC, Alias, SA, Hyde KD (2013) Bioactive metabolites from macrofungi: ethnopharmacology, biological activities and chemistry. Fungal Diversity 62: 1–40. https://doi.org/10.1007/s13225-013-0265-2

Dai YC, Cui BK, Yuan HS, Li BD (2007) Pathogenic wood-decaying fungi in China. Forest Pathology 37: 105–120. https://doi.org/10.1111/j.1439-0329.2007.00485.x

Dai YC, Zhou LW, Hattori T, Cao Y, Stalpers JA, Ryvarden L, Buchanan P, Oberwinkler F, Hallenberg N, Liu PG, Wu SH (2017) *Ganoderma lingzhi* (Polyporales, Basidiomycota): the scientific binomial for the widely cultivated medicinal fungus Lingzhi. Mycological Progress 16: 1051–1055. https://doi.org/10.1007/s11557-017-1347-4

Dang HN, Wang CL, Lay HL (2018) Effect of nutrition, vitamin, grains, and temperature on the mycelium growth and antioxidant capacity of *Cordyceps militaris* (strains AG-1 and PSJ-1). Journal of Radiation Research and Applied Sciences 11: 130–138. https://doi.org/10.1016/j.jrras.2017.11.003

Gottlieb AM, Wright JE (1999) Taxonomy of *Ganoderma* from southern South America: sub genus *Ganoderma*. Mycological Research 103(6): 661–673. https://doi.org/10.1017/S0953756298007941

Hall TA (1999) BioEdit: a user-friendly biological sequence alignment editor and analysis program for Windows 95/98/NT. Nucleic Acids Symposium Series 41: 95–98.

Hapuarachchi KK, Karunarathna SC, Raspé O, De Silva KHWL, Thawthong A, Wu XL, Kakumyan P, Hyde KD, Wen TC (2018a) High diversity of *Ganoderma* and *Amauroderma* (Ganodermataceae, Polyporales) in Hainan Island, China. Mycosphere 9(5): 931–982. https://doi.org/10.5943/mycosphere/9/5/1

Hapuarachchi KK, Karunarathna SC, Phengsintham P, Kakumyan P, Hyde KD, Wen TC (2018b) *Amauroderma* (Ganodermataceae, Polyporales) – bioactive compounds, beneficial properties and two new records from Laos. Asian Journal of Mycology 1: 121–136. https://doi.10.5943/ajom/1/1/10

Hapuarachchi KK, Karunarathna SC, McKenzie EHC, Wu XL, Kakumyan P, Hyde KD, Wen TC (2019) High phenotypic plasticity of *Ganoderma sinense* (Ganodermataceae, Polyporales) in China. Asian Journal of Mycology 2(1) : 1–47. https://doi.org/10.5943/ajom/2/1/1

Hu LL, Ma QY, Huang SZ, Guo ZK, Guo JC, Dai HF, Zhao YX (2013) Two new phenolic compounds from the fruiting bodies of *Ganoderma tropicum*. Bulletin of the Korean Chemical Society 34: 884–886. https://doi.org/10.5012/bkcs.2013.34.3.884

Huelsenbeck JP, Ronquist F (2001) MRBAYES: Bayesian inference of phylogenetic trees. Bioinformatics 17: 754–755. https://doi.org/10.1093/bioinformatics/17.8.754

Index Fungorum (2019) Index Fungorum. http://www.indexfungorum.org/names/names.asp [2019-1-25]

Jargalmaa S, Eimes JA, Park MS, Park JY, Oh SY, Lim YW (2017) Taxonomic evaluation of selected *Ganoderma* species and database sequence validation. Peer Journal 5: 1–16. https://doi.org/10.7717/peerj.3596

Jo WS, Cho YJ, Cho DH, Park SD, Yoo YB, Seok SJ (2009) Culture conditions for the mycelial growth of *Ganoderma applanatum*. Mycobiology 37: 94–102. https://doi.org/10.4489/MYCO.2009.37.2.094

Kadiri M (1998) Spawn and fruit body production of *Pleurotus sajor-caju* in Abeokuta, Nigeria. Nigeria Journal of Botany 11; 125–131.

Karsten PA (1881) Enumeralio boletinearum et polyporearum fennicarum, systemate novo dispositarum. Revue de Mycologie 3: 16–19.

Katoh K, Standley DM (2013) MAFFT multiple sequence alignment software version 7: improvements in performance and usability. Molecular Biology and Evolution 30: 772–780. https://doi.org/10.1093/molbev/mst010

Kreisel H, Schauer F (1987) Methoden des mykologischen Laboratoriums. VEB Gustav Fischer Verlag, Jena, 181 pp.

Largent DL (1986) How to Identify Mushrooms to Genus (3rd edn). Mad River Press, California, 166 pp.

Larget B, Simon DL (1999) Markov Chain Monte Carlo algorithms for the Bayesian analysis of phylogenetic trees. Molecular Biology and Evolution 16: 750–759. https://doi.org/10.1093/oxfordjournals.molbev.a026160

Lee UY, Jayasinghe C, Imtiaj A, Hur H, Lee GW, Lee TS (2008) Favorable culture conditions for mycelial growth of Korean wild strains in *Ganoderma lucidum*. Mycobiology 36: 28–33. https://doi.org/10.4489/MYCO.2008.36.1.028

Lima-Júnior NC, Gibertoni TB, Malosso E (2014) Delimitation of some neotropical laccate *Ganoderma* (Ganodermataceae): molecular phylogeny and morphology. Revista de Biologia Tropical 62 (3): 1197–1208. https://doi.org/10.15517/rbt.v62i3.12380

Liu YJ, Whelen S, Hall BD (1999) Phylogenetic relationships among ascomycetes: evidence from an RNA polymerase II subunit. Molecular Biology and Evolution 16: 1799–1808. https://doi.org/10.1093/oxfordjournals.molbev.a026092

Lodge DJ, Ammirati FJ, O'Dell TE, Mueller GM (2004) Collecting and describing macrofungi. In: Mueller GM., Bills GF, Foster MS (Eds) Biodiversity of Fungi Inventory and Monitoring Methods. Elsevier Academic Press, London, 128–154.

Loyd AL, Richter BS, Jusino MA, Truong C, Smith ME, Blanchette RA, Smith JA (2018) Identifying the "mushroom of immortality": assessing the *Ganoderma* species composition in commercial Reishi products. Frontiers in Microbiology 9: 1–14. https://doi.org/10.3389/fmicb.2018.01557

Luangharn T, Karunarathna SC, Khan S, Xu JC, Mortimer PE, Hyde KD (2017) Antibacterial activity, optimal culture conditions and cultivation of the medicinal *Ganoderma australe*, new to Thailand. Mycosphere 8(8): 1108–1123. https://doi.org/10.5943/mycosphere/8/8/11

Magday JC Jr, Bungihan ME, Dulay RMR (2014) Optimization of mycelial growth and cultivation of fruiting body of Philippine wild strain of *Ganoderma lucidum*. Current Research in Environmental & Applied Mycology 4: 162–172. https://doi.org/10.5943/cream/4/2/4

Miettinen O, Larsson KH (2006) *Trechispora elongata* species nova from North Europe. Mycotaxon 96: 193–198.

Miller MA, Pfeiffer W, Schwartz T (2010) Creating the CIPRES Science Gateway for inference of large phylogenetic trees. Proceedings of the Gateway Computing Environments Workshop (GCE). Institute of Electrical and Electronics Engineers, Louisiana, 1–8. https://doi.org/10.1109/GCE.2010.5676129

Moncalvo JM, Buchanan PK (2008) Molecular evidence for long distance dispersal across the Southern Hemisphere in the *Ganoderma applanatum-australe* species complex (Basidiomycota) Mycological Research 112: 425–436. https://doi.org/10.1016/j.mycres.2007.12.001

Moncalvo JM, Ryvarden L (1997) A nomenclatural study of the Ganodermataceae Donk. Synopsis Fungorum 11: 1–114.

Nylander JAA, (2004) MrModeltest v.2 program distributed by the author. Evolutionary Biology Centre, Uppsala University.

Park YJ, Kwon OC, Son ES, Yoon DE, Han W, Nam JY, Yoo YB, Lee CS (2012) Genetic diversity analysis of *Ganoderma* species and development of a specific marker for identification

of medicinal mushroom *Ganoderma lucidum*. African Journal of Microbiology Research 6(25): 5417–5425.

Pilotti CA, Sanderson FR, Aitken AB, Armstrong W (2004) Morphological variation and host range of two *Ganoderma* species from Papua New Guinea. Mycopathologia 158: 251–265. https://doi.org/10.1023/B:MYCO.0000041833.41085.6f

Pilotti CA (2005) Stem rots of oil palm caused by *Ganoderma boninense*: pathogen biology and epidemiology. Mycopathologia 159: 129–137. https://doi.org/10.1007/s11046-004-4435-3

Rambaut A (2012) FigTree version 1.4.0. http://tree.bio.ed.ac.uk/software/soft-ware/figtree/

Richter C, Wittstein K, Kirk PM, Stadler M (2015) An assessment of the taxonomy and chemotaxonomy of *Ganoderma*. Fungal Diversity 71: 1–15. https://doi.org/10.1007/s13225-014-0313-6

Ridgeway R (1912) Color Standards and Color Nomenclature. Ridgeway, Washington DC, 12–225. https://doi.org/10.5962/bhl.title.144788

Ríos JL, Andújar I, Recio MC, Giner RM (2012) Lanostanoids from fungi: a group of potential anticancer compounds. Journal of Natural Products 75: 2016–2044. https://doi.org/10.1021/np300412h

Ryvarden L (2004) Neotropical polypores Part 1. Synopsis Fungorum. Fungiflora, Oslo, 227 pp.

Sanoamuang N (2010) Wild Mushrooms of Thailand: Biodiversity and Utilization. Universal Graphic and Trading, Bangkok, 424 pp.

Silvestro D, Michalak I (2011) raxmlGUI: a graphical front-end for RAxML. Organisms Diversity and Evolution 12(4): 335–337. https://doi.org/10.1007/s13127-011-0056-0

Simonic J, Stajic M, Glamoclija J, Vukojevic J, Duletic-Lausevic S, Brceski I (2008) Optimization of submerged cultivation conditions for extra- and intracellular polysaccharide production by medicinal Lingzhi or Reishi mushroom *Ganoderma lucidum* (W. Curt.: Fr.) P. Karst. (Aphyllophoromycetideae). International Journal of Medicinal Mushrooms 10(4): 351–360. https://doi.org/10.1615/IntJMedMushr.v10.i4.80

Stamatakis A (2014) RAxML Version 8: A tool for phylogenetic analysis and post-analysis of large phylogenies. Bioinformatics 30: 1312–1313. https://doi.org/10.1093/bioinformatics/btu033

Swofford DL (2002) PAUP*. Phylogenetic analysis using parsimony (*and Other Methods), Version 4.0 beta version. Sinauer Associates, Sunderland, Massachusetts.

Teng BS, Wang CD, Yang HJ, Wu JS, Zhang D, Zheng M, Fan ZH, Pan D, Zhou P (2011) A protein tyrosine phosphatase 1B activity inhibitor from the fruiting bodies of *Ganoderma lucidum* (Fr.) Karst and its hypoglycemic potency on streptozotocin-induced type 2 diabetic mice. Journal of Agricultural and Food Chemistry 59: 6492–6500. https://doi.org/10.1021/jf200527y

Thawthong A, Hapuarachchi KK, Wen TC, Raspé O, Thongklang N, Kang JC, Hyde KD (2017) *Ganoderma sichuanense* (Ganodermataceae, Polyporales) new to Thailand. MycoKeys 22: 27–43. https://doi.org/10.3897/mycokeys.22.13083

Vilgalys R, Hester M (1990) Rapid genetic identification and mapping of enzymatically amplified ribosomal DNA from several *Cryptococcus* species. Journal of Bacteriology 172(8): 4238–4246. https://doi.org/10.1128/jb.172.8.4238-4246.1990

Wang DM, Wu SH, Su C., Peng JT, Shih YH, Chen LC (2009) *Ganoderma multipileum*, the correct name for "*G. lucidum*" in tropical Asia. Botanical Studies 50: 451–458.

Wang XC, Xi RJ, Wang DM, Yao YJ (2012) The species identity of the widely cultivated *Ganoderma*, "*G. lucidum*" (Lingzhi) in China. PLoS ONE 7(7): e40857. https://doi.org/10.1371/journal.pone.0040857

White TJ, Bruns T, Lee S, Taylor JW (1990) Amplification and direct sequencing of fungal ribosomal RNA genes for phylogenetics. In: Innis MA, Gelfand DH, Sninsky JJ, White TJ (Eds) PCR Protocols: a Guide to Methods and Applications. Academic Press, New York, 315–322. https://doi.org/10.1016/B978-0-12-372180-8.50042-1

Wu XL, Mao XL, Tuli GE, Song B, Li TH, Zhao YX, Chen SL, Zeng NK, Huang SZ, Wen TC, Deng CY (2013) Medicinal fungi of China. Science Press, Beijing, 375 pp.

Yang ZL, Feng B (2013) What is the Chinese "Lingzhi"?—a taxonomic mini-review. Mycology 4: 1–4.

Yao YJ, Wang XC, Wang B (2013) Epitypification of *Ganoderma sichuanense* J.D. Zhao & X.Q. Zhang (Ganodermataceae). Taxon 62: 1025–1031. https://doi.org/10.12705/625.10

Zhang SS, Wang YG, Ma QY, Huang SZ, Hu LL, Dai HF, Yu ZF, Zhao YX (2015) Three new lanostanoids from the mushroom *Ganoderma tropicum*. Molecules 20: 3281–3289. https://doi.org/10.3390/molecules20023281

Zhou LW, Cao Y, Wu SH, Vlasák J, Li DW, Li MJ, Dai YC (2015) Global diversity of the *Ganoderma lucidum* complex (Ganodermataceae, Polyporales) inferred from morphology and multilocus phylogeny. Phytochemistry 114: 7–15. https://doi.org/10.1016/j.phytochem.2014.09.023

MycoKeys 51: 85–96 (2019)
doi: 10.3897/mycokeys.51.33262
http://mycokeys.pensoft.net

RESEARCH ARTICLE

A peer-reviewed open-access journal
MycoKeys
Launched to accelerate biodiversity research

Reinstatement of the corticioid genus *Leifia* (Hymenochaetales, Basidiomycota) with a new species *L. brevispora* from Hubei, Central China

Shi-Liang Liu[1*], Yusufjon Gafforov[2,3*], Xian-Ying Zhang[2,4], Hong-Ling Wang[4], Xue-Wei Wang[2,5], Li-Wei Zhou[1,2]

1 *State Key Laboratory of Mycology, Institute of Microbiology, Chinese Academy of Sciences, Beijing 100101, China* **2** *Institute of Applied Ecology, Chinese Academy of Sciences, Shenyang 110016, China* **3** *Laboratory of Mycology, Institute of Botany, Academy of Sciences of the Republic of Uzbekistan, 32 Durmon yuli Street, Tashkent, 100125, Uzbekistan* **4** *College of Life Engineering, Shenyang Institute of Technology, Fushun 113122, China* **5** *University of Chinese Academy of Sciences, Beijing 100049, China*

Corresponding author: *Li-Wei Zhou* (liwei_zhou1982@im.ac.cn)

Academic editor: *Bao-Kai Cui* | Received 22 January 2019 | Accepted 9 April 2019 | Published 8 May 2019

Citation: Liu S-L, Gafforov Y, Zhang X-Y, Wang H-L, Wang X-W, Zhou L-W (2019) Reinstatement of the corticioid genus *Leifia* (Hymenochaetales, Basidiomycota) with a new species *L. brevispora* from Hubei, Central China. MycoKeys 51: 85–96. https://doi.org/10.3897/mycokeys.51.33262

Abstract

The monotypic genus *Leifia* was previously considered to be a later synonym of *Odonticium*. With the morphological and phylogenetic evidence provided by an additional four East Asian specimens, we propose to reinstate *Leifia* as an independent genus in Hymenochaetales. *Leifia* morphologically differs from *Odonticium* by its grandinioid hymenophore with hyphal strands, numerous thick-walled cystidia with an invaginated apical end and narrowly and thick-walled basidia. The phylogeny generated from the current data set of ITS and 28S regions indicates that *Leifia* forms a sister clade to *Odonticium*. Besides the generic type *Leifia flabelliradiata* in the *Leifia* clade, two specimens, collected from Hubei, Central China, are newly introduced as *Leifia brevispora*. This new species is the second species of *Leifia* and differs from the generic type by its shorter basidiospores and distribution in warm-temperate to subtropical areas in East Asia. The additional two specimens, collected from Da Lat, Viet Nam, differ morphologically, both from each other and from known species of *Leifia*, but more samples need to be examined before further taxonomic decisions can be made.

* These authors contributed equally.

Keywords
Morphology, *Odonticium*, phylogeny, taxonomy, wood-inhabiting fungi, 1 new taxon

Introduction

Leifia Ginns is a monotypic genus of wood-inhabiting basidiomycetes introduced by Ginns (1998). The basionym of its type is *Phanerochaete flabelliradiata* J. Erikss. & Hjortstam that was described from Norway (Eriksson et al. 1981). Burdsall (1985) regarded *P. flabelliradiata* as a deviating element in *Phanerochaete* P. Karst. and transferred it to *Tubulicrinis* Donk. Hjortstam (1986) accepted the concept of *Phanerochaete* sensu Burdsall (1985), but he considered that *Tubulicrinis flabelliradiatus* (J. Erikss. & Hjortstam) Burds. did not fit the concept of *Tubulicrinis* or any other known genus and thus erected a new genus *Granulocystis* Hjortstam to accommodate this species. Unfortunately, *Granulocystis* is an illegitimate later homonym for *Granulocystis* Hindák, a genus of green algae (Code of Nomenclature Art. 53.1, Turland 2018). Therefore, Ginns (1998) introduced *Leifia* replacing *Granulocystis*. By examining Russian specimens of *Leifia flabelliradiata* (J. Erikss. & Hjortstam) Ginns, Zmitrovich (2001) combined this species to *Odonticium* Parmasto as *O. flabelliradiatum* (J. Erikss. & Hjortstam) Zmitr. that is the currently accepted name of this species in MycoBank and Index Fungorum. Correspondingly, *Leifia* is treated as a synonym of *Odonticium*.

Till now, Larsson et al. (2006) is the single paper which includes the species *Odonticium flabelliradiatum* in a phylogenetic analysis. Although *Odonticium flabelliradiatum* grouped with *O. romellii* (S. Lundell) Parmasto, the generic type of *Odonticium* and two species of *Repetobasidium* J. Erikss. with a full Bayesian posterior probability (BPP) support in the *Rickenella* Raithelh. clade of Hymenochaetales, Larsson et al. (2006) considered that this clade might not be reliable due to the lack of morphological similarities and still used the name *Leifia flabelliradiata* rather than *O. flabelliradiatum*. However, no further taxonomic opinion relating to *Leifia* was provided in Larsson et al. (2006).

In 2017, four specimens close to *Odonticium flabelliradiatum* were collected from Central China and Vietnam, which draw our attention to the taxonomic status and diversity of *Leifia*. Based on morphological and molecular evidence, we propose the reinstatement of *Leifia* and reveal a higher diversity of this genus.

Materials and methods

Specimens studied are deposited in the herbarium of Institute of Applied Ecology, Chinese Academy of Sciences (IFP). Morphological photos were taken with a digital camera Canon E12 (Tokyo, Japan) in the field. Morphological observations were made with Nikon SMZ 645 and SMZ 1000 stereomicroscopes and a Nikon Eclipse 80i light microscope (Tokyo, Japan) at magnifications up to 1000×. Microscopic procedures followed Hjortstam et al. (1987). Basidiocarp sections were prepared in Melzer's reagent, lactic acid Cotton Blue (CB) and 3% potassium hydroxide (KOH). All microscopic measurements were made in CB. When presenting the variation of basidiospore

sizes, 5% of the measurements were excluded from each end of the range and are given in parentheses. The following abbreviations are used in the text: L = mean basidiospore length (arithmetic average of all measured basidiospores), W = mean basidiospore width (arithmetic average of all measured basidiospores), Q = variation in the L/W ratios between the specimens studied, n (a/b) = number of spores (a) measured from given number (b) of specimens.

The four specimens newly collected were subjected to polymerase chain reaction (PCR) directly with the Phire Plant Direct PCR kit (Finnzymes Oy, Espoo, Finland), following the manufacturer's instructions. The nuc rDNA ITS1-5.8S-ITS2 (ITS barcode) and 28S regions were amplified using the primer pairs ITS1-F (Gardes and Bruns 1993) or ITS5 and ITS4 (White et al. 1990) and LR0R and LR7 (Vilgalys and Hester 1990), respectively. The PCR procedure was as follows: initial denaturation at 98°C for 5 min, followed by 39 cycles at 98 °C for 5 s, 59 °C for 5 s (ITS region)/48 °C for 5 s (28S region) and 72 °C for 5 s, with a final extension at 72 °C for 10 min. The PCR products were sequenced at the Beijing Genomics Institute, China, with the same primers used for PCR. All newly generated sequences were deposited in GenBank (Table 1).

The current dataset for phylogenetic analysis was mainly adopted from Larsson et al. (2006), where, to avoid redundance, taxa in the *Rickenella* clade including *Leifia flabelliradiata* were mostly referred to, while taxa in other clades were representatively selected (Table 1). *Sistotrema brinkmannii* (Bres.) J. Erikss. was selected as an outgroup taxon. Besides taxa in Hymenochaetales, *Protodontia piceicola* (Kühner ex Bourdot) G.W. Martin and *Exidiopsis calcea* (Pers.) K. Wells from Auriculariales were also included as additional ingroup taxa. The ITS and 28S datasets were separately aligned with MAFFT 7.110 (Katoh and Standley 2013) with the G-INI-I option (Katoh et al. 2005) and then the two resulting alignments were concatenated as a single alignment deposited in TreeBASE (study no. 23768). The best-fit evolutionary model for this concatenated alignment was estimated as GTR+I+G with jModel Test (Guindon and Gascuel 2003; Posada 2008). Maximum likelihood (ML) and Bayesian Inference (BI) methods were conducted to perform phylogenetic analysis, respectively, using raxmlGUI 1.2 (Silvestro and Michalak 2012; Stamatakis 2006) and MrBayes 3.2 (Ronquist et al. 2012). In the ML analysis, bootstrap (BS) values were tested under the auto FC option (Pattengale et al. 2010). In the BI analysis, two independent runs were employed. Each run had four chains of 10 000 000 generations and started from random trees. Chain convergence was determined with Tracer 1.5 (http://tree.bio.ed.ac.uk/software/tracer/). After sampling every 1000th generation, the first 25% of sampled trees was removed, whereas the other 75% was subjected to construction of a 50% majority consensus tree and calculation of BPPs. The ML and BI methods generated congruent topologies in main lineages. Therefore, the topology generated in the ML analysis is presented and the BS values and BPPs, simultaneously above 50% and 0.7, respectively, are shown at the nodes.

To further differentiate the taxa of *Leifia*, the distance matrix of the alignment of their ITS sequences (5.8S and ITS2 region) were estimated using MEGA5 (Tamura et al. 2011) under the parameters of maximum composite likelihood model, uniform rates amongst sites and pairwise deletion of gaps/missing data treatment.

Results

From four studied specimens, four ITS and four 28S sequences were newly generated (Table 1). These sequences were incorporated in the dataset of Larsson et al. (2006) with an emphasis of taxa in the *Rickenella* clade. The current dataset included 62 taxa, each with an ITS and a 28S sequence. The concatenated alignment had 2426 characters. The BS search in the ML analysis stopped after 350 replicates. In the BI analysis, all chains were converged as suggested by the effective sample sizes of all parameters above 3300 and by the potential scale reduction factors close to 1000.

The current phylogeny (Figure 1) recovered Hymenochaetales as a strongly supported clade (94%, 1.00). Amongst Hymenochaetales, the *Oxyporus* (Bourdot & Galzin) Donk clade, the *Kneiffiella* P. Karst. clade, the *Hyphodontia* J. Erikss. clade and the Hymenochaetaceae clade were recovered like those in Larsson et al. (2006), although the latter two clades received no statistical support (Figure 1). The so-called *Coltricia* Gray clade in Larsson et al. (2006) here consisted entirely of corticioid species currently referred to *Lyomyces* P. Karst., *Palifer* Stalpers & P.K. Buchanan and *Xylodon* (Pers.) Gray, while *Coltricia perennis* (L.) Murrill nested within the Hymenochaetaceae clade (Figure 1). The *Rickenella* clade of Larsson et al. (2006), the focus group for this study, did not group together well, but *Odonticium romellii* and *Leifia flabelliradiata* formed a strongly supported clade (91%, 1.00; Figure 1) like that in Larsson et al. (2006). The four newly sequenced specimens, also in this clade, had a closer relationship with *L. flabelliradiata* (100%, 1.00; Figure 1) than with *Odonticium*. Besides the lack of morphological similarities between *Odonticium* and *Leifia*, the branch length separating *Odonticium* from *Leifia* and related taxa also indicated that the two genera should be treated as independent.

In the *Leifia* clade, four newly sequenced specimens formed two subclades: *LWZ 20170820-46* and *LWZ 20170820-48* (99%, 0.76) and *LWZ 20171015-36* and *LWZ 20171015-38* (58%, 0.86), which were both separated from *L. flabelliradiata*. The distance matrix of ITS sequences (Table 2) indicated that *LWZ 20171015-36* and *LWZ 20171015-38* represented two distinct lineages (4.4%), while *LWZ 20170820-46* and *LWZ 20170820-48* represented one lineage distinctly different from *LWZ 20171015-36* (3.5%) and *LWZ 20171015-38* (2.9%) and moderately from *L. flabelliradiata* (1.3%).

Table 1. Specimens used for the phylogenetic analyses.

Species [a]	Voucher/strain number	GenBank accession number		Sequence reference	Origin
		ITS	LSU		
Atheloderma mirabile	TAA 169235	DQ873592	DQ873592	Larsson et al. (2006)	Estonia
Basidioradulum radula	AFTOL-ID 451	DQ234537	AY700184	Unpublished	unknown
Blasiphalia pseudogrisella	Lutzoni 930728-3	U66437	U66437	Lutzoni (1997)	unknown
Coltricia perennis	DSH 93-198	DQ234559	AF287854	Hibbett et al. (2000)	unknown
Coniferiporia weirii	JV 0407/8J	KR350569	KR350557	Zhou et al. (2016)	USA
Cylindrosporus flavidus	Dai 13213	KP875564	KP875561	Zhou (2015)	China
Cyphellostereum laeve	JJ 020909	EU118621	EU118621	Larsson (2007a)	Sweden
Exidiopsis calcea	KHL 11075	AY463406	AY586654	Larsson et al. (2004)	Sweden

Species [a]	Voucher/strain number	GenBank accession number		Sequence reference	Origin
		ITS	LSU		
Fomitiporella caryophylli	CBS 448.76	AY558611	AY059021	Wagner and Fischer (2002); Jeong et al. (2005)	India
Fomitiporia hartigii	CBS 162.30	AY558621	AF311005	Jeong et al. (2005)	Russia
Fulvifomes fastuosus	CBS 213.36	AY558615	AY059057	Jeong et al. (2005)	Philippines
Fulvoderma scaurum	LWZ 20130909-2	MF860780	MF860731	Zhou et al. (2018a)	China
Globulicium hiemale	Hjm 19007	DQ873595	DQ873595	Larsson et al. (2006)	Sweden
Hymenochaete adusta	CBS 759.91	AY558594	AF385161	Jeong et al. (2005)	Unknown
Hyphoderma capitatum	KHL 8464 (GB)	DQ677491	DQ677491	Larsson (2007b)	Sweden
Hyphoderma orphanellum	NH 12208 (GB)	DQ677500	DQ677500	Larsson (2007b)	Russia
Hyphoderma sibiricum	KHL 4141 (GB)	DQ677503	DQ677503	Larsson (2007b)	Sweden
Hyphodontia alutaria	KHL 11889	DQ873603	DQ873603	Larsson et al. (2006)	Sweden
Hyphodontia arguta	Hjm 18726	DQ873605	DQ873605	Larsson et al. (2006)	Sweden
Hyphodontia sp.	H Berglund 1117	DQ873633	DQ873634	Larsson et al. (2006)	Sweden
Kneiffiella abieticola	KHL 12498	DQ873601	DQ873601	Larsson et al. (2006)	Sweden
Kneiffiella barba-jovis	KHL 11730	DQ873609	DQ873610	Larsson et al. (2006)	Sweden
Kneiffiella curvispora	KHL	DQ873615	DQ873616	Larsson et al. (2006)	Finland
Kneiffiella floccosa	Berglund 150-02	DQ873618	DQ873618	Larsson et al. (2006)	Sweden
Leifia brevispora	LWZ 20170820-46	MK343469	MK343473	This study	China
Leifia brevispora	LWZ 20170820-48	MK343470	MK343474	This study	China
Leifia flabelliradiata	KG Nilsson 36270	DQ873635	DQ873635	Larsson et al. (2006)	Sweden
Leifia sp. 1	LWZ 20171015-36	MK343471	MK343475	This study	Vietnam
Leifia sp. 2	LWZ 20171015-38	MK343472	MK343476	This study	Vietnam
Loreleia marchantiae	Lutzoni 930826-1	U66432	U66432	Lutzoni (1997)	unknown
Lyomyces crustosus	KHL 11731	DQ873614	DQ873614	Larsson et al. (2006)	Finland
Lyomyces griseliniae	KHL 12971 (GB)	DQ873651	DQ873651	Larsson et al. (2006)	Costa Rica
Lyomyces pruni	Ryberg 021018	DQ873624	DQ873625	Larsson et al. (2006)	Sweden
Odonticium romellii 1	H 6059319	MF319073	MF318929	Korotkin (2017)	Finland
Odonticium romellii 2	KHL s. n.	DQ873639	DQ873639	Larsson et al. (2006)	Norway
Palifer verecundus	KHL 12261 (GB)	DQ873642	DQ873643	Larsson et al. (2006)	USA
Peniophorella praetermissum	KHL 13164 (GB)	DQ873597	DQ873597	Larsson et al. (2006)	Estonia
Peniophorella puberum	KHL 13154 (GB)	DQ873599	DQ873599	Larsson et al. (2006)	Estonia
Protodontia piceicola	KHL 11763 (GB)	DQ873660	DQ873660	Larsson et al. (2006)	Sweden
Repetobasidium conicum	KHL 12338	DQ873647	DQ873647	Larsson et al. (2006)	USA
Rickenella fibula 1	AD86033	AY463464	AY586710	Larsson et al. (2004)	Sweden
Rickenella fibula 2	TENN 071482	MF319083	MF318943	Korotkin (2017)	USA
Rickenella mellea	Lamoure 74-20h 1/9.91	U66438	U66438	Lutzoni (1997)	unknown
Rigidoporus corticola	KHL 13217 (GB)	DQ873641	DQ873641	Larsson et al. (2006)	Estonia
Sidera lunata	JS 15063	DQ873593	DQ873593	Larsson et al. (2006)	Norway
Sistotrema brinkmannii	KHL 14078 (GB)	KF218967	KF218967	Larsson and Kotiranta (2013)	Sweden
Skvortzovia furfuraceum	KHL 11738 (GB)	DQ873648	DQ873648	Larsson et al. (2006)	Finland
Skvortzovia furfurella	KHL 10180 (GB)	DQ873649	DQ873649	Larsson et al. (2006)	Puerto Rico
Skvortzovia georgica	KHL 12019 (GB)	DQ873645	DQ873645	Larsson et al. (2006)	Norway
Skvortzovia pinicola	KHL 12224 (GB)	DQ873637	DQ873637	Larsson et al. (2006)	USA
Sphaerobasidium minutum	KHL 11714	DQ873652	DQ873653	Larsson et al. (2006)	Finland
Sphagnomphalia revibasidiata	Lutzoni 930826-1	U66441	U66441	Lutzoni (1997)	unknown
Trichaptum abietinum	NH 12842 (GB)	AF347104	AF347104	Larsson et al. (2004)	Finland
Tubulicrinis globisporus	KHL 12133	DQ873655	DQ873655	Larsson et al. (2006)	Sweden
Tubulicrinis hirtellus	KHL 11717 (GB)	DQ873657	DQ873657	Larsson et al. (2004)	Finland
Tubulicrinis inornatus	KHL 11763 (GB)	DQ873659	DQ873659	Larsson et al. (2004)	Finland
Tubulicrinis subulatus	KHL11079	AY463478	AY586722	Larsson et al. (2004)	Sweden
Xylodon asperus	KG Nilsson s. n.	DQ873606	DQ873607	Larsson et al. (2006)	Sweden
Xylodon brevisetus	KHL 12386	DQ873612	DQ873612	Larsson et al. (2006)	Sweden
Xylodon detriticus	K.G. Nilsson 990902	DQ677507	DQ677507	Larsson (2007b)	Sweden
Xylodon nespori	B Nordon 030915	DQ873622	DQ873622	Larsson et al. (2006)	Sweden
Xylodon rimosissimus	Ryberg 021031 (GB)	DQ873627	DQ873628	Larsson et al. (2006)	Sweden

[a] Species names are adopted from recent taxonomic proposals.

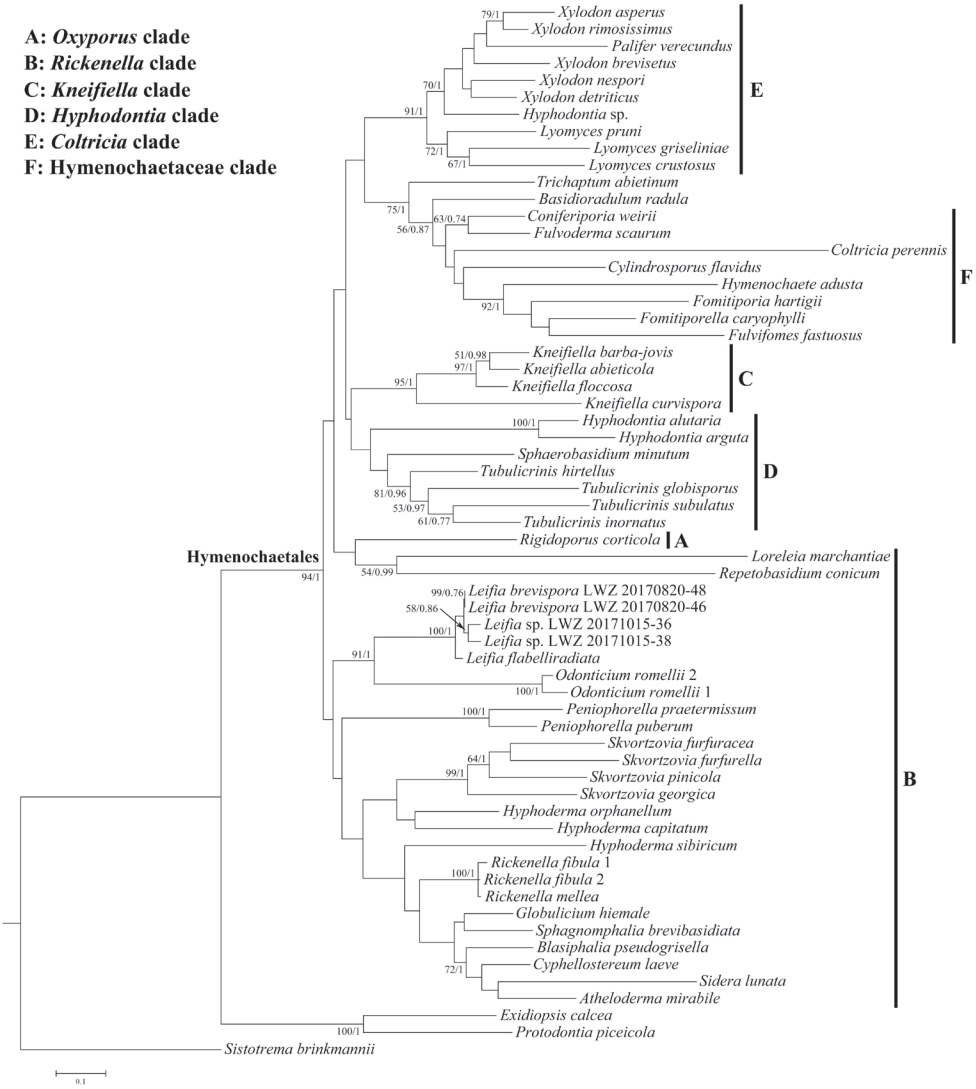

Figure 1. Phylogenetic relationship between *Odonticium romellii* and *Leifia*, based on the concatenated dataset of ITS and 28S regions. The topology was generated from the maximum likelihood analysis and the bootstrap values and Bayesian posterior probability, simultaneously above 50% and 0.7, respectively, are shown at the nodes. The clade names are adapted from Larsson et al. (2006) and the species names from recent taxonomic proposals.

Table 2. Distance matrix of the alignment of ITS sequences (5.8S and ITS2 region) from *Leifia* specimens.

	Species	1	2	3	4	5
1	*L. flabelliradiata*					
2	*L. brevispora* (LWZ 20170820-46)	0.013				
3	*L. brevispora* (LWZ 20170820-48)	0.013	0.000			
4	*L.* sp. (LWZ 20171015-36)	0.043	0.035	0.035		
5	*L.* sp. (LWZ 20171015-38)	0.036	0.029	0.029	0.044	

Taxonomy

***Leifia brevispora* Gafforov, S.L. Liu & L.W. Zhou, sp. nov.**
Figures 2 and 3
MycoBank MB829252

Diagnosis. The species is distinct from *Leifia flabelliradiata* by shorter basidiospores and by being distributed in warm-temperate to subtropical areas in East Asia.

Typification. CHINA. Hubei Province, Wudangshan Town, Wudangshan National Forest Park, on fallen angiosperm branch, 20 Aug 2017, *LWZ 20170820-46* (**holotype** in IFP 019239). GenBank: ITS = MK343469; 28S = MK343473.

Etymology. *brevispora* (Latin), referring to short basidiospores.

Basidiomata. Annual, resupinate, inseparable from substrate, effused, up to 0.6 mm thick. Hymenophore grandinioid to subodontioid. Margin white, smooth or minutely fibrous, sometimes bearing hyphal strands, thinning out, up to 2 mm wide. Aculei cream to buff in colour, rounded to ellipsoid, 2–3 per mm, up to 0.5 mm long, several being clustered together when dry. Subiculum white, up to 100 μm thick.

Microscopic structures. Hyphal system monomitic; generative hyphae without clamp connections. Subicular hyphae hyaline, thin- to thick-walled, occasionally branched, frequently septate, more or less parallel to substrate, 2–4 μm wide. Aculeus (subhymenial) hyphae hyaline, distinctly thick-walled, mainly vertically intertwined,

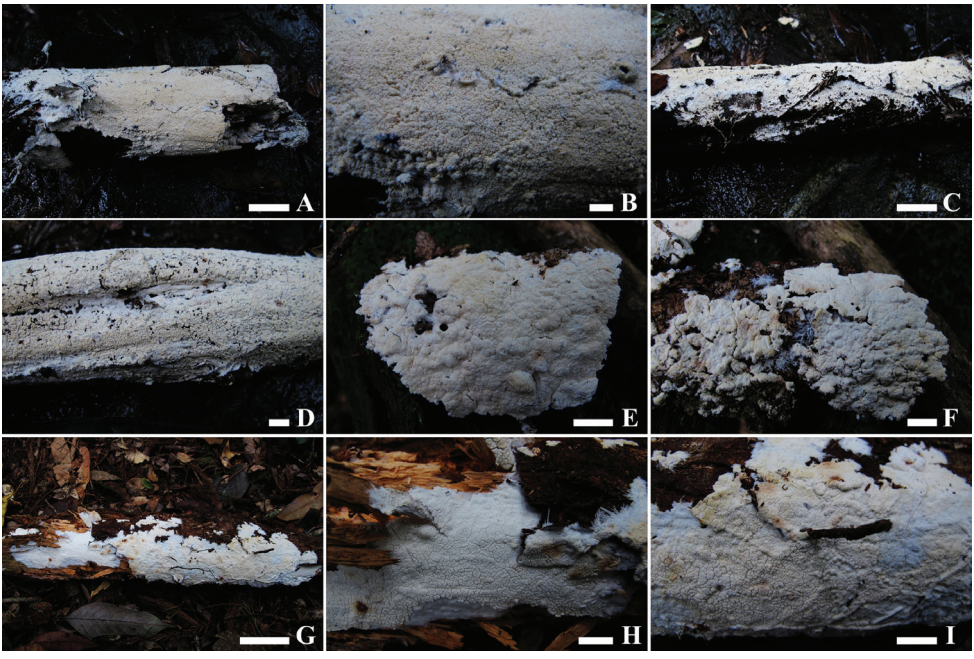

Figure 2. Basidiocarps of *Leifia* in situ. A-B. *L. brevispora* (LWZ 20170820-46, holotype). C-D. *L. brevispora* (LWZ 20170820-48, paratype). E-F. *Leifia* sp. (LWZ 20171015-36). G-I. *Leifia* sp. (LWZ 20171015-38). Scale bars: A, C, G: 5 cm; B, D–F, H–I: 1 cm.

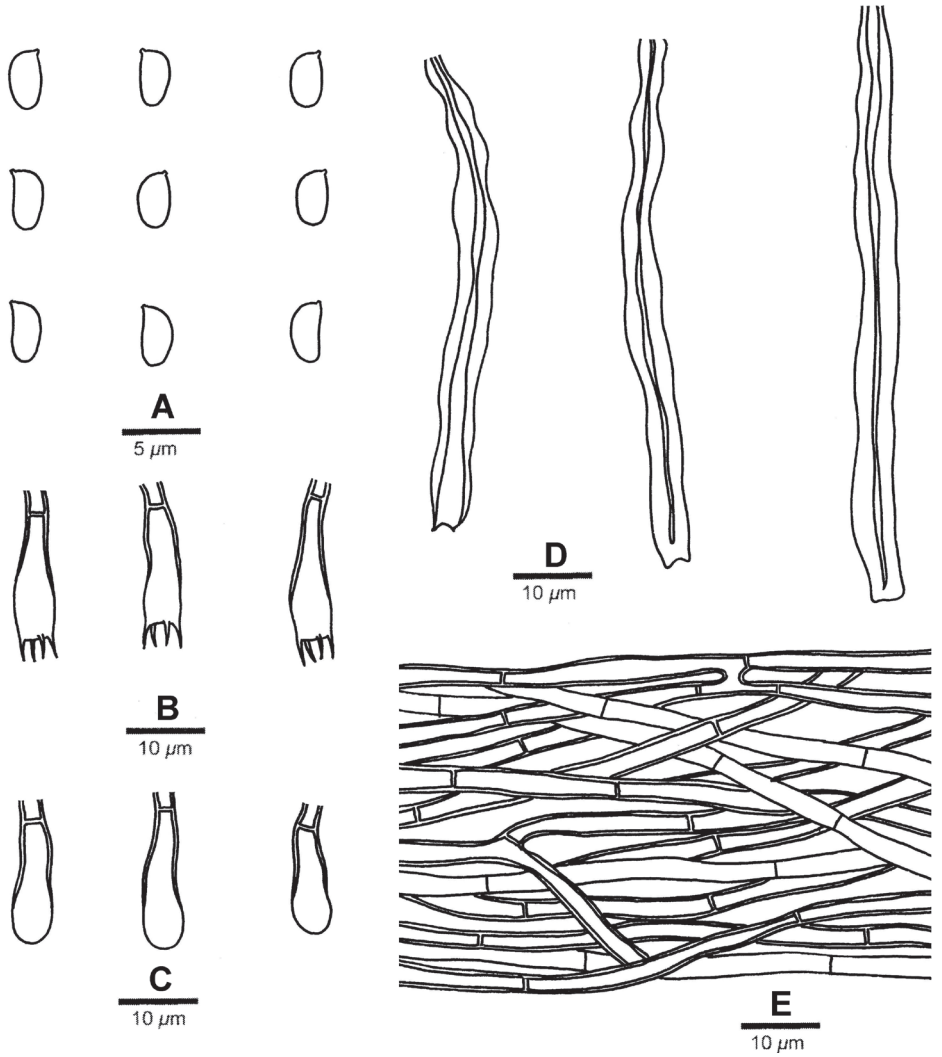

Figure 3. Microscopic structures of *Leifia brevispora* (drawn from LWZ 20170820-46, holotype). A. basidiospores. B. basidia. C. basidioles. D. cystidia. E. subicular hyphae.

2–4 μm wide. Cystidia hyaline, thick-walled, tubular with an invaginated apical end, 60–100 × 5–7 μm, swelling in KOH. Basidia hyaline, thick-walled, clavate to cylindrical, with four sterigmata each 2–3 μm long and a simple septum at the base, 14–18 × 4.5–5.5 μm. Basidioles similar in shape to basidia, but smaller. Basidiospores ellipsoid, hyaline, thin-walled, smooth, inamyloid and indextrinoid, acyanophilous, 3.8–4.5(–5) × (1.8–)2–2.5 μm, L = 4.13 μm, W = 2.14 μm, Q = 1.92–1.96 (60/2).

Other specimen examined. CHINA. Hubei Province, Wudangshan Town, Wudangshan National Forest Park, on fallen angiosperm branch, 20 Aug 2017, *LWZ 20170820-48* (IFP 019240).

Notes. The grandinioid hymenophore, simple-septate hyphae, distinctly thick-walled cystidia with an invaginated apical end and ellipsoid to subovate basidiospores with a straight or concave side, indicate that the new species is the second member of *Leifia*. Moreover, the phylogeny inferred from the ITS and 28S dataset also confirm the taxonomic position of *L. brevispora*. The generic type of *Leifia*, *L. flabelliradiata*, differs from *L. brevispora* by having longer basidiospores (4.5–5.5 × 2–2.5 μm) and a distribution in Europe (Eriksson et al. 1981).

Discussion

In this study, the newly generated ITS and 28S sequences were incorporated into the dataset of Larsson et al. (2006) and, in the resulting phylogeny (Figure 1), clades are labelled A-F as in Larsson et al. (2006). The differences of phylogeny observed between the current study and Larsson et al. (2006) might reflect that the ITS and 28S dataset itself is not enough to reliably resolve the relationships within Hymenochaetales. Similar to Larsson et al. (2006), *Leifia* formed a sister lineage to *Odonticium* with strong support in the current phylogeny (Figure 1). The five taxa of *Leifia* and the two of *Odonticium* were clearly separated and recovered as independent, fully supported clades. Morphologically, *Leifia* is well distinguished from *Odonticium* by its grandinioid hymenophore with hyphal strands, numerous thick-walled cystidia with an invaginated apical end and narrowly and thick-walled basidia (Eriksson et al. 1981). Therefore, we propose to resurrect *Leifia* as an independent genus in Hymenochaetales.

Amongst the four newly sequenced taxa in *Leifia* clade, *LWZ 20170820-46* and *LWZ 20170820-48* represent the new species *L. brevispora*, while *LWZ 20171015-36* and *LWZ 20171015-38*, both collected from Bidoup Nui Ba National Park, Da Lat, Viet Nam, seem to represent two undescribed taxa. *LWZ 20171015-36* differs from *L. brevispora* and *L. flabelliradiata* by fairly thick basidiocarps and *LWZ 20171015-38* differs by having basidia and basidioles that swell in KOH. Moreover, *LWZ 20171015-38* grows on fallen branches of *Pinus*, while the other three specimens were all collected from angiosperm substrates. Although the morphological characters of *LWZ 20171015-36* and *LWZ 20171015-38* are unique in *Leifia*, we feel more samples need to be examined before describing them as new species.

Acknowledgements

The research was financed by the National Natural Science Foundation of China (Project Nos. 31570014 & 31770008), Youth Innovation Promotion Association CAS (No. 2017240) and Chinese Academy of Sciences President's International Fellowship Initiative (Grant No. 2018VBB0021). We thank Dr. Barbara Wilson (Corvallis, Oregon, US) for suggestions on Latin name of species.

References

Burdsall Jr HH (1985) A contribution to the taxonomy of the genus *Phanerochaete* (Corticiaceae, Aphyllophorales). Mycologia Memoir 10: 1–165.

Eriksson J, Hjortstam K, Ryvarden L (1981) The Corticiaceae of North Europe 6. Fungiflora, Oslo, 1051–1276.

Gardes M, Bruns TD (1993) ITS primers with enhanced specifity for Basidiomycetes: application to identification of mycorrhizae and rusts. Molecular Ecology 2: 113–118. https://doi.org/10.1111/j.1365-294X.1993.tb00005.x

Ginns J (1998) Genera of the North American Corticiaceae sensu lato. Mycologia 90: 1–35. https://doi.org/10.2307/3761008

Guindon S, Gascuel O (2003) A simple, fast and accurate method to estimate large phylogenies by maximum-likelihood. Systematic Biology 52: 696–704. https://doi.org/10.1080/10635150390235520

Hibbett DS, Gilbert LB, Donoghue MJ (2000) Evolutionary instability of ectomycorrhizal symbioses in basidiomycetes. Nature 407: 506–508. https://doi.org/10.1038/35035065

Hjortstam K (1986) Notes on Corticiaceae (Basidiomycetes) XIV. Mycotaxon 25: 273–277.

Hjortstam K, Larsson KH, Ryvarden L (1987) The Corticiaceae of North Europe 1. Fungiflora, Oslo, 1–59.

Jeong WJ, Lim YW, Lee JS, Jung HS (2005) Phylogeny of *Phellinus* and related genera inferred from combined data of ITS and mitochondrial SSU rDNA sequences. Journal of Microbiology & Biotechnology 15: 1028–1038.

Katoh K, Kuma K, Toh H, Miyata T (2005) MAFFT version 5: improvement in accuracy of multiple sequence alignment. Nucleic Acids Research 33: 511–518. https://doi.org/10.1093/nar/gki198

Katoh K, Standley DM (2013) MAFFT multiple sequence alignment software version 7: improvements in performance and usability. Molecular Biology and Evolution 30: 772–780. https://doi.org/10.1093/molbev/mst010

Korotkin HB (2017) Stable isotopes, phylogenetics, and experimental data indicate a unique nutritional mode for *Rickenella fibula*, a bryophyte-associate in the Hymenochaetales. MsD Theses, University of Tennessee, Knoxville, 114 pp.

Larsson KH (2007a) Re-thinking the classification of corticioid fungi. Mycological Research 111: 1040–1063. https://doi.org/10.1016/j.mycres.2007.08.001

Larsson KH (2007b) Molecular phylogeny of *Hyphoderma* and the reinstatement of *Peniophorella*. Fungal Biology 111: 186–195. https://doi.org/10.1016/j.mycres.2006.10.002

Larsson KH, Parmasto E, Fischer M, Langer E, Nakasone KK, Redhead SA (2006) Hymenochaetales: a molecular phylogeny for the hymenochaetoid clade. Mycologia 98: 926–936. https://doi.org/10.1080/15572536.2006.11832622

Larsson KH, Kotiranta H (2013) *Sistotrema luteoviride* sp. nov. (Cantharellales, Basidiomycota) from Finland. Acta Mycologica 48: 219–225. https://doi.org/10.5586/am.2013.023

Larsson KH, Larsson E, Koljalg U (2004) High phylogenetic diversity among corticioid homobasidiomycetes. Mycological Research 108: 983–1002. https://doi.org/10.1017/S0953756204000851

Lutzoni FM (1997) Phylogeny of lichen- and non-lichen-forming omphalinoid mushrooms and the utility of testing for combinability among multiple data sets. Systematic Biology 46: 373–406. https://doi.org/10.2307/2413688

Pattengale ND, Alipour M, Bininda-Emonds ORP, Moret BME, Stamatakis A (2010) How many bootstrap replicates are necessary? Journal of Computational Biology 17: 337–354. https://doi.org/10.1089/cmb.2009.0179

Posada D (2008) jModelTest: phylogenetic model averaging. Molecular Biology and Evolution 25: 1253–1256. https://doi.org/10.1093/molbev/msn083

Ronquist F, Teslenko M, van der Mark P, Ayres D, Darling A, Höhna S, Larget B, Liu L, Suchard MA, Huelsenbeck JP (2012) MrBayes 3.2: efficient Bayesian phylogenetic inference and model choice across a large model space. Systematic Biology 61: 539–542. https://doi.org/10.1093/sysbio/sys029

Silvestro D, Michalak I (2012) raxmlGUI: a graphical front end for RAxML. Organisms, Diversity & Evolution 12: 335–337. https://doi.org/10.1007/s13127-011-0056-0

Stamatakis A (2006) RAxML-VI-HPC: maximum likelihood based phylogenetic analyses with thousands of taxa and mixed models. Bioinformatics 22: 2688–2690. https://doi.org/10.1093/bioinformatics/btl446

Tamura K, Peterson D, Peterson N, Stecher G, Nei M, Kumar S (2011) MEGA5: Molecular evolutionary genetic analysis using maximum likelihood, evolutionary distance, and maximum parsimony methods. Molecular Biology and Evolution 28: 2731–2739. https://doi.org/10.1093/molbev/msr121

Turland NJ, Wiersema JH, Barrie FR, Greuter W, Hawksworth DL, Herendeen PS, Knapp S, Kusber WH, Li DZ, Marhold K, May TW, McNeill J, Monro AM, Prado J, Price MJ, Smith GF (2018) International Code of Nomenclature for algae, fungi, and plants (Shenzhen Code) adopted by the Nineteenth International Botanical Congress Shenzhen, China, July 2017. Regnum Vegetabile 159. Koeltz Botanical Books, Glashütten, 254 pp. https://doi.org/10.12705/Code.2018

Vilgalys R, Hester M (1990) Rapid genetic identification and mapping of enzymatically amplified ribosomal DNA from several *Cryptococcus* species. Journal of Bacteriology 172: 4238–4246. https://doi.org/10.1128/jb.172.8.4238-4246.1990

Wagner T, Fischer M (2002) Proceedings towards a natural classification of the worldwide taxa *Phellinus* s.l. and *Inonotus* s.l., and phylogenetic relationships of allied genera. Mycologia 94: 998–1016. https://doi.org/10.2307/3761866

White TJ, Bruns T, Lee S, Taylor J (1990) Amplification and direct sequencing of fungal ribosomal RNA genes for phylogenetics. In: Innis MA, Gelfand DH, Sninsky JJ, White TJ (Eds) PCR protocols: a guide to methods and application. Academic Press, New York, 315–322. https://doi.org/10.1016/B978-0-12-372180-8.50042-1

Zhou LW (2015) *Cylindrosporus flavidus* gen. et comb. nov. (Hymenochaetales, Basidiomycota) segregated from *Onnia*. Phytotaxa 219: 276–282. https://doi.org/10.11646/phytotaxa.219.3.7

Zhou LW, Ji XH, Vlasák J, Dai YC (2018) Taxonomy and phylogeny of *Pyrrhoderma*: a redefinition, the segregation of *Fulvoderma* gen. nov. and four new species. Mycologia 110: 872–889. https://doi.org/10.1080/00275514.2018.1474326

Zhou LW, Vlasák J, Dai YC (2016) Taxonomy and phylogeny of *Phellinidium* (Hymenochaetales, Basidiomycota): a redefinition and the segregation of *Coniferiporia* gen. nov. for forest pathogens. Fungal Biology 120: 988–1001. https://doi.org/10.1016/j.funbio.2016.04.008

Zmitrovich IV (2001) Contribution to the taxonomy of corticoid fungi. I. The genera *Athelia*, *Byssomerulius*, *Hyphoderma*, *Odonticium*. Mikologiya I Fitopatologiya 35: 9–19.

MycoKeys 51: 97–106 (2019)
doi: 10.3897/mycokeys.51.34956
http://mycokeys.pensoft.net

RESEARCH ARTICLE

A peer-reviewed open-access journal
MycoKeys
Launched to accelerate biodiversity research

Erysiphe deutziicola sp. nov. (Erysiphaceae, Ascomycota), a powdery mildew species found on *Deutzia parviflora* (Hydrangeaceae) with unusual appendages

Peng-Lei Qiu[1], Uwe Braun[2], Yu Li[1], Shu-Yan Liu[1,3]

1 *Jilin Agricultural University, Engineering Research Center of Chinese Ministry of Education for Edible and Medicinal Fungi, No. 2888 Xincheng Street, Changchun 130118, Jilin Province, China* **2** *Martin Luther University, Institute of Biology, Geobotany and Botanical Garden, Herbarium, Neuwerk 21, 06099 Halle (Saale), Germany* **3** *Laboratory of Plant Pathology, College of Plant Protection, Jilin Agricultural University, No. 2888 Xincheng Street, Changchun130118, Jilin Province, China*

Corresponding author: *Shu-Yan Liu* (liussyan@163.com)

Academic editor: *N. Wijayawardene* | Received 30 March 2019 | Accepted 4 April 2019 | Published 8 May 2019

Citation: Qiu P-L, Braun U, Li Y, Liu S-Y (2019) *Erysiphe deutziicola* sp. nov. (Erysiphaceae, Ascomycota), a powdery mildew species found on *Deutzia parviflora* (Hydrangeaceae) with unusual appendages. MycoKeys 51: 97–106. https://doi.org/10.3897/mycokeys.51.34956

Abstract

A powdery mildew (Erysiphales) has recently been collected on leaves of an ornamental shrub *Deutzia parviflora* in Baihua Mountain, Beijing, China. Microscopic examination of the chasmothecia suggested a species belonging to *Erysiphe* sect. *Erysiphe*, above all due to mycelioid chasmothecial appendages, although circinate apices of the appendages were rather in favour of *Erysiphe* sect. *Uncinula*, which is a fairly rare combination of appendage characteristics in *Erysiphe*. Phylogenetic analyses of ITS and 28S rDNA sequences demonstrated that the two examined powdery mildew collections on *D. parviflora* clustered together as an independent lineage within *Erysiphe* with 100% bootstrap support, representing a species of its own, which is phylogenetically allied to, but clearly distinct from *Erysiphe deutziae* and, in addition, morphologically quite different from all known *Erysiphe* species on hosts belonging to the Hydrangeaceae. The new species on *D. parviflora* is described as *Erysiphe deutziicola*.

Keywords

Erysiphales, powdery mildew, pathogen, ITS, 28S rDNA, phylogeny

Introduction

The family Hydrangeaceae comprises 17 genera and about 220 species distributed in temperate and subtropical regions of the Americas, Pacific islands, Asia and Europe (Kubitzki 2004). One of the largest genera, *Deutzia*, includes important ornamentals and is known to be used to treat enuresis, malaria and scabies in China (He 1990). Amongst the genera of Hydrangeaceae, *Deutzia*, *Hydrangea*, *Schizophragma*, *Jamesia* and *Philadelphus* have been reported as hosts of powdery mildews (Braun and Cook 2012). Nine species are currently known on hosts of these genera, viz., *Erysiphe deutziae* (Bunkina) U. Braun & S. Takam. on *Deutzia*, *E. hydrangeae* (Z.X. Chen & R.X. Gao) U. Braun & S. Takam. on *Hydrangea*, *E. poeltii* U. Braun on *Hydrangea*, *E. schizophragmatis* (Tanda & Y. Nomura) U. Braun & S. Takam. on *Hydrangea* and *Schizophragma*, *E. yanshanensis* T.Z. Liu & U. Braun on *Hydrangea*, *Golovinomyces orontii* on *Hydrangea*, *Phyllactinia jamesiae* U. Braun on *Jamesia*, *P. philadelphi* (Jacz.) Bunkina on *Philadelphus* and *Pseudoidium hortensiae* (Jørst.) U. Braun & R.T.A. Cook on *Hydrangea*. *Erysiphe deutziae* has been the only powdery mildew species hitherto found on *Deutzia* spp. (Braun and Cook 2012). This species was originally described as *Microsphaera deutziae* (Bunkina 1973). In 1977, this species was recorded from the Russian Far East and Japan (Nomura 1997). Braun and Takamatsu (2000) re-allocated *M. deutziae* to *Erysiphe* based on the phylogenetic analysis of ITS rDNA sequences (Braun and Takamatsu 2000). Later, this powdery mildew was introduced to Europe with records from France, Germany, Poland and Switzerland (Bolay et al. 2005) and the UK (Denton and Henricot 2007). In recent years, this pathogen was also reported on *Deutzia* in Korea (Park et al. 2010) and China (Nguyen et al. 2018).

In 2018, leaves of *D. parviflora* with clearly dense powdery layers were collected twice. Microscopic examination suggested the unusual appendages of chasmothecia of the fungus are apparently distinct from *E. deutziae* on *Deutzia*. In order to circumscribe this species, morphological and molecular phylogenetic analyses, based on ITS and 28S rDNA sequences, were conducted for the characterisation and identification of a new *Erysiphe* species, *E. deutziicola*, found in China on *D. parviflora*.

Materials and methods

Morphological studies

In May 2018, *D. parviflora* plants with typical white powdery mildew symptoms were first noticed and collected in the nature reserve of Baihua Mountain of Beijing, China (115°34.20'E; 39°50.40'N) and later, in October, the sexual morph was found. The two specimens were deposited in the Herbarium of Mycology of Jilin Agricultural University (**HMJAU**) under the accession number HMJAU-PM91860 and HMJAU-PM91861, respectively. The dried specimens were put in lactic acid for light microscopic examinations (Zeiss Axio Scope A1, Germany).

DNA extraction and sequencing

Genome DNA was extracted using chasmothecia of HMJAU-PM91860 and conidia and mycelia from the asexual specimen HMJAU-PM91861 by the Chelex-100 method (Walsh et al. 1991; Hirata and Takamatsu 1996). Two specimens of *Erysiphe deutziae* on *Deutzia parviflora* var. *amurensis* (Nguyen et al. 2018) were also used for the DNA extraction and amplification, since 28S rDNA sequences of *E. deutziae* were not yet available in GenBank. The DNA amplification and sequencing were conducted according to the procedure described by Qiu et al. (2018).

Molecular phylogenetic analyses

The newly obtained sequence data (28S rDNA, including domains D1 and D2 and ITS, including the 5.8S rDNA) from two powdery mildew specimens on *D. parviflora* were aligned to confirm the homology. The new sequences were deposited in GenBank under accession numbers MK656288 (ITS) and MK656309 (28S) from HMJAU-PM91860 and MK656289 (ITS) and MK656310 (28S) from HMJAU-PM91861. The combined datasets of ITS and 28S rDNA sequences from the two specimens were aligned with closely related sequences of *Erysiphe* spp. retrieved from GenBank (Table 1) including sequences from some species occurring on hosts belonging to the Hydrangeaceae using MUSCLE implemented in the MEGA 7 programme (Kumar et al. 2016). Alignments were further manually refined and deposited in TreeBASE (http://www.treebase.org/) under the accession number of S24214.

Table 1. Vouchers, hosts and GenBank accession numbers of the sequences used in this study.

Species	Voucher	Host	Host family	Accession number	Sequence size (bp)	Reference
Erysiphe adunca	MUMH 171	*Salix futura*	Salicaceae	LC028968	1326	Takamatsu et al. 2015b
E. arcuata	MUMH 2741	*Carpinus tschonoskii*	Betulaceae	AB252473	1335	Braun et al. 2006
E. arcuata	MUMH 3620	*C. tschonoskii*	Betulaceae	AB252474	1335	Braun et al. 2006
E. blasti	MUMH 0002	*Laurus umbellata*	Lauraceae	LC009905	1317	Takamatsu et al. 2015a
E. deutziae	HMJAU91777	*Deutzia parviflora* var. *amurensis*	Hydrangeaceae	MH027420 (ITS)	671	Nguyen et al. 2018
				MK656311 (28S)	637	This study
E. deutziae	HMJAU91771	*D. parviflora* var. *amurensis*	Hydrangeaceae	MG674082 (ITS)	670	Nguyen et al. 2018
				MK656312 (28S)	637	This study
E. deutziicola	HMJAU-PM91860	*D. parviflora*	Hydrangeaceae	MK656288 (ITS)	666	**This study**
				MK656309 (28S)	636	
E. deutziicola	HMJAU-PM91861	*D. parviflora*	Hydrangeaceae	MK656289 (ITS)	666	**This study**
				MK656310 (28S)	636	
E. epigena	MUMH 2193	*Quercus variabilis*	Fagaceae	AB292720	1403	Takamatsu et al. 2007
E. heraclei	MUMH 2484	*Conium maculatum*	Umbelliferae	LC010021	1355	Takamatsu et al. 2015a
E. huayinensis	MUMH 4644	*Isodon umbrosus*	Lamiaceae	LC010072	1314	Takamatsu et al. 2015a
E. huayinensis	MUMH 0087	*I. trichocarpus*	Lamiaceae	LC010080	1362	Takamatsu et al. 2015a
E. hydrangeae	MUMH 0514	*Hydrangea paniculata*	Hydrangeaceae	LC028983	1361	Takamatsu et al. 2015b

E. izuensis	MUMH 4651	*Rhododendron reticulatum*	Ericaceae	LC010076	1350	Takamatsu et al. 2015a
E. juglandis	TPU 1745	*Pterocarya rhoifolia*	Juglandaceae	LC010090	1276	Takamatsu et al. 2015a
E. pileae	MUMH 2987	*Pilea pumila*	Urticaceae	LC010059 (ITS)	552	Takamatsu et al. 2015a
				LC010058 (28S)	754	
E. pedaliacearum	MUMH 412	*Sesamum indicum*	Pedaliaceae	LC342968	1516	Shin et al. 2018
E. phyllanthi	MUMH 0099	*Phyllanthus flexuosus*	Euphorbiaceae	LC009921	1351	Takamatsu et al. 2015a
E. sedi	MUMH 2576	*Sedum* sp.	Crassulaceae	LC010046	1321	
E. schizophragmatis	MUMH 4642	*Hydangea petiolaris*	Hydrangeaceae	LC029001	1356	Takamatsu et al. 2015b
Pseudoidium hortensiae	MUMH 0071	*Hydrangea macrophylla*	Hydrangeaceae	LC009915	1249	Takamatsu et al. 2015a
Pse. neolycopersici	MUMH 0066	*Lycopersicon esculentum*	Solanaceae	LC009912	1344	Takamatsu et al. 2015a

A phylogenetic tree was obtained from the combined data using the maximum-parsimony (MP) method in PAUP 4.0. The MP analysis was performed with the heuristic search option using the tree-bisection-reconstruction (TBR) algorithm with 100 random sequence additions to find the global optimum tree. The gaps were treated as missing data. The bootstrap analysis (1000 replications) was used for testing the strength of the internal branches of the resulting trees (Felsenstein 1985). Tree scores, including tree length, consistency index (CI), retention index (RI) and rescaled consistency index (RC) were also calculated. Bootstrap (BS) values of 60% or higher are indicated.

Results

Phylogenetic analysis

The alignments of ITS and 28S rDNA sequences obtained from the two specimens examined are identical to each other. A total of 22 combined sequence data, including sequences from *Pseudoidium hortensiae*, *E. hydrangeae*, *E. schizophragmatis* and *E. deutziae*, four powdery mildew species on hosts of the Hydrangeaceae, were used to construct the phylogenetic tree. The sequence of *E. adunca* (LC028968) was used as outgroup. The original alignment dataset comprises of 1232 characters. We manually deleted 111 characters and the remaining 1121 characters were finally used for constructing the phylogenetic tree, where 105 characters were variable but not informative and 175 characters were phylogenetically informative for parsimony analysis. The analysis produced three equally parsimonious trees. The best MP tree (TL = 525, CI = 0.6895, RI = 0.7175, RC = 0.4947) with the highest likelihood score is shown in Figure 1. The phylogenetic analysis confirmed that the new sequences obtained from the powdery mildew on *D. parviflora* formed an independent clade supported by a bootstrap value of 100%.

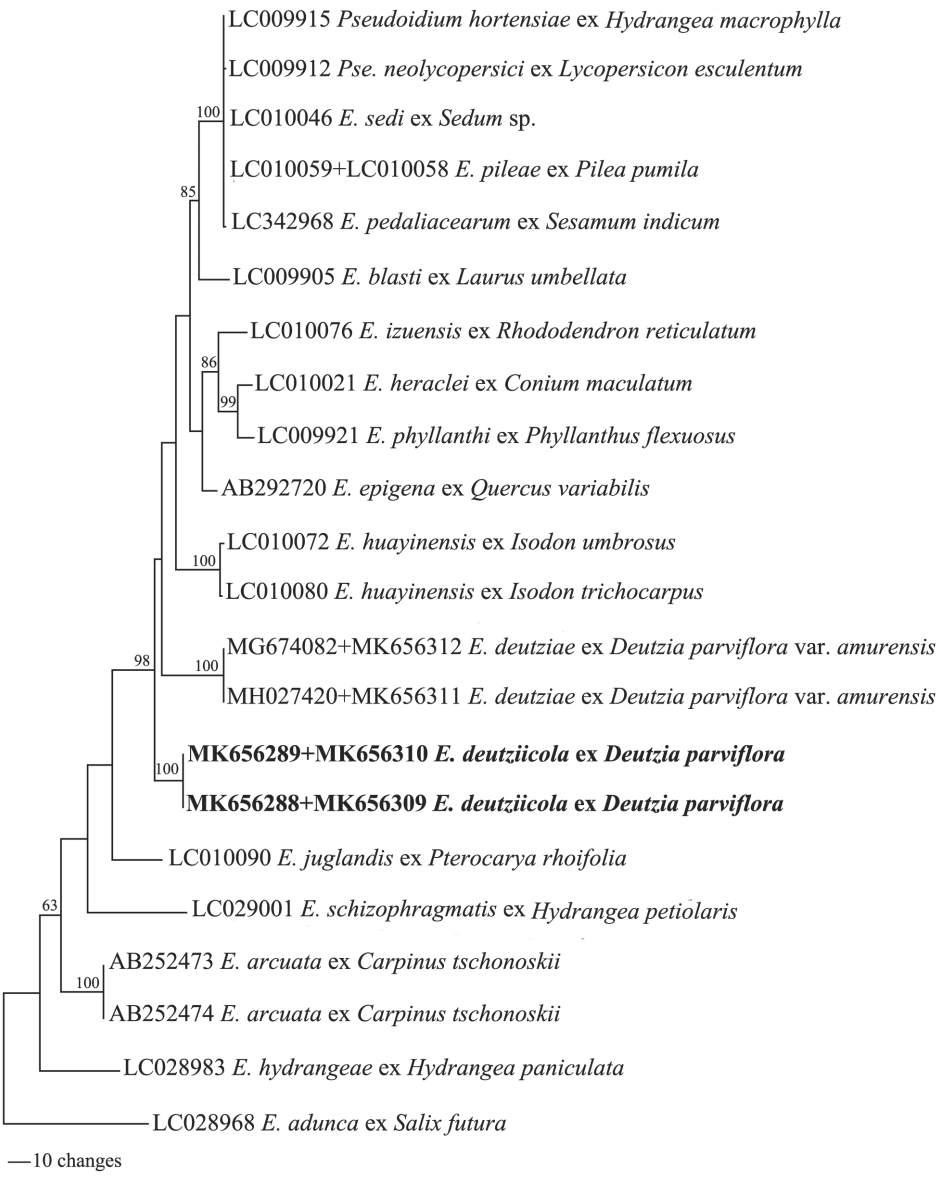

Figure 1. Maximum parsimony phylogram of *Erysiphe deutziicola* and its allied species constructed from the combination of ITS and 28S rDNA sequences. *Erysiphe adunca* (LC028968) was used as outgroup. Bootstrap values (> 60%) by the maximum parsimony (MP) method are shown on the respective branches. The sequences pertaining to *E. deutziicola* are shown in bold face.

Taxonomy

Erysiphe deutziicola **P.-L. Qiu, S.-Y. Liu & Y. Li, sp. nov.**
Figure 2
MycoBank: MB830253

Etymology. Named after the host genus, *Deutzia*, + -icola (dweller).

Diagnosis. Differs from all known *Erysiphe* species on hosts belonging to the Hydrangeaceae in having very long conidiophores, up to 235.0 µm and chasmothecia with mycelioid appendages, circinate at the apex.

Type. CHINA. Beijing City, Baihua Mountain, on leaves of *Deutzia parviflora*, 19 October 2018, P.-L. Qiu, S.-R. Tang & L. Liu, HMJAU-PM91860 (holotype) and HMAS 248089 (isotype) in the Herbarium Mycologicum Academiae Sinica (HMAS), Beijing; ibid., on leaves of *D. parviflora*, 26 May 2018, P.-L. Qiu, S.-R. Tang & D.-N. Jin, HMJAU-PM91861 (paratype).

Description. Forming distinct white colonies, very small and dense, covering both sides of the leaves, causing discolourations of entire leaves or even malformations. Mycelium amphigenous, effuse and persistent. Hyphal appressoria distinctly lobed, solitary (Figure 2, A). Conidiophores, short to very long, 54.5−171.0(−235) × 5.8−8.0 µm, arising from the upper surface of hyphal mother cells (Figure 2, B−D). Foot-cells straight, (23−)30.5−75.0 × 5.7−7.7 µm, followed by 1 to 3(−4) cells, 13−80 µm in length. Conidia formed singly, hyaline, ellipsoid-ovoid or oblong, 18.6−35.5 × 10−14 µm with a length/width ratio varying from 1.4−3.0(−3.3) (Figure 2, E−G). Germ tubes on the conidia with lobed apex or longitubus pattern, apex simple or somewhat swollen, produced laterally, near the middle or in perihilar position (Figure 2, H−J). Chasmothecia, amphigenous, scattered, 70−100.0 µm diam. (Figure 2, K). Peridium cells irregularly polygonal, 3.5–12.5 µm diam. (Figure 2, M). Appendages 6−14 per chasmothecium, mycelioid, hyaline, aseptate, extremely long and flexuous, 1.3−7.0 times as long as the chasmothecial diameter, up to 600 µm, 3–9 µm wide in the lower half, apices mostly sinuous-geniculate or branched, circinate at the near apex, coils relatively loose and wide (Figure 2, L). Asci 4–6 per chasmothecium, broad obovoid-saccate or clavate, short-stalked or sessile, 48−71.5 × 28.5−49.5 µm (Figure 2, N−R). Ascospores ovoid or ellipsoid, 5−8 in each ascus, 13.0−20.5 × 10.5−14.5 µm (Figure 2, S−T).

Host range and distribution. On *Deutzia parviflora* (Hydrangeaceae) in Beijing, China.

Discussion

For taxonomic purposes within the genus *Erysiphe*, the characteristics of the appendages are the most effective way to assign species to morphological, non-phylogenetic sections of *Erysiphe* that were introduced in Braun and Takamatsu (2000) and Braun and Cook (2012). Of the nine species recorded on hosts of the Hydrangeaceae, only *E. poeltii*

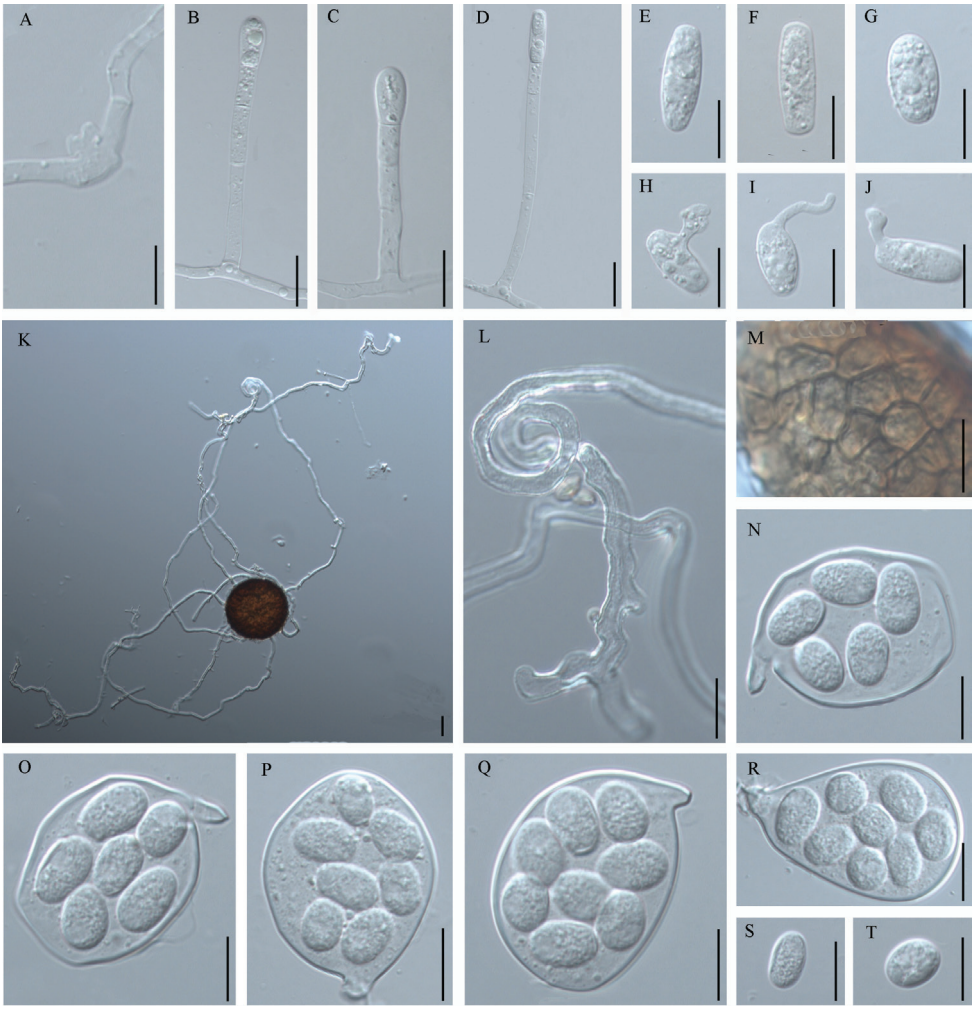

Figure 2. Morphology of *Erysiphe deutziicola* on *Deutzia parviflora*. **A** Lobed hyphal appresorium **B–D** Conidiophores **E–G** Conidia **H** Lobed germ tube arising from the lateral of conidium **I** Germ tube showing longitubus pattern arising from a conidium in perihilar position **J** Slightly lobed germ tube arising from the perihilar position of a conidium **K** Chasmothecium **L** Appendage with sinuous-geniculate, branched and circinate apex **M** Peridium cells **N** Ascus with 5 ascospores **O** Ascus with six ascospores **P** Ascus with seven ascospores **Q** Ellipsoid ascus with eight ascospores **R** Clavate ascus with eight ascospores **S** Ellipsoid ascospore **T** Ovoid ascospore. Scale bars: 20 μm.

pertains to *Erysiphe* sect. *Erysiphe* characterised by mycelioid chasmothecial appendages. The mycelioid appendages of *E. poeltii* are unbranched and later become yellowish to brownish, but remain paler or hyaline in the upper half. The appendages of *E. deutziicola* are completely hyaline, mostly sinuous-geniculate or branched in the apical region and sometimes distinctly circinate at the apex. *Erysiphe deutziae* is currently the only species on *Deutzia* spp., but it differs from *E. deutziicola* by its typically dichotomously branched appendages. The shorter, straight, stiff uncinuloid chasmothecial appendages

Table 2. Morphological comparison of *Erysiphe deutziicola* and closely related species in Braun and Cook (2012).

Species name	Host family	Conidia (µm)	Length of conidiophores (µm)	Diameter of chasmothecia (µm)	Appendages		Number of asci	Ascospores	
					Number	morphology		Number	Colour
Erysiphe deutziicola	Hydrangeaceae	18.6–35.6 × 10.2–14.1	54.7–171.0 (–234.7)	71.0–100.0	6–14	mycelioid	4–6	5–8	colourless
E. abeliae	Caprifoliaceae	– †	–	(85–) 95–120	10–40	mycelioid	4–8	6–8	yellowish
E. braunii	Asteraceae	35–45 × 17–23	80–110	90–130	18–36	mycelioid	6–16	2–3	colourless
E. deutziae	Hydrangeaceae	25–35 (–40) × (16.5–) 17.5–20 (–22)	50–75	70–150	4–16	dichotomous	2–6	4–8	colourless
E. hydrangeae	Hydrangeaceae	–	–	120–225	19–40 (–48)	circinate	(5–) 6–12 (–21)	(4–) 5–8	colourless
E. poeltii	Hydrangeaceae	26–33 × 13–18	–	75–110	5–20	mycelioid	(3–) 4–5 (–6)	5–8	colourless
E. schizophragmatis	Hydrangeaceae	27–38 × 14–18	up to 90	80–120	7–22	circinate	6–13	4–5	colourless
E. yanshanensis	Hydrangeaceae	average 26.5 × 14	45–80	average 120	5–23	circinate	(3–) 4–9 (–11)	(2–) 5–7 (–8)	yellowish
Pseudoidium hortensiae	Hydrangeaceae	(18–) 25–40 (–45) × (9–) 12–19 (–22)	40–130 (–175)	–	–	–	–	–	–

† "–" means no related information

with uncinated-circinate tips are characteristic for *E. hydrangeae*, *E. schizophragmatis* and *E. yanshanensis* and easily distinguish these species from *E. deutziicola*. Recently published phylogenetic examinations revealed that *Pseudoidium hortensiae* belongs to the *Erysiphe aquilegiae* complex (Shin et al. 2018) suggesting that *Pse. hortensiae* is a member of sect. *Erysiphe*, although chasmothecia of this species have not yet been found (Braun and Cook 2012). There are two additional species with chasmothecial appendages similar to those of *E. deutziicola*, viz., *E. abeliae* R.Y. Zheng & G.Q. Chen and *E. braunii* Y. Nomura. which have been described. However, the appendages in *E. braunii* on *Saussurea* are quite distinct by being pluriseptate and not coiled at the tip and the asci are 2–3-spored (Braun and Cook 2012). *Erysiphe deutziicola* differs from *E. abeliae* in having fewer, much longer appendages (numbers 6−14 vs. 10−40, 1.3−7.0 times as long as the chasmothecial diameter vs. mostly 1–2 times) and fewer asci (4−6 per chasmothecium vs. 4−8). In addition, the ascospores of *E. abeliae* are yellowish vs. colourless in *E. deutziicola*.

The phylogenetic analysis revealed that *Erysiphe deutziicola* clustered in a separate clade with 100% bootstrap support, distant from all included *Erysiphe* species occurring on hosts of the Hydrangeaceae and it further confirmed that this species represents a species of its own. The detail morphological traits of *E. deutziicola* and other *Erysiphe* species on hosts of the Hydrangeaceae, as well as morphologically similar species on hosts of other plant families, are shown in Table 2.

Acknowledgements

The authors sincerely acknowledge Prof. Susumu Takamatsu for reading the full text, for critical comments and for corrections. We appreciate the laboratories of Engineering Research Center of Chinese Ministry of Education for Edible and Medicinal Fungi and College of Plant Protection in Jilin Agricultural University, Changchun, China. This work was supported by the National Natural Science Foundation of China [grant programme numbers 31670022, 31470153].

References

Braun U, Takamatsu S (2000) Phylogeny of *Erysiphe*, *Microsphaera*, *Uncinula* (Erysipheae) and *Cystotheca*, *Podosphaera*, *Sphaerotheca* (Cystotheceae) inferred from rDNA ITS sequences – some taxonomic consequences. Schlechtendalia 4: 1–33.

Braun U, Takamatsu S, Heluta V, Limkaisang S, Divarangkoon R, Cook R, Boyle H (2006) Phylogeny and taxonomy of powdery mildew fungi of *Erysiphe* sect. *Uncinula* on *Carpinus* species. Mycological Progress 107(5): 139–153. https://doi.org/10.1007/s11557-006-0509-6

Braun U, Cook RTA (2012) Taxonomic Manual of the Erysiphales (powdery mildews). Fungal Biodiversity Centre, CBS Biodiversity Series No. 11, 707 pp.

Bolay A, Braun U, Delhey R, Kummer V, Piątek M, Wołczańska A (2005) *Erysiphe deutziae* – a new epidemic spread in Europe. Cryptogamie Mycologie 26(4): 293–298.

Bunkina IA (1973) Novye vidy i formy muchnisto-rosyanykh gribov yuga Primorskogo Kraya (Dal'niy Vostok). Novosti Sistematiki Nizshikh Rastenii 10: 79–83.

Denton G, Henricot B (2007) First report of powdery mildew on *Deutzia* spp. in the UK. Plant Pathology 56(2): 353. https://doi.org/10.1111/j.1365-3059.2007.01534.x

Felsenstein J (1985) Confidence limits on phylogenies: an approach using the bootstrap. Evolution 39(4): 783–791. https://doi.org/10.2307/2408678

He P (1990) Taxonomy of *Deutzia* (Hydrangeaceae) from Sichuan, China. Phytologia 69(5): 332–339.

Hirata T, Takamatsu S (1996) Nucleotide diversity of rDNA internal transcribed spacers extracted from conidia and cleistothecia of several powdery mildew fungi. Mycoscience 37(3): 283–288. https://doi.org/10.1007/BF02461299

Kubitzki K (2004) The Families and Genera of Vascular Plants, Volume VI Flowering Plants, Dicotyledons: Celastrales, Oxalidales, Rosales, Cornales, Ericales. Springer-Verlag Berlin Heidelberg, 489 pp. https://doi.org/10.1007/978-3-662-07257-8_1

Kumar S, Stecher G, Tamura K (2016) MEGA7: Molecular Evolutionary Genetics Analysis version 7.0 for bigger datasets. Molecular Biology and Evolution 33(7): 1870–1874. https://doi.org/10.1093/molbev/msw054

Nguyen VN, Guan GX, Zhao FY, Tang SR, Li Y, Liu SY (2018) *Erysiphe deutziae* causes powdery mildew on *Deutzia parviflora* var. *amurensis* in China. Forest Pathology 48(5): e12454. https://doi.org/10.1111/efp.12454

Nomura Y (1997) Taxonomical Study of Erysiphaceae of Japan. Yokendo Ltd., 281 pp.

Park MJ, Choi YJ, Hong SB, Shin HD (2010) Powdery mildew of crenate deutzia caused by *Erysiphe deutziae* in Korea. The Plant Pathology Journal 26(3): 294. https://doi.org/10.5423/PPJ.2010.26.3.294

Qiu PL, Nguyen VN, Guan GX, Li Y, Takamatsu S, Liu SY (2018) Occurrence of powdery mildew caused by *Golovinomyces orontii* on *Lactuca sativa* var. *ramosa* (lettuce) in China. Crop Protection 110: 108–111. https://doi.org/10.1016/j.cropro.2018.04.005

Shin HD, Meeboon J, Takamatsu S, Adhikari MK, Braun U (2018) Phylogeny and taxonomy of *Pseudoidium pedaliacearum*. Mycological Progress 18(1–2): 237–246. https://doi.org/10.1007/s11557-018-1429-y

Takamatsu S, Braun U, Limkaisang S, Kom-Un S, Sato Y, Cunnington JH (2007) Phylogeny and taxonomy of the oak powdery mildew *Erysiphe alphitoides* sensu lato. Mycological Research 111(7): 809–826. https://doi.org/10.1016/j.mycres.2007.05.013

Takamatsu S, Ito H, Shiroya Y, Kiss L, Heluta V (2015a) First comprehensive phylogenetic analysis of the genus *Erysiphe* (Erysiphales, Erysiphaceae) I. the *Microsphaera* lineage. Mycologia 107(3): 475–489. https://doi.org/10.3852/15-007

Takamatsu S, Ito Arakawa H, Shiroya Y, Kiss L, Heluta V (2015b) First comprehensive phylogenetic analysis of the genus *Erysiphe* (Erysiphales, Erysiphaceae) II: the *Uncinula* lineage. Mycologia 107(5): 903–914. https://doi.org/10.3852/15-062

Walsh PS, Metzger DA, Higuchi R (1991) Chelex 100 as a medium for simple extraction of DNA for PCR-based typing from forensic material. Biotechniques 10(4): 506–513. https://doi.org/10.2144/000113897

MycoKeys 51: 107–123 (2019)
doi: 10.3897/mycokeys.51.33529
http://mycokeys.pensoft.net

RESEARCH ARTICLE

A peer-reviewed open-access journal
MycoKeys
Launched to accelerate biodiversity research

Two new species of *Phylloporus* (Fungi, Boletales) from tropical *Quercus* forests in eastern Mexico

Leticia Montoya[1], Edith Garay-Serrano[1], Victor M. Bandala[1]

1 *Red Biodiversidad y Sistemática, Instituto de Ecología A.C., P.O. Box 63, Xalapa, Veracruz, 91000, México*

Corresponding author: *Victor M. Bandala* (victor.bandala@inecol.mx)

Academic editor: *A. Vizzini* | Received 6 February 2019 | Accepted 29 March 2019 | Published 8 May 2019

Citation: Montoya L, Garay-Serrano E, Bandala VM (2019) Two new species of *Phylloporus* (Fungi, Boletales) from tropical *Quercus* forests in eastern Mexico. MycoKeys 51: 107–123. https://doi.org/10.3897/mycokeys.51.33529

Abstract

We present a proposal of two new species of *Phylloporus* discovered in tropical oak forests from central Veracruz, Mexico. Both species were distinguished based on macro and micro-morphologic features and supported with a molecular phylogenetic analysis, based on sequences of nuc rDNA ITS, D1, D2 and D3 domains of nuc 28S rDNA (LSU), and transcription elongation factor 1-alpha (tef-1α). In the phylogenetic reconstruction inferred, the new species clustered in two different clades related to species from USA, Costa Rica and Panama. The recollection of fructifications in monodominant stands of either *Quercus oleoides* or *Q. sapotifolia*, allowed recognizing the distribution of one of the *Phylloporus* species under both *Quercus* species, and the other under *Q. oleoides* only. Detailed macro and microscopic descriptions accompanied by illustrations, photos and a taxonomic discussion are provided.

Keywords

ectomycorrhizal fungi, Neotropical fungi, oak forest

Introduction

The genus *Phylloporus* is widely distributed worldwide with approximately 100 species occurring among conifers and broad-leaf trees as potential hosts (Neves 2007; Ortiz-Santana et al. 2007; Neves and Halling 2010; Neves et al. 2010, 2012; Zeng et al. 2013; Ye et al. 2014). Recent research on *Phylloporus* systematics revealed that some species placed under this genus in the past are related to other groups. Such is the case of *P. boletinoides*, that was found to be genetically distant, representing an independent genus, described recently as *Phylloporopsis* (Farid et al. 2018). *Erythrophylloporus*

Ming Zhang & T.H. Li recently described, is a lamellate lineage in the Boletaceae, having morphological resemblance to *Phylloporus* (Zhang and Li 2018). Additionally, a high species diversity is being detected in the genus; for example in China, Zeng et al. (2013) recognized at least 21 phylogenetic species of *Phylloporus*, 17 of which represented newly discovered taxa. Most *Phylloporus* species have a tropical and subtropical range of occurrence, although some species, e.g. *P. imbricatus* and *P. pachycystidiatus*, are known to occur in alpine ecosystems (Zeng et al. 2013; Ye et al. 2014). In the Neotropics, an important diversity of *Phylloporus* has been documented since the early works by Singer (1973, 1978) and Singer and Gómez (1984), to more recent contributions by Ortiz et al. (2007), Neves and Halling (2010) and Neves et al. (2012). In the Neotropics, *Quercus*, *Pinus*, *Abies*, *Alnus*, *Dicymbe*, and *Neea*, represent some potential ectomycorrhizal hosts of *Phylloporus* spp. mentioned in the literature (Singer 1978, Montoya et al. 1987; Montoya and Bandala 1991, Ortiz-Santana et al. 2007, Neves 2007, Neves and Halling 2010).

In Mexico, *Phylloporus* has been collected mainly in temperate and mesophytic forests. *Phylloporus guzmanii* Montoya & Bandala, and *P. fagicola* Montoya & Bandala were described as new species, the former found in *Pinus* and *Pinus-Quercus* forests, while the latter in mesophyll forest under *Fagus grandifolia* var. *mexicana* (Montoya and Bandala 1991, 2011). Other records in Mexico correspond to *P. bellus* (Massee) Corner, *P. rhodoxanthus* (Schw.) Bres. (inhabiting *Quercus* and mixed *Pinus-Quercus*, *Pinus-Abies* forests), *P. centroamericanus* Singer & Gómez and *P. foliiporus* (Murr.) Singer (in *Quercus* and mesophyll forests), *P. phaeoxanthus* var. *simplex* Singer & Gómez and *P. leucomycelinus* (Singer) Singer (in *Quercus* forest) (Singer 1957, 1978; Singer and Gómez 1984; Montoya et al. 1987; Montoya and Bandala 1991; García 1999).

Mexico harbors the greatest center of *Quercus* species diversity with about 160–165 species of the 500–600 known worldwide (Valencia 2004, Nixon 2006; Cavender-Bares 2016). Some species of *Quercus* dominate the canopy of lowland tropical forest relicts in the country (Challenger and Soberón 2008). In the state of Veracruz (eastern Mexico) such forest ecosystems currently cover around 905 km^2, and are listed by CONABIO as priority terrestrial regions considered Pleistocene relicts (Arriaga et al. 2000). Such tropical *Quercus* forests are seriously fragmented but still shelter populations of diverse biological groups, including endemic species of flora and ectomycorrhizal fungi associated with native *Quercus* trees. Many species of this trophic group of fungi in their tropical range are poorly known in Mexico.

As part of a weekly monitoring of macrofungi in two lowland relicts of tropical *Quercus* forests in eastern Mexico, we have detected, among other ectomycorrhizal fungi, the common presence of *Phylloporus* fructifications. After a macro- and micromorphological study of the collections, that included molecular phylogenetic analyses based on ITS, LSU and tef-1α sequences, we concluded that the specimens represent two new species inhabiting the tropical *Quercus* forests from eastern Mexico.

Material and methods

Sampling and morphological study

A weekly monitoring developed during June-October 2016–2017 in two tropical *Quercus* forests from Central Veracruz (eastern Mexico) were the basis of the present study, including some collections made in 2009 and 2012. The two forests are within private properties, one located at Zentla Co. (850 m alt.) and the other one at Alto Lucero Co. (400–500 m alt.); both forests present monodominant stands of *Q. oleoides* Schltdl. & Cham. and *Q. sapotifolia* Liebm. where the *Phylloporus* samples were gathered.

Macromorphological and color studies of specimens were conducted on different growth stages of fresh material. In the description of each species, alphanumeric nomenclature of colors is based on Kornerup and Wanscher (1967) (e.g. 3A4–5) and Munsell color chart (1994) (e.g. 2.5YR 4/4). Basidiomes were dried in a hot air dehydrator (45 °C) for a week. Measurements and colors of micromorphological structures were recorded in 3% KOH and Melzer´s solution. Thirty five basidiospores per collection were measured in lateral view. Basidiospore sizes are accompanied by the symbols: $\bar{X}$, representing the range of X (where X is the average of basidiospores length and width in each collection) and $\bar{Q}$ refers to the range of Q (where Q is the average of the ratio of basidiospore length/basidiospore width in each collection). Line drawings were made under a compound microscope (Nikon Eclipse E400) using an attached drawing tube. Line drawings were made under a compound microscope, using an attached drawing tube. Specimen vouchers are kept at XAL herbarium (Thiers B., continuously updated, Index Herbariorum: http://sweetgum.nybg.org/science/ih/).

DNA extraction, PCR and sequencing

Genomic DNA was extracted from tissue of dried basidiomes according to Montoya et al. (2014). The ITS region of the nuclear ribosomal RNA gene was amplified using the primers ITS1F/ITS4 (White et al. 1990; Gardes and Bruns 1993), the LSU rRNA gene, D1–D3 domains, using primers LR0R/LR21, NL4, LR5 (Hopple y Vilgalys 1999, O´Donnell 1993, Vilgalys and Hester 1990), and the transcription elongation factor 1-alpha (tef-1α) with primers tef1F/tef1R or EF1-2F/EF1-2R (Morehouse et al. 2003, Zeng et al. 2013). PCR conditions for amplification, and procedures for purification of PCR products follow Montoya et al. (2014) and Herrera et al. (2018). Once sequences were assembled and edited, they were deposited at GenBank (http://www.ncbi.nlm.nih.gov) under accession numbers provided in Table 1.

Phylogenetic analysis

ITS, LSU and tef-1α sequences of *Phylloporus* generated in this study and sequences of closely related species downloaded after a BLAST search from GenBank database (http://www.ncbi.nlm.nih.gov/), were incorporated in independent datasets (one for each molecular marker) in the PhyDE program v.0.9971 (Müller et al. 2010). Each dataset (TreeBASE accession 23913) was independently aligned on the online Mafft service (Katoh et al. 2017) and inconsistencies were adjusted manually. The best evolutionary model for every dataset was calculated with MEGA 6.06 (Tamura et al. 2013). A concatenated dataset with previously aligned sequences of ITS + LSU + tef-1α was integrated. Maximum Likelihood (ML) analysis for every dataset and concatenated multilocus dataset were performed for phylogenetic inference, with 1000 bootstrap replicates in the same program. Phylogenetic analyses were also performed with MrBayes v 3.2.6 (Ronquist et al. 2012) for 1,000,000 of replicates. The phylogenies from ML and BI analyses were displayed using Mega 6.06 and FigTree v1.4.3 (Rambaut 2016) respectively.

Results

Eighteen fresh collections of *Phylloporus* were gathered in the tropical *Quercus* forests studied. Twenty four ITS, LSU and tef-1α sequences (indicated in bold in Table 1) were obtained from eight specimens, and together with 146 sequences of worldwide *Phylloporus* species worldwide were included in the phylogenetic analyses developed (Fig. 1). The best resolution in the phylogenetic analyses was obtained in the combined dataset (nrLSU, tef-1α and ITS). In the individual datasets, both species here described were recognized as independent clades with good BS values. We present here the concatenated three-locus phylogenetic tree (Fig. 1), where the sequences of the Mexican specimens clustered in two strongly supported isolated clades, suggesting that they can be recognized as two different species. Sequences supporting three collections grouped in one clade (BS= 100%, PP= 1.0) sister to sequences of specimens from USA and Panama, identified by Neves et al. (2012) as *P. leucomycelinus* and *P. caballeroi*. Another group of five sequences from Mexican specimens also cluster in a well-supported clade (BS= 89%, PP= 1.0) sister to a sequence identified by those authors as *P. purpurellus* from Costa Rica. Within this latter Mexican clade, sequences recorded as NC 7285-1 and as NC 7286-1, of an unidentified *Phylloporus* species from USA, appear nested in the phylogeny, suggesting that they belong to the same taxon (Fig. 1). Considering the distinctive set of morphological features that the Mexican *Phylloporus* specimens possess (see descriptions below) and with the results of the phylogenetic analysis, we concluded that they represent two new *Phylloporus* species in tropical *Quercus* forests from eastern Mexico and both are proposed here.

Table 1. Specimens and sequences considered in this study.

Species	Voucher	Locality	GenBank accession number		
			LSU	ITS	*tef-1*α
P. alborufus	MAN022	Costa Rica	JQ003678	JQ003624	–
P. arenicola	JT27954	USA	JQ003704	–	–
P. bellus	HKAS 56763	China	JQ967196	JQ967239	JQ967153
	REH8710	USA	JQ003686	JQ003618	–
	REH7733	Costa Rica	JQ003661	–	–
P. bogoriensis	DED7785	Indonesia	JQ003680	JQ003625	–
P. brunneiceps	HKAS 56903	China	JQ967198	JQ967241	JQ967155
	HKAS 59727	China	JQ967201	JQ967244	JQ967158
P. caballeroi	REH7906	Panama	JQ003662	JQ003638	–
P. castanopsidis	MAN104	Thailand	JQ003689	JQ003642	–
	MAN118	Thailand	JQ003693	JQ003646	–
P. centroamericanus	MAN037	Costa Rica	JQ003664	JQ003634	–
P. cyanescens	REH8681	Australia	JQ003684	JQ003621	–
P. dimorphus	MAN128	Thailand	JQ003697	JQ003648	–
P. foliiporus	JLM1677	USA	JQ003687	JQ003641	–
P. gajari	HKAS 81585	Bangladesh	KP780423	KP780419	–
P. imbricatus	HKAS 54647	China	JQ967202	JQ967245	JQ967159
	HKAS 54861	China	JQ967205	JQ967248	JQ967162
P. leucomycelinus	MB05-007	USA	JQ003666	JQ003653	–
	MB00-043	USA	JQ003677	JQ003628	–
	HKAS 74678	USA	JQ967206	JQ967249	JQ967163
P. luxiensis	HKAS 57036	China	JQ967207	JQ967250	JQ967164
	HKAS 57048	China	JQ967209	JQ967252	JQ967166
P. maculatus	HKAS 59730	China	JQ678698	JQ678696	JQ967194
P. orientalis	REH8731	Australia	JQ003700	–	–
	REH8755	Australia	JQ003701	JQ003651	–
P. pachycystidiatus	HKAS 54540	China	JQ967211	JQ967254	JQ967168.1
P. parvisporus	HKAS 54768	China	JQ967214	JQ967257	JQ967171
P. pelletieri	K 128205	England	JQ967215	JQ967258	–
P. phaeoxanthus	MAN064	Costa Rica	JQ003670	–	–
P. purpurellus	MAN050	Costa Rica	JQ003672	JQ003630	–
P. quercophilus	Garay 373a	Mexico	MK226557	MK226549	MK314105
	Gutiérrez 29	Mexico	MK226556	MK226548	MK314104
	Montoya 5239	Mexico	MK226558	MK226550	MK314106
P. rhodoxanthus	JLM1808	USA	JQ003688	JQ003654	–
	REH8714	USA	JQ003675	JQ003629	–
	SAR 89.457	USA	U11925	–	–
P. rimosus	Caro 69	Mexico	MK226552	MK226544	
	César 61	Mexico	MK226555	MK226547	
	Garrido14	Mexico	MK226553	MK226545	
	Gutiérrez 37	Mexico	MK226551	MK226543	
	Montoya 4834	Mexico	MK226554	MK226546	
	NC-7285/1	USA	–	AY456356	–
	NC-7286/1	USA	–	AY456355	–
P. rubeolus	HKAS 52573	China	JQ967216	JQ967259	JQ967172
P. rubiginosus	MAN117	Thailand	JQ003692	JQ003645	–
	MAN119	Thailand	JQ003694	JQ003647	–
P. rubrosquamosus	HKAS 54559	China	JQ967219	JQ967262	JQ967175
P. rufescens	HKAS 59722	China	JQ967220	JQ967263	JQ967176
P. scabripes	REH8531	Belize	JQ003683	JQ003623	–
	REH8558	Belize	–	JQ003622	–
P. yunnanensis	HKAS 52225	China	JQ967222	JQ967265	JQ967178
	HKAS 52527	China	JQ967223	JQ967266	JQ967179
P. sp. 1	HKAS 74679	China	JQ967228	JQ967271	JQ967184
P. sp.10	HKAS 74689	China	JQ967237	JQ967280	JQ967192
P. pruinatus	HKAS 74687	China	JQ967235	JQ967278	JQ967190
P. sp. 7	HKAS 74688	China	JQ967236	JQ967279	JQ967191
P. sp.	LAM 0417	Malaysia	KY091029	–	–
	MAN131	Thailand	JQ003698	JQ003649	–
	PDD 104656	New Zealand	KP191688	–	–
Xerocomus magniporus	HKAS 59820	China	JQ678699	JQ678697	JQ967195
Xerocomus perplexus	MB00-005	USA	JQ003702	JQ003657	KF030438
Xerocomus subtomentosus	K 167686	England	JQ967238	JQ967281	JQ967193

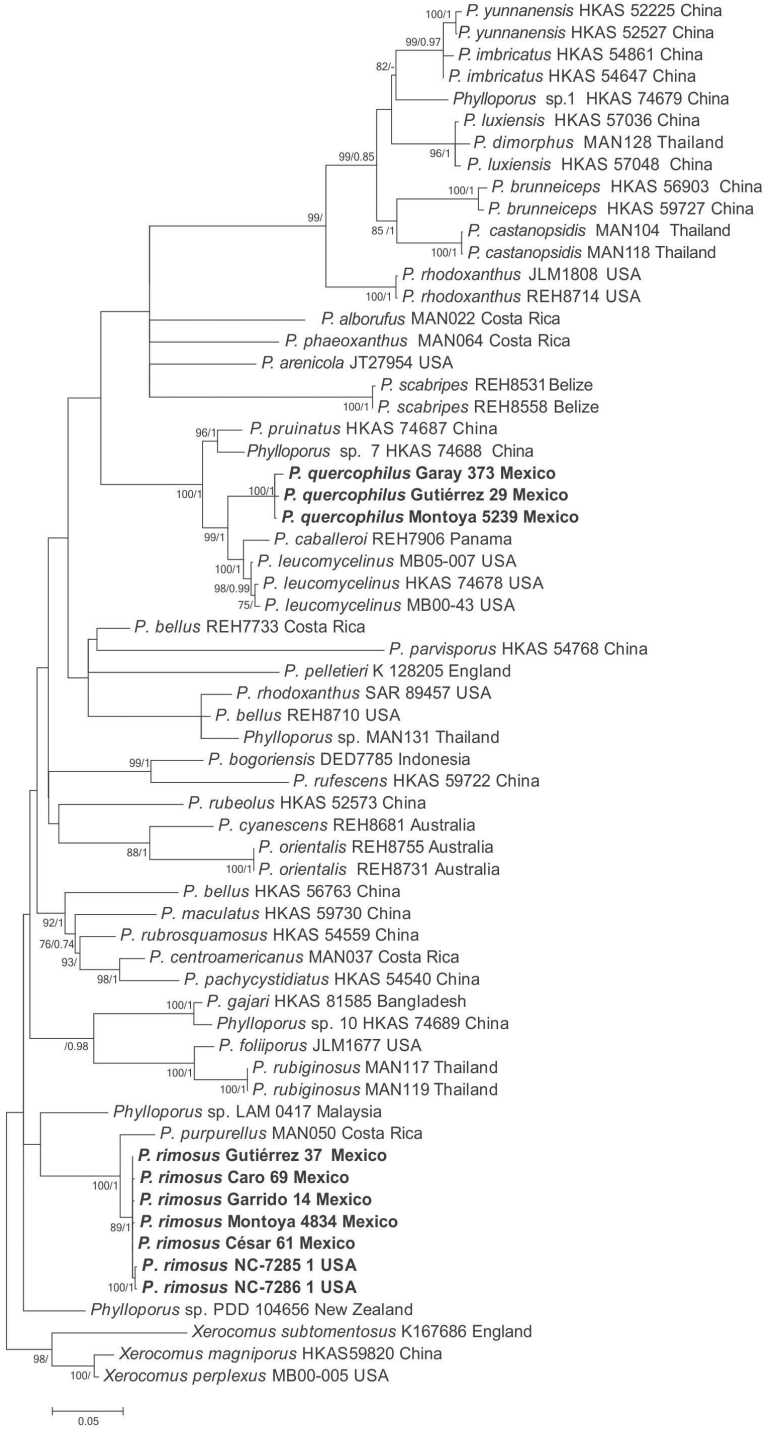

Figure 1. Concatenated three-locus (nrLSU, tef-1α and ITS) phylogenetic analysis by maximum likelihood of *Phylloporus* species. Bootstrap values (BS> 75) / Posterior probabilities (PP > 0.85) are indicated above branches. New species are indicated in bold letters.

Description of the new species

Phylloporus rimosus **Bandala, Montoya & Garay, sp. nov.**
MycoBank: MB 829439
Figs 2a, b, 3, 4

Holotype. MEXICO. Veracruz: Municipality of Coatepec, Vaquería, gregarious in soil, under *Quercus oleoides* Schltdl. & Cham., 27 June 2012, Montoya 4834 (XAL).

Diagnosis. Recognized by the combination of pileus vinaceous to grayish-vinaceous, surface becoming rimose-areolate with development, the stipe apex with ribbed appearance and scabrous or even with tiny rigid scales and gills staining blue. Its stature (pileus 27–80 mm diam., stipe 27–80 × 7–12 mm), basidiospores and pleurocystidia size and shape, prevents confusion with *P. purpurellus* Singer or with *P. scabripes* B. Ortiz & M.A. Neves.

Gene sequences ex-holotype. MK226546 (ITS), MK226554 (LSU), MK314102 (tef-1α).

Etymology. Referring to the rimose pileus surface.

Figure 2. Basidiomes of *Phylloporus* species. **a, b** *P. rimosus* (**a** Garrido 3, **b** Montoya 5232a) **c** *P. quercophilus* (LM5239 holotype). Scale bars: 10 mm.

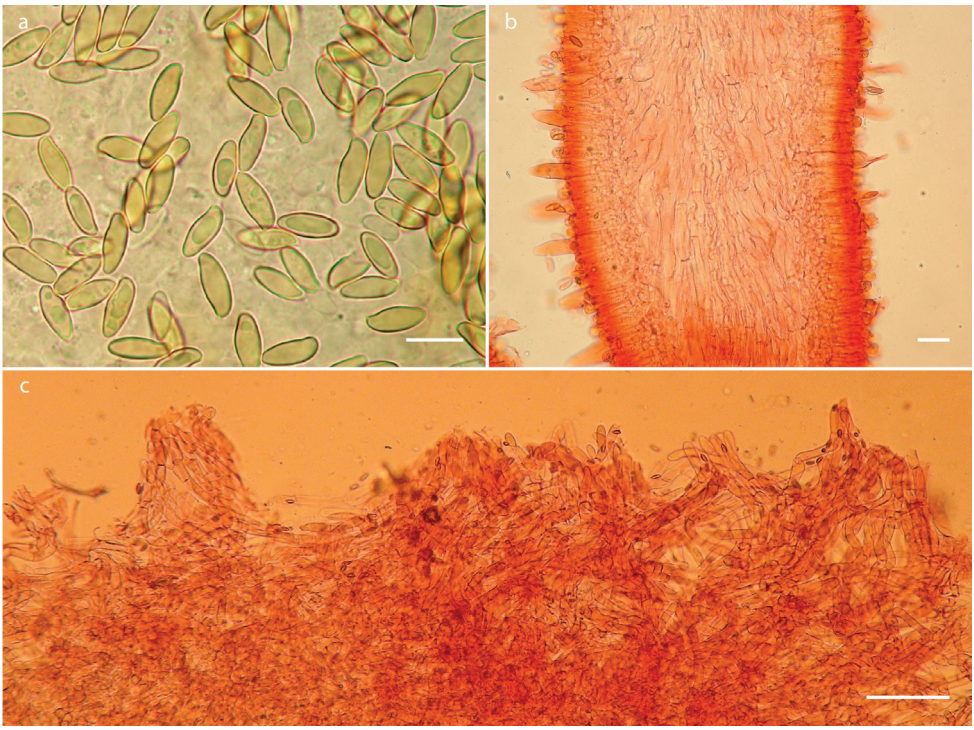

Figure 3. *Phylloporus rimosus* (Montoya 4834, holotype). **a** Basidiospores **b** hymenophoral trama **c** longitudinal section of pileipellis. Scale bars: 10 µm (**a**), 25 µm (**b**), 100 µm (**c**).

Description. ***Pileus*** 27–80 mm diam, convex to plane-convex, at times faintly depressed at center or even infundibuliform; surface velvety, uniform but frequently rimose-areolate, or fracturing and forming rivulose patches, cracked when seen under lens, vinaceous to grayish-vinaceous (7D4–D5, 7C4; 5YR 3/4, 4/3, 4/4–25Y 6/6), darker in some areas especially towards the margin, or yellowish, reddish-yellow, reddish-brown or even yellowish-beige (10YR 5/4, 6/6) in other parts especially towards the center, some specimens even reddish-vinaceous (7E8–E7) with brownish tinges (7D6–6E8), mature specimens fading to brownish when exposed to the sun; margin slightly incurved, edge entire, at times undulate. ***Lamellae*** subdecurrent to decurrent, 9–15 mm broad, close, bright yellow (3A7, 5A6–A7; 5Y8/8; 4A16), mustard yellow with age (4A6–A7; 4B7–B8), staining blue or greenish-blue when handled, stains becoming reddish or brownish-vinaceous after several minutes, old specimens or specimens long exposed to the sun developing reddish spots at lamellae sides or even dark brownish red or brown at edge; somewhat sinuous when the hymenophore is seen frontally, veined or anastomosed mostly in the area below the pileus and intervenose or even somewhat labyrinthiform, especially when young; lamellullae of different sizes, edge entire. ***Stipe*** 27–80 × 7–12 mm, cylindrical, curved, somewhat sinuous, compact, apex with ribbed appearance by decurrent lines of the lamellae,

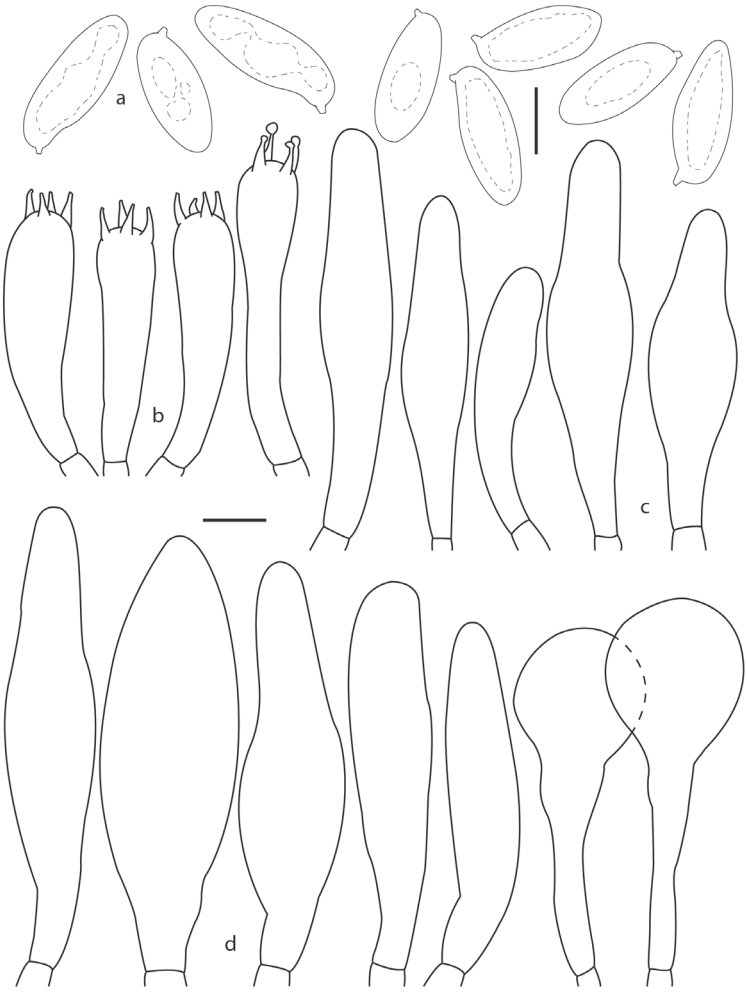

Figure 4. *Phylloporus rimosus* (Montoya 4834, holotype). **a** Basidiospores **b** basidia **c** cheilocystidia **d** pleurocystidia. Scale bars: 5 µm (**a**), 10 µm (**b–d**).

surface pruinose, scabrous or even with tiny rigid scales, cracked after long exposure to the sun, beige (10YR 6/6–8) or pale yellow (4A/2), or whitish at the bottom of the surface and covered with a reddish or oxide-red (25YR 4/6) pruina, at the middle area reddish-beige (8D16), at times caespitose. ***Basal mycelium*** whitish-cream with some yellow spots or even mustard yellow (5Y8/6). ***Context*** yellow, staining pinkish or pinkish-brown. KOH 3% reddish (10YR 3/6 to 2.5YR 3/4) on pileus, stipe surface and context; NH_4OH 10% greenish-blue (5Y 2.5/1) on pileus surface, the center of the stain becoming reddish (2.5YR 3/6), brownish at the hymenium, negative in the context and faintly green or negative on stipe surface. ***Odor*** mild to slightly citric. ***Taste*** mild.

Basidiospores (9–) 9.5–14 (–15) × 3.5–5 µm, $\bar{X}$ = 11–12.3 × 4.3–4.6 µm, $\bar{Q}$ = 2.5 2.8 µm, subfusiform, with suprahilar depression, somewhat ventricose, apex attenuated, yellow to amber yellow in KOH, wall slightly thickened (up to 0.5 µm thick). ***Basidia*** 29–50 (–55) × 7–10 (–11) µm, clavate, tetrasporic, rarely trisporic, hyaline, thin walled, unclamped. ***Pleurocystidia*** 42–105 (–120) × 9–27 µm, narrowly to broadly utriform, at times cylindrical or subclavate, rarely sphaeropedunculate (52–58 × 20–23 µm), thin-walled, at times thickened in some areas, some with incrustations, hyaline, abundant, unclamped. ***Cheilocystidia*** (33–) 34–70 (–75) × 8–17 (–19) µm, narrowly utriform, hyaline, thin-walled, at times thickened towards the apex, unclamped. ***Pileipellis*** a trichodermis, with anticlinally oriented hyphae, tightly interwoven, frequently disposed in mounds, hyphae 8–16 µm broad, wall slightly thickened (up to 1 µm), hyaline yellowish-brown; terminal elements 23–64 × 8–14 µm, cylindrical, slightly inflated, other or clavate, pale yellowish-brown. ***Pileus trama*** hyphae 5–16 µm broad, in a lax interwoven arrangement, hyaline, thin walled. ***Hymenophoral trama*** arranged in a more or less regular central strand and somewhat divergent on both sides of the strand, with cylindrical hyphae 7–19 µm broad; some slightly inflated, hyaline, thin-walled, unclamped.

Habitat. In soil, solitary or gregarious, in tropical oak forest, under *Quercus oleoides* and *Q. sapotifolia*.

Additional studied material. MEXICO. Veracruz: Alto Lucero Co., NE Mesa de Venticuatro, 4 Oct 2016, Garrido14; 19 Sep 2017, Gutiérrez 37. Zentla Co. Road Puentecilla-La Piña, 2 July 2009, Ramos 195. Around town of Zentla, 15 June 2016, Montoya 5232a; Montoya 5238; 23 June 2016, Gutiérrez 5, Hervert 84; 30 June 2016, Cesar 61, Hervert 93; 6 July 2016, Caro 69; 30 Aug 2016, Garrido 3; 24 Aug 2017, Garay 368; 7 Sep 2017, César 84 (all at XAL).

Phylloporus quercophilus **Montoya, Bandala & Garay, sp. nov.**
MycoBank: MB 829440
Figs 2c, 5, 6

Holotype. MEXICO. Veracruz: Municipality of Zentla, around town of Zentla, 850 m a.s.l., in soil, in small groups, at tropical oak forest, under *Quercus oleoides* 15 June, 2016, Montoya 5239 (XAL).

Diagnosis. Its reddish pileus tinges together with, context staining reddish, basidiospores 9–13 × 3–4 µm and narrowly utriform or subcylindrical cystidia and its habitat distinguish it from close related species, such as *P. caballeroi* Singer.

Gene sequences ex-holotype. MK226550 (ITS), MK226558 (LSU), MK314106 (tef-1α).

Etymology. In reference to the habitat.

Description. ***Pileus*** 15–65 mm diam., hemispheric at first, then becoming convex to plane-convex,; surface velvety, reddish-vinaceous (8D7, 8E7–8), dark reddish-brown (9E6–7), brown (7C5) with pinkish tinges to pinkish-vinaceous (7C6) with paler zones and dark vinaceous tinges (7D6–D7); margin straight to slightly decurved to

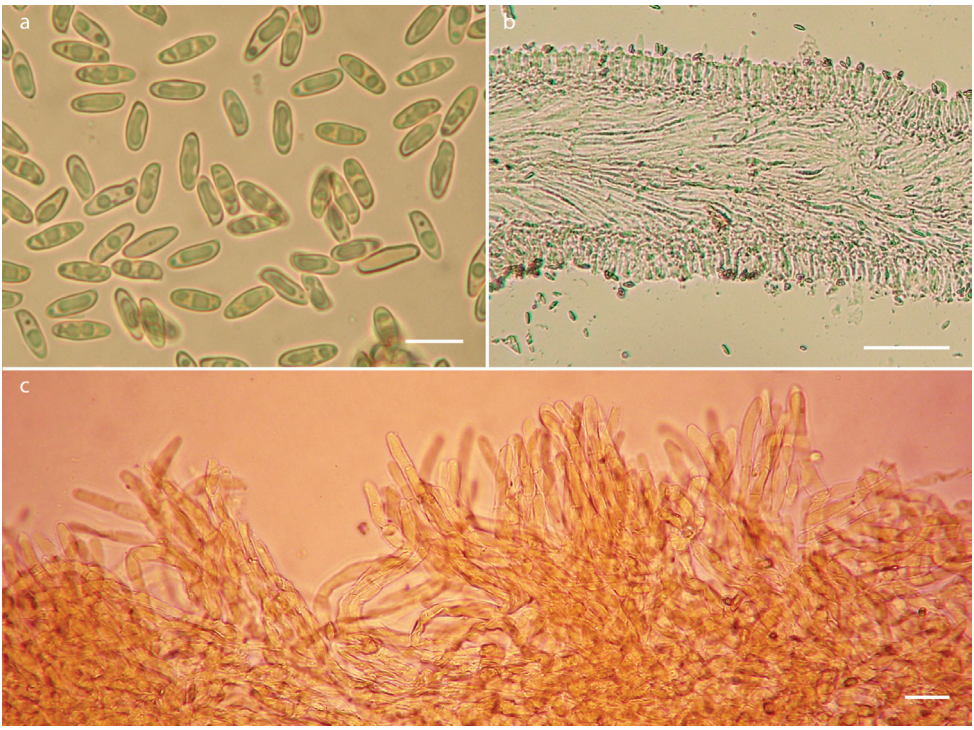

Figure 5. *Phylloporus quercophilus* (Montoya 5239, holotype). **a** Basidiospores **b** hymenophoral trama **c** longitudinal section of pileipellis. Scale bars: 10 µm (**a**), 100 µm (**b**), 25 µm (**c**).

incurved, undulate. ***Lamellae*** 5–8 mm width, adnate to subdecurrent, close to slightly subdistant, yellow (3A5, 3B7), mustard-yellow (4B7–B8), staining pale brown or blue-greenish when handled, veined or anastomosed mostly below pileus surface and with interparietal veins, margin finely fimbriate, lamellullae of different sizes, with reddish spots. ***Stipe*** 25–55 × 3–13 mm, central, attenuated towards the base, sinuous, compact, reddish-vinaceous (9E7), middle and basal part yellowish to pale brown, bright yellow (3A2, 4A6), with olive to pinkish-vinaceous tinges when young, frequently with a reddish pruina and fine appressed scales over the apex, surface smooth, with peeling fibers especially in mature specimens. ***Basal mycelium*** whitish to yellowish. ***Context*** dirty whitish, staining reddish especially towards the pileus area where it is hygrophanous; stipe at times fistulose but mostly compact, especially at apical area. KOH 3% blackish on pileus, greenish to brown in lamellae, negative in context; NH_4OH 10% bluish on pileus, or bluish-greenish at the beginning, later blackish in pileus and stipe, dark grayish-blue in context and lamellae. ***Odor*** fruity. ***Taste*** mild.

Basidiospores 9–13 × 3–4 µm, $\bar{X}$ = 10–10.7 × 3.6–3.7 µm, $\bar{Q}$ =2.7–2.9 µm, subcylindrical, with a faint suprahilar depression, attenuated towards apical area and with rounded apex, frontal view subcylindrical, hyaline, with very pale greenish tinges, wall slightly thickened (up to 0.5 µm) 10 to 30% in a field of view dextrinoid. ***Basidia***

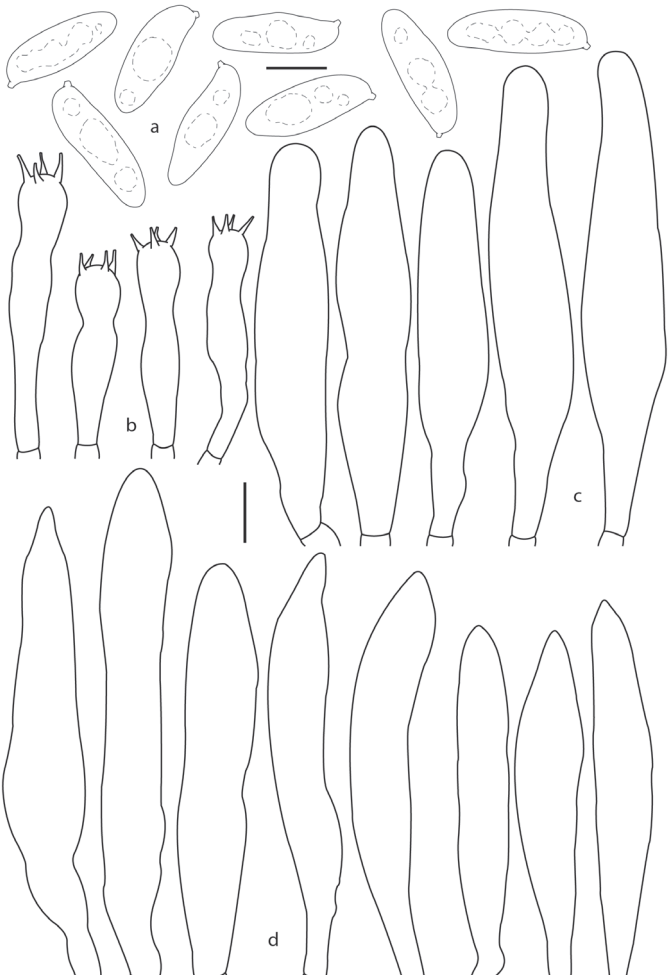

Figure 6. *Phylloporus quercophilus* (Montoya 5239, holotype). **a** Basidiospores **b** basidia **c** pleurocystidia **d** cheilocystidia. Scale bars: 5 μm (**a**), 10 μm (**b–d**).

28–42 (–46) × 6–10 μm, clavate, tetrasporic, hyaline, unclamped. ***Pleurocystidia*** 50–102 × 8–16 μm, narrowly utriform, subutriform or irregularly subcylindric, hyaline, pale yellowish, not incrusted, thin walled, at times the wall slightly thickened up to 1 μm, unclamped. ***Cheilocystidia*** 42–90 × 8–14 μm, hyaline, narrowly fusiform to subcylindrical, thin-walled, at times incrusted, unclamped. ***Pileipellis*** a trichodermis composed of more or less erect and tightly interwoven hyphae, at times disposed in mounds, hyphae 7–14 μm broad, thin walled, unclamped; terminal elements 20–48 × 7–14 μm, hyaline, other cells with pale yellow contents, this layer yellowish-brown in KOH at lower magnifications, thin walled, unclamped. ***Pileus trama*** hyphae 6–13 μm broad, in a compact interwoven arrangement, cylindrical to subcylindrical, hyaline, thin walled, at times incrusted in a faintly circumferential striate pattern, un-

clamped. ***Hymenophoral trama*** divergent; hyphae 6–12 µm broad, thin-walled (< 1 µm thick), at times with resinous like incrustations, some hyphae with a faintly striate appearance, hyaline, unclamped.

Habitat. In soil, in small groups or solitary, in tropical oak forest, under *Quercus oleoides* Schltdl. & Cham.

Additional studied material. MEXICO. Veracruz: Zentla Co., around town of Zentla, 850 m a.s.l., 12 July 2017, Gutiérrez 29; 24 Aug 2017, Garay 366; 7 Sep 2017, Garay 373a (all at XAL).

Discussion

The multilocus phylogeny inferred demonstrated that *Phylloporus rimosus* and *P. quercophilus* are genetically distant, clustered in separate well-supported clades, and apart from other *Phylloporus* species. Both were found co-habiting in the *Quercus* forests studied. Although they are somewhat similar in their general habit, when comparing the pileus surface, the velvety texture in *P. rimosus* becomes rimose-areolate with development, while in *P. quercophilus* the surface remains uniform. *Phylloporus rimosus* has more robust basidiomes, with a thicker, scabrous and more rigid stipe. The basidiospore sizes, shape and color are different, being larger in *P. rimosus* [(9–) 9.5–14 (–15) × 3.5–5 µm, $\bar{X}$ = 11–12.3 × 4.3–4.6 µm *vs*. 9–12.5 × 3–4 µm, $\bar{X}$ = 10 –10.7 × 3.6–3.7 µm] more ventricose and attenuated towards the apex, and more pigmented, in contrast to *P. quercophilus*. The cystidia appear wider (8–27 µm *vs*. 8–16 µm) and more versiform (including sphaeropedunculate pleurocystidia) in *P. rimosus*. Another difference is that the latter has a hymenophoral trama with the hyphae arranged in a regular central strand and somewhat divergent on both sides, while in *P. quercophilus* that trama is distinctly divergent.

In the phylogenetic analysis (Fig 1) *P. rimosus* grouped close to a Costa Rican specimen identified as *P. purpurellus* Singer by Neves et al. (2012). According to Singer (1973) the basidiomes of *P. purpurellus* in comparison with the Mexican species, present a tiny habit, with pileus only up to 26 mm diam. and stipe 30 × 4–4.5 mm; shorter basidiospores (7.5–11.3 × 3.3–4 µm) and with cystidia 48–65 × 8.5–12 µm shorter and narrower. In the analysis, the *P. rimosus* clade includes two ITS sequences (NC 7285-1, NC 7286-1) obtained from basidiomes growing in a Loblolly pine (*Pinus taeda*) plantation from North Carolina, USA (after Edwards et al. (2004). Both sequences are inferred to be conspecific with the *P. rimosus* Mexican collections. Loblolly pine is widely distributed in the SE United States (USDA, https://www.fs.fed.us/database/feis/plants/tree/pintae/all.html). Currently, the provenance of our specimens and those of Edwards et al. (2004), reveal that *P. rimosus* displays a range at the eastern portions of both USA and Mexico.

Phylloporus quercophilus appeared as a sister species (Fig 1) to specimens identified by Neves et al. (2012) and Zeng et al. (2013) as *P. caballeroi* Singer and *P. leucomycelinus* Singer. *Phylloporus caballeroi* described by Singer (1973) from Argentina,

differs from *P. quercophilus* by the pileus with olivaceous tinges, lamellae in a closer arrangement, context not staining reddish, and association with *Alnus*. Neves and Halling (2010) offered a broader concept of *P. caballeroi*, and congruent with the original diagnosis, they cite similar basidiospores [4–5 (–6) µm diam. (Q= 2.21)] and ampullaceous cystidia. *Phylloporus leucomycelinus* differs from *P. quercophilus* by the smalller basidiomes (pileus 28–34 mm diam; stipe 27–45 × 3–5 mm), with deep red-brown pileus, lamellae brownish yellow to yellow-brown with olive tinge, and shorter [50–71 × (6–) 11–12] ampullaceous cystidia (Singer 1978).

Considering some morphological and color resemblance, *P. rimosus* and *P. quercophilus* should be compared with *P. scabripes* B. Ortiz and M.A. Neves from Belize, *P. bellus* (Massee) Corner and *P. rufescens* Corner from Singapore (Corner 1970; Singer and Gómez 1984; Ortiz-Santana et al. 2007). However, they are genetically distinct according to the phylogeny inferred here (Fig. 1) [that include sequences produced by Neves et al. (2012) and Zeng et al. (2013)]. *Phylloporus scabripes* is similar to *P. rimosus* because of its distinctly scabrous stipe surface, an unusual feature for a species of *Phylloporus*. The former species differs however, from *P. rimosus* by shorter basidiospores [9.8–12.8 × 3.2–4.8 µm *vs*. (9–) 9.5–14 (–15) × 3.5–5 µm] and shorter and broader pleurocystidia [43.2–80 × 13.6–15.2 µm *vs.* 42–105 (–120) × 9–27 µm)]. The pleurocystidia size also distinguishes *P. scabripes* from *P. quercophilus* (50–102 × 8–16 µm) as also the pileus color of *P. scabripes* ["...pale reddish brown (6D4), paler to tan with age (near 5C4..."] is paler and brownish in range, not as vinaceous, as in both of the Mexican taxa, and the context of *P. scabripes* does not stain reddish. Moreover, *P. scabripes* apparently lacks cheilocystidia.

We concur with Zeng et al. (2013) that the name *P. bellus* has been too widely applied. So we refer here to the original description (Corner 1970) which defines this species with shorter basidiomes than those of *P. rimosus* [stipe (30–40 × 4–10 mm)], with narrower lamellae (4–7 mm width) and shorter basidiospores [8.5–10 × 4.5–5.5 (–6) µm]. The basidiospores of *P. bellus* are even shorter than in *P. quercophilus*. The Asian species *P. bellus* differs also from both Mexican taxa by the context not staining reddish. On the contrary, *P. rufescens* Corner shares with both Mexican taxa the reddening of the context but it finally turns black on exposure (Corner 1970), which does not occur either in *P. rimosus* or in *P. quercophilus*. Other differences among *P. rufescens* and the Mexican species are the shorter size of basidiospores (8–9 × 4–5 µm) and more robust basidiomes (pileus 50–140 mm diam and stipe 25–120 × 6–25 mm).

In Costa Rica, Singer and Gomez (1984) concluded that *Phylloporus* species are present in tropical montane zones forming ectomycorrhiza with *Quercus* spp. and *Alnus jorullensis*. They observed however, that this group of fungi did not occur in lower mountains of the country, and suggested that, it is possibly extremely rare there or perhaps, it is not adapted to *Q. oleoides* or that unknown edaphic or climatic limitations prevent its distribution. Current records of *Phylloporus* in tropical monodominant stands of *Q. oleoides* here described suggest the potential ectomycorrhizal association of *Phylloporus* with this tree species. Additionally, *P. rimosus* represents a first report of *Phylloporus* growing in association with *Q. sapotifolia* trees and even with *Pinus taeda*.

Acknowledgments

We recognize the support of CONACYT (CB 252431) to study the EcM fungi associated with tropical species of *Quercus* in Veracruz, Mexico. E. Garay is grateful for the postdoctoral scholarship grant from Fondo SEP-CONACYT for the project CB-252431 and from the INECOL. We acknowledge the assistance in field and laboratory of Biol. D. Ramos (Instituto de Ecología, A.C.). We appreciate the support given by CONACYT (225382) to the Laboratorio de Presecuenciación, Red Biodiversidad y Sistemática, INECOL. IBT Bertha Pérez assisted us in molecular procedures. We appreciate the English revision by Dr. Andrew Vovides, INECOL.

References

Arriaga L, Espinoza JM, Aguilar C, Martínez E, Gómez L, Loa E, Larson J (2000) Regiones prioritarias terrestres de México. Comisión Nacional para el Conocimiento y Uso de la Biodiversidad. México, DF. https://doi.org/10.5962/bhl.title.118644

Cavender-Bares J (2016) Diversity, distribution, and ecosystem services of the North American oaks. International Oaks 27: 37–48.

Challenger A, Soberón J (2008) Los ecosistemas terrestres. Capital natural de México. 1: 87–108.

Corner EJH (1970) *Phylloporus* Quél. and *Paxillus* Fr. In Malaya and Borneo. Nova Hedwigia 20: 793–822.

Edwards J, Cripliver L, Gillespie AR, Johnsen KH, Scholler M, Turco RF (2004) Nitrogen availability alters macrofungal basidiomycete community structure in optimally fertilized loblolly pine forests. New Phytologist 162: 755–770. https://doi.org/10.1111/j.1469-8137.2004.01074.x

Farid A, Gelardi M, Angelini C, Franck AR, Costanzo F, Kaminsky L, Ercole E, Baroni TJ, White AL, Garey JR, Smith ME, Vizzini A (2018) *Phylloporus* and *Phylloboletellus* are no longer alone: *Phylloporopsis* gen. nov. (Boletaceae), a new smooth-spored lamellate genus to accommodate the American species *Phylloporus boletinoides*. Fungal Systematics and Evolution 2: 341–359. https://doi.org/10.3114/fuse.2018.02.10

García JJ (1999) Estudio sobre la taxonomía, ecología y distribución de algunos hongos de la familia Boletaceae (Basidiomycetes, agaricales) de México. Tesis de maestría en Ciencias Forestales, Facultad de Ciencias Forestales, Universidad Autónoma de Nuevo León, Linares, México. https://doi.org/10.5154/r.rchscfa.2017.09.057

Gardes M, Bruns TD (1993) ITS primers with enhanced specificity for basidiomycetes application to the identification of mycorrhizae and rusts. Molecular Ecology 2:113–118. https://doi.org/10.1111/j.1365-294x.1993.tb00005.x

Herrera M, Bandala VM, Montoya L (2018) *Cantharellus violaceovinosus*, a new species from tropical *Quercus* forests in eastern Mexico. MycoKeys 32: 91–109. https://doi.org/10.3897/mycokeys.32.22838.figure2

Hopple J, Vilgalys R (1999) Phylogenetic relationships in the mushroom genus *Coprinus* and dark-spored allies based on sequence data from the nuclear gene coding for the large ribo-

somal subunit RNA: divergent domains, outgroups and monophyly. Molecular Phylogenetics and Evolution 13: 1–19. https://doi.org/10.1006/mpev.1999.0634

Katoh K, Rozewicki J, Yamada KD (2017) MAFFT online service: multiple sequence alignment, interactive sequence choice and visualization. Briefings in bioinformatics. https://doi.org/10.1093/bib/bbx108

Kornerup A, Wanscher JH (1967) Methuen handbook of colour. 2th ed. Methuen. London.

Montoya L, Bandala VM (1991) Studies on the genus *Phylloporus* in Mexico I. Discussion of the known species and description of a new species and a new record. Mycotaxon 41: 471–482.

Montoya L, Bandala VM (2011) A new *Phylloporus* from two relict *Fagus grandifolia* var. *mexicana* populations in a montane cloud forest. Mycotaxon 117: 9–18. https://doi.org/10.5248/117.9

Montoya L, Bandala VM, Guzmán G (1987) Nuevos registros de hongos del estado de Veracruz, IV.Agaricales II. Revista Mexicana de Micología 3: 83–107. https://doi.org/10.21829/abm63.2003.921

Montoya L, Bandala VM, Garay E (2014) Two new species of *Lactarius* associated with *Alnus acuminata* subsp. *arguta* in Mexico. Mycologia 106: 949–962. https://doi.org/10.3852/14-006

Morehouse EA, James TY, Ganley ARD, Vilgalys R, Berger L, Murphy PJ, Longcore JE (2003) Multilocus sequence typing suggests the chytrid pathogen of amphibians is a recently emerged clone. Molecular Ecology 12: 395–403. https://doi.org/10.1046/j.1365-294x.2003.01732.x

Munsell Soil Colour Charts (1994) Macbeth, New Windsor.

Müller J, Müller K, Neinhuis C, Quandt D (2010) PhyDE Phylogenetic Data Editor, version 0.9971. Program distributed by the authors. http://www.phyde.de

Neves MA (2007) Toward a revision of the genus *Phylloporus* (Boletaceae): systematics phylogeny of species from various parts of the world. Doctor of Philosophy dissertation, Graduate Faculty in Biology (ProQuest, Ed.). University of New York, New York.

Neves MA, Halling RE (2010) Study on species of *Phylloporus* I: Neotropics and North America. Mycologia 102: 923–943. https://doi.org/10.3852/09-215

Neves, MA, Henkel TW, Halling RE (2010) *Phylloporus colligatus* sp. nov., a new gilled bolete from Guyana. Mycotaxon 111: 143–148. https://doi.org/10.5248/111.143

Neves MA, Binder M, Halling RE, Soytong K (2012) The phylogeny of selected *Phylloporus* species, inferred from nrLSU and ITS sequences, and descriptions of new species from the Old World. Fungal Diversity 55: 109–123. https://doi.org/10.1007/s13225-012-0154-0

Nixon KC (2006) Global and neotropical distribution and diversity of oak (genus *Quercus*) and oak forests. Ecology and conservation of neotropical montane oak forests. Springer, Berlin, Heidelberg, 3–13. https://doi.org/10.1007/3-540-28909-7_1

O´Donnell K (1993) *Fusarium* and its near relatives In: Reynolds DR, Taylor JW (Eds) The Fungal Holomorph: Mitotic, Meiotic and Pleomorphic Speciation in Fungal Systematics. Edited by Wallingford, UK. CAB International 1993: 225–233.

Ortiz-Santana B, Jean D, Baroni TJ, Both EE (2007) Boletes from Belize and the Dominican Republic. Fungal Diversity 27: 247–416.

Rambaut A (2016) FigTree v1.4.3. Institute of Evolutionary Biology, Univ of Edinburgh. http://tree.bio.ed.ac.uk/software/figtree

Ronquist F, Teslenko M, van der Mark P, Ayres DL, Darling A, Höhna S, Larget B, Liu L, Suchard MA, Huelsenbeck JP (2012) MrBayes 3.2: efficient Bayesian phylogenetic inference and model choice across a large model space. Systematic Biology 61: 539–542. https://doi.org/10.1093/sysbio/sys029

Singer R (1957) Fungi mexicani, series prima, Agaricales. Sydowia 11: 354–374.

Singer R (1973) Diagnoses fungorurn novorurn Agaricalium. Sydowia Beih 7: 1–106.

Singer R (1978) Notes on Bolete taxonomy II. Persoonia 9:421–438.

Singer R, Gómez LD (1984) The Basidiomycetes of Costa Rica III. The genus *Phylloporus* (Boletaceae). Brenesia 22: 163–181.

Tamura K, Stecher G, Peterson D, Filipski A, Kumar S (2013) MEGA6: molecular evolutionary genetics analysis version 6.0. Molecular Biology and Evolution 30: 2725–2729. https://doi.org/10.1093/molbev/mst197

Valencia AS (2004) *Quercus* (Fagaceae) diversity in Mexico. Botanical Sciences 75: 33–53.

Vilgalys R, Hester M (1990) Rapid genetic identification and mapping of enzymatically amplified ribosomal DNA from several *Cryptococcus* species. Journal of Bacteriology 172: 4238–4246. https://doi.org/10.1128/jb.172.8.4238-4246.1990

White TJ, Bruns T, Lee S, Taylor J (1990) Amplification and direct sequencing of fungal ribosomal RNA genes for phylogenetics. In: Innis MA,Gelfand DH, Sninsky JJ,White TJ (Eds) PCR protocols: a guide to methods and applications. Academic Press, New York, 315–322. https://doi.org/10.1016/b978-0-12-372180-8.50042-1

Ye L, Mortimer P, Xu J, Karunarathna SC, Hyde KD (2014) The Genus *Phylloporus* (Boletaceae, Boletales), from Mekong River Basin (Yunnan Province, China). Chiang Mai Journal Science 41: 798–810.

Zeng NK, Tang LP, Li YC, Tolgor B, Zhu XT, Zhao Q, Yang ZL (2013) The genus *Phylloporus* (Boletaceae, Boletales) from China: morphological and multilocus DNA sequence analyses. Fungal Diversity 58: 73–101. https://doi.org/10.1007/s13225-012-0184-7

Zhang M, Li TH (2018) *Erythrophylloporus* (Boletaceae, Boletales), a new genus inferred from morphological and molecular data from subtropical and tropical China. Mycosystema 37: 1111–1126.